國 立 交 通 大 學

機械工程學系

碩士論文

藉部分區域穩定理論之坤-震八卦多重交織導數同步

Kun-Zhen Hexagram Multiple Symplectic Derivative Synchronization by Partial Region Stability Theory

研 究 生：黃啟任

指導教授：戈正銘　教授

中華民國一零一年六月

藉部分區域穩定理論之坤-震八卦多重交織導數同步

Kun-Zhen Hexagram Multiple Symplectic Derivative Synchronization by Partial Region Stability Theory

研究生：黃啟任　　Student：Qi-Ren Huang

指導教授：戈正銘　　Advisor：Zheng-Ming Ge

國立交通大學

機械工程研究所

碩士論文

A Thesis

Submitted to Institute of Mechanical Engineering

College of Engineering

National Chiao Tung University

In Partial Fulfillment of the Requirement

For the Degree of master of science

In

Mechanical Engineering

June 2012

Hsinchu, Taiwan, Republic of China

中華民國一零一年六月

藉部分區域穩定理論之坤-震八卦多重交織導數同步

學生： 黃啟任　　指導教授：戈正銘

摘要

廣義同步是存在著主人與僕人狀態之間的一個函數關係。一個新型的渾沌同步，藉由部分區域穩定理論之多重交織導數同步，得到與原系統狀態變量和其他不同系統構成的“夥伴”關係。利用數值模擬來驗證部分區域穩定理論之多重交織導數同步的有效性。

在中國哲學中，陰代表是負或陰柔，而陽是代表正或陽剛。陰跟陽在中國哲學中兩個是互相對立的，然而太極結合陰陽，這可能意味著宇宙的起源。八卦是中國哲學的一部分，他們擁有各自的方位、數字、以及代表性。作為例証，本論文主要研究坤卦與震卦，結合了在上面的坤卦與在下面震卦得到六十四卦的坤-震卦。坤-震卦代表不同的混沌系統，並藉由部分區域穩定理論達成多重交織導數同步。

Kun Trigram Symplectic Derivative Chaos Synchronization by Partial Region Stability Theory

Student：Qi-Ren Huang　　Advisor：Zheng-Ming Ge

Abstract

The generalized synchronization is that there exists a functional relationship between the states of the master and those of the slave. A new type of chaotic synchronization, multiple chaotic symplectic derivative synchronization, is obtained with the state variables of the original system and of another different order system as constituents of the functional relation of “partners”. Numerical simulations are provided to verify the effectiveness of the proposed scheme.

In Chinese philosophy, Yin means negative, historical, or feminine principle while Yang is positive, contemporary, or masculine principle. Yin and Yang are two fundamental opposites in Chinese philosophy, and “Tai Ji”, the great one, is the combination of Yin and Yang, which maybe the origin of Cosmos. The eight trigrams is a part of Chinese philosophy, and they have their own direction, figure, and representation. In this thesis,as examples,Kun trigram and Zhen trigram are studied. Combining Kun trigram in upper place and Zhen trigram in lower place can get Kun-Zhen hexagram. Kun-Zhen hexagram can be annotated by chaos and its synchronization.

誌謝

本論文得以完成，首先必須感謝我的指導老師 戈正銘教授的耐心指導與教誨。戈老師有教無類與因才施教的教育方式使我在課業上與做研究方面獲得極大的幫助。在研究過程中，也讓我學習如何發現問題以及解決問題。戈老師也不厭其煩的修訂論文，讓論文加以完整。老師專業領域上的成就以及對於文學、史學、哲學涵養上，也讓學生受匪淺。

在這段兩年的碩士生涯裏，非常感謝李仕宇、何俊諺、蔡尚恩、王翔平、江振賓、李永厚學長在渾沌知識的指導與經驗傳承，在研究遇到瓶頸之時，給予我寶貴的意見；也感謝我的同學張登順、紀亭宇、李健華，與他們相處不論在課業上或是生活上都有獲得很大的幫助。

最後，感謝我的家人，您們全力支持，讓我可以不必擔心課業以外的事務，使我無後顧之憂地攻讀碩士。雖然與家人分隔兩地，但是在外求學的我，依然還是可以感受到家庭的溫暖，感謝您們的教養，使我順利拿到碩士學位。也感謝女友瑋儒，一直以來有你的支持與體諒，妳讓我在疲勞之時得以繼續撐下去的動力。最後，僅以此論文獻給你們。

CONTENTS

Chapter 1

Introduction

Nonlinear dynamics has been extensively used in physics, mathematics, engineers, economics and philosophy studying in the past few decades. Chaos theory as a part of nonlinear dynamics has been widely used in various fields such as power converters, weather prediction, information processing, population dynamics, chemical reactions, biological systems, secure communications, etc [1-8]. Accepted chaos theory pioneer is Lorenz [9]. He discovered chaos in a simple system of three autonomous ordinary differential equations to describe the simplified Rayleigh-Benard problem.

In Chinese philosophy, Yin means negative, feminine or past, while Yang means positive, masculine or present. Yin and Yang are two fundamental opposites in Chinese philosophy [10]. In this research, Chen-Lee system[5] is studied. There are many articles in studying contemporary Chen-Lee system for time $0 \to +\infty$ which is called Yang Chen-Lee system, of which the chaos is called Yang chaos. Indeed we can also study the historical Chen-Lee system for time $0 \to -\infty$ which is called Yin Chen-Lee system of which the chaos is called Yin chaos. Furthermore, by Chinese philosophy, Tai Ji chaos, i.e. Great One chaos, which consists of Yin chaos and Yang chaos, of Chen-Lee system is studied.

Symplectic synchronization is defined as $y = H(x, y, t)$, where x, y are the state vectors of the "Partner A" and of the "Partner B", respectively [11]. The final desired state y of the "Partner B" not only depends upon the state of Partner A x but also depends upon the the state of Partner B y itself. Therefore the " Partner B" is not

a traditional pure slave obeying the “master” completely but plays a role to determine the final desired state of the “slave” system.

Let

$$G(x,y,t)=F(x,y,t) \tag{1.1}$$

Since x and y are presented at both the right hand side and the left hand side of the equality,it is called double symplectic synchronization where x,y are state vectors of Partner A and Partner B,respectively,*G(x,y,t)* and *F(x,y,t)* are given vector functions of *x,y* and time.

New strategy to achieve multiple symplectic derivative synchronization is presented. Furthermore, by Chinese philosophy, Tai Ji chaos, i.e. Great One chaos, which consists of Yin chaos and Yang chaos. Finally, combining Kun trigram in upper place and Zhen trigram in lower place can get Kun-Zhen hexagram. Kun-Zhen hexagram can be annotated by chaos and its synchronization.

Chapter 2

Yin Chaos Yang Chaos and

Tai Ji Chaos of Chen-Lee Systems

2.1 Preliminary

Yin and Yang are two fundamental opposites in Chinese philosophy. Chaos of contemporary Chen-Lee system, i.e. Yang chaos of Chen-Lee system, has been investigated completely. In this research, chaos of historical Chen-Lee system, i.e. Yin chaos of Chen-Lee system, is studied with comparison to that of Yang chaos by time histories of states, phase portraits, bifurcation diagrams and Lyapunov exponents. Furthermore, by Chinese philosophy, Tai Ji chaos, i.e. Great One chaos, which consists of Yin chaos and Yang chaos, of Chen-Lee system is studied.

2.2Yang Chen-Lee system

Chen-Lee system for time interval $0 \to +\infty$ is called Yang Chen-Lee system:

$$\begin{cases} \dfrac{dx_1(t)}{dt} = -x_2(t)x_3(t) + ax_1(t) \\ \dfrac{dx_2(t)}{dt} = x_1(t)x_3(t) + bx_2(t) \\ \dfrac{dx_3(t)}{dt} = x_1(t)x_2(t)/3 + cx_3(t) \end{cases} \tag{2.1}$$

Chaos of Yang Chen-Lee system appears when initial condition(x_{10}, x_{20}, x_{30}) = (0.2, 0.2, 0.2) and Yang parameters a=3, b=-5 and c=-1.0. The behaviors of corresponding Yang chaos are shown in Figs 2.1~2.3 by time histories, 2D and 3D phase portraits.

2.3 Yin Chen-Lee system

By replacing variable$(x_1(t), x_2(t), x_3(t), t)$ with$(x_1(-t), x_2(-t), x_3(-t), -t)$ in Eq. (2.1) to study the past $(t: 0 \to -\infty)$ of the system, Yin Chen-Lee system is described as follows:

$$\begin{cases} \dfrac{dx_1(-t)}{d(-t)} = \dfrac{-dx_1(-t)}{dt} = -x_2(-t)x_3(-t) + ax_1(-t) \\ \dfrac{dx_2(-t)}{d(-t)} = \dfrac{-dx_1(-t)}{dt} = x_1(-t)x_3(-t) + bx_2(-t) \\ \dfrac{dx_3(-t)}{d(-t)} = \dfrac{-dx_1(-t)}{dt} = \dfrac{x_1(-t)x_2(-t)}{3} + cx_3(-t) \end{cases} \tag{2.2}$$

The simulation results are tabulated in Table 2.1.

Table 2.1. Dynamic behaviors of Yin Chen-Lee system for different signs of parameters

a	b	c	states
-	+	+	Chaos and periodic
+	-	+	Approach to infinite
+	+	-	Approach to infinite
-	-	+	Approach to infinite
-	+	-	Approach to infinite
-	-	-	Approach to infinite

Table 1 shows dynamic behaviors of Yin Chen-Lee system for different signs of parameters. It shows that chaos of Yin Chen-Lee system appears for initial condition*(x_{10}, x_{20}, x_{30})* = (0.2, 0.2, 0.2) and parameters *a*=-3.0, *b*=5.0 and *c*=1.0 only. The chaotic behaviors are shown in Figs 2.4~2.6 by time histories, 2D and 3D phase portraits.

2.4 Further Simulation results

In order to learn the difference and similarity between Yang and Yin Chen-Lee system, the bifurcation diagrams and Lyapunov exponents are also used. The simulation results are shown in three cases:

Case 1: Paremeter *a* is varied and *b, c* are fixed. Bifurcation diagrams and Lyapunov exponents are shown in Figs 2.7~2.10. The simulation results are compared from Table 2.2 and Table2. 3.

Table 2.2. Dynamic behaviors of Yang chaos for parameter *a*

Range of parameter *a*	Behaviors of chaos
0.00～0.03	Periodic trajectory
0.04～0.7	Chaos
0.71～1.29	Periodic trajectory
1.3～1.4	Chaos
1.41	Periodic trajectory
1.42～1.47	Chaos
1.48	Periodic trajectory
1.49～2.80	Chaos
2.81	Periodic trajectory
2.82～3.29	Chaos
3.3～4.4	Periodic trajectory

Table 2.3. Dynamic behaviors of Yin chaos for parameter *a*

Range of parameter *a*	Behaviors of chaos
0～-0.04	Periodic trajectory
-0.05～-0.7	Chaos
-0.71～-1.29	Periodic trajectory
-1.3～-2.79	Chaos
-2.81	Periodic trajectory
-2.82～-3.29	Chaos
-3.3～-4.4	Periodic trajectory

Table 2.2 and Table 2.3 show the dynamic behaviors of chaos and periodic motion in varied ranges of parameter *a* and fixed parameters *b*, *c* of Yang and Yin Chen-Lee system. From these results, the Yin chaos and Yang chaos are different in many details. For example, when $-2.79 \le a \le 1.3$ chaotic trajectories appear in Yin system while chaos appears in Yang system when $2.82 \le a \le 3.29$ Other differences can be discovered in the Tables. These phenomena match with the jargon of Chinese philosophy: Yin chaos and Yang chaos are "difference in same and same in difference".

Case 2: Paremeter *b* is varied and *a*, *c* are fixed. Bifurcation diagrams and Lyapunov exponents are shown in Figs 2.11~2.14. From these results, the Yin chaos and Yang chaos are similar as a whole. The simulation results are listed in Table2. 4 and Table2. 5.

Table 2.4. Dynamic behaviors of Yang chaos for parameter *b*

Range of parameter *b*	Behaviors of chaos
-4～-4.61	Periodic trajectory
-4.62～-8.9	Chaos
-8.91～-8.92	Periodic trajectory
-8.93～-9.1	Chaos
-9.11～-9.67	Periodic trajectory
-9.68～-10	Chaos

Table 2.5. Dynamic behaviors of Yin chaos for parameter *b*

Range of parameter *b*	Behaviors of chaos
4～4.61	Periodic trajectory
4.62～9.09	Chaos
9.1～9.66	Periodic trajectory
9.67～10	Chaos

Table 2.4 and Table 2.5 show the dynamic behaviors of chaos and periodic motion in varied ranges of parameter *b* and fixed parameters *a*, *c* of Yang and Yin Chen-Lee system. From them, the Yin chaos and Yang chaos are different in many details. For example, when $-4.62 \geq b \geq -8.9$ and $-8.93 \geq b \geq -9.1$, Yang Chen-Lee system has chaotic behaviors while chaos appears in Yin system when $4.62 \leq b \leq 9.09$. Other differences can be discovered in the Tables.

Case 3: Paremeter *c* is varied and *a*, *b* are fixed. Bifurcation diagrams and Lyapunov exponents are shown in Fig. 2.15~2.18. The simulation results are listed in Table 2.6 and Table 2.7.

Table 2.6. Dynamic behaviors of Yang chaos for parameter *c*

Range of parameter *c*	Behaviors of chaos
0.00～-0.02	Periodic trajectory
-0.03～-1.34	Chaos
-1.35～-2	Periodic trajectory

Table 2.7. Dynamic behaviors of Yin chaos for parameter *c*

Range of parameter *c*	Behaviors of chaos
0.00～1.32	Chaos
1.33～2.00	Periodic trajectory

Observing the corresponding ranges of Yin system, they seem nearly the negative ranges of Yang Chen-Lee system.

2.5 Tai Ji Chen-Lee system

"Tai Ji" Chen-Lee system, i.e. "Great One" Chen-Lee system, consists of Yin and Yang Chen-Lee system for time $-\infty$ to ∞. The jargon "Tai Ji" in Chinese philosophy, i.e. Yi classic, means the original chaotic substance which is the origin of the cosmos.

The chaotic behaviors for time $-\infty$ to ∞ are shown in Figs 2.19~2.22 by time histories, 2D and 3D phase portraits.

Bifurcation diagrams of chaotic Yang and Yin Chen-Lee system in Figs 2.7, 2.9, Figs 2.11, 2.13 and Figs 2.15, 2.17 respectively, are nearly symmetrical as a whole. Put them together, and reverse the time order of Yin chaos, the time histories and phase portraits of Tai Ji Chen-Lee system are shown in Figs 2.19~2.21.

Obviously, they are not the same. The bifurcation diagrams of Yang, Yin and Tai Ji Chen-Lee systems are shown in Figs 2.22~2.30.

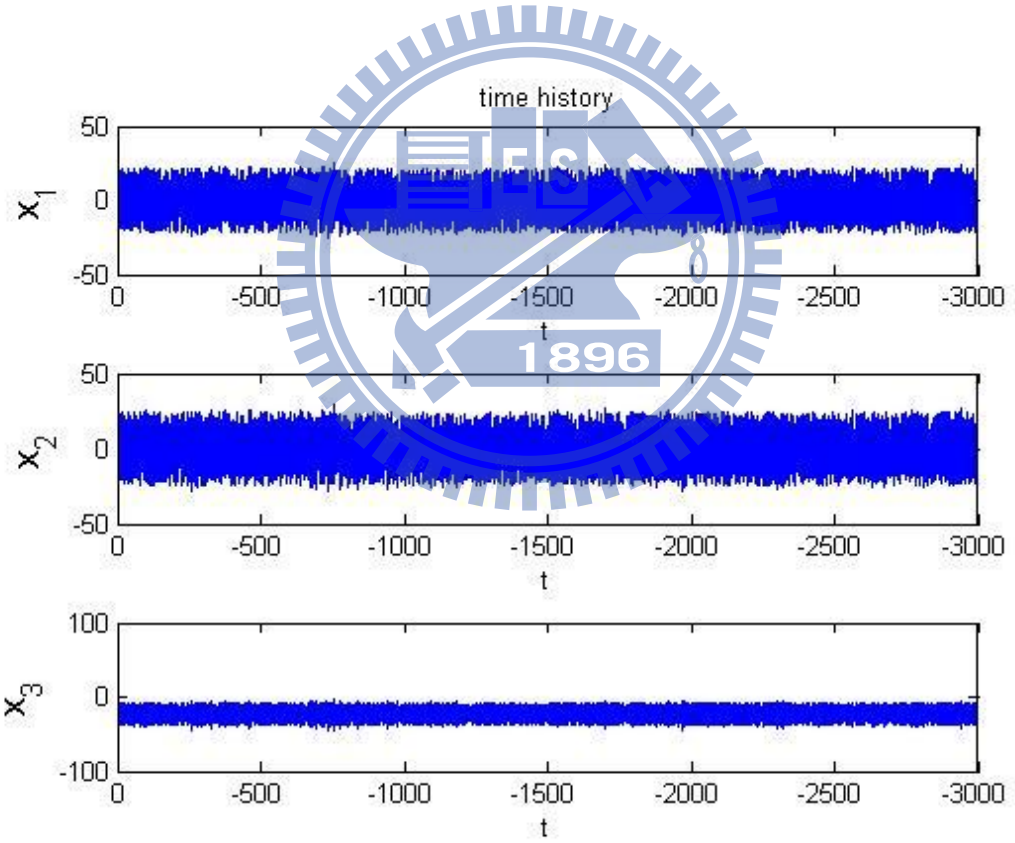

Fig. 2.1 Time histories of Yang Chen-Lee chaos for Yang Chen-Lee system with a=3.0, b=-5.0 ,c=-1.0 and t in seconds.

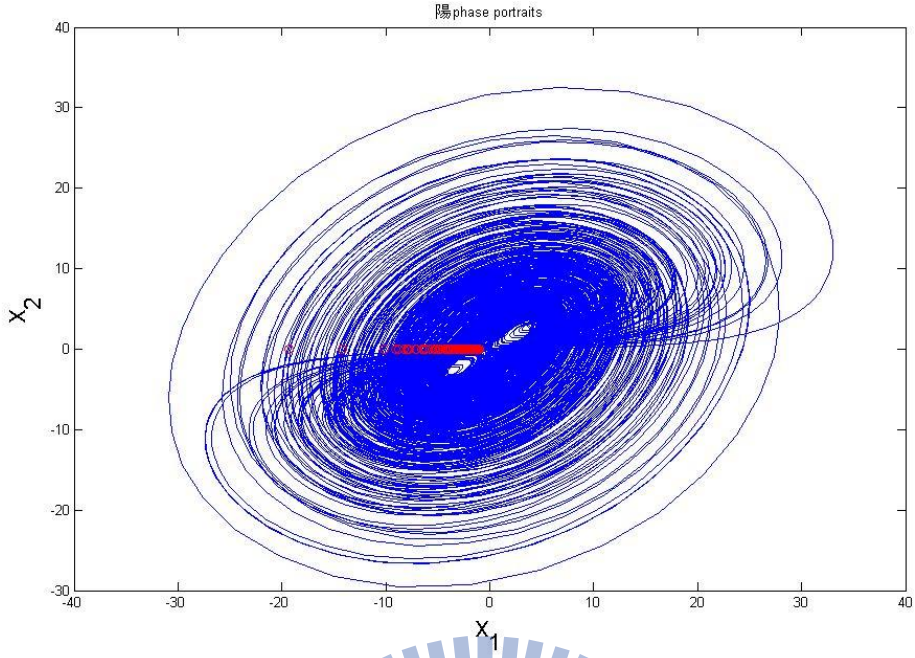
陽phase portraits
40
30
20
10
0
-10
-20
-30
-40
-30
-20
-10
0
10
20
30
40
x2
x1

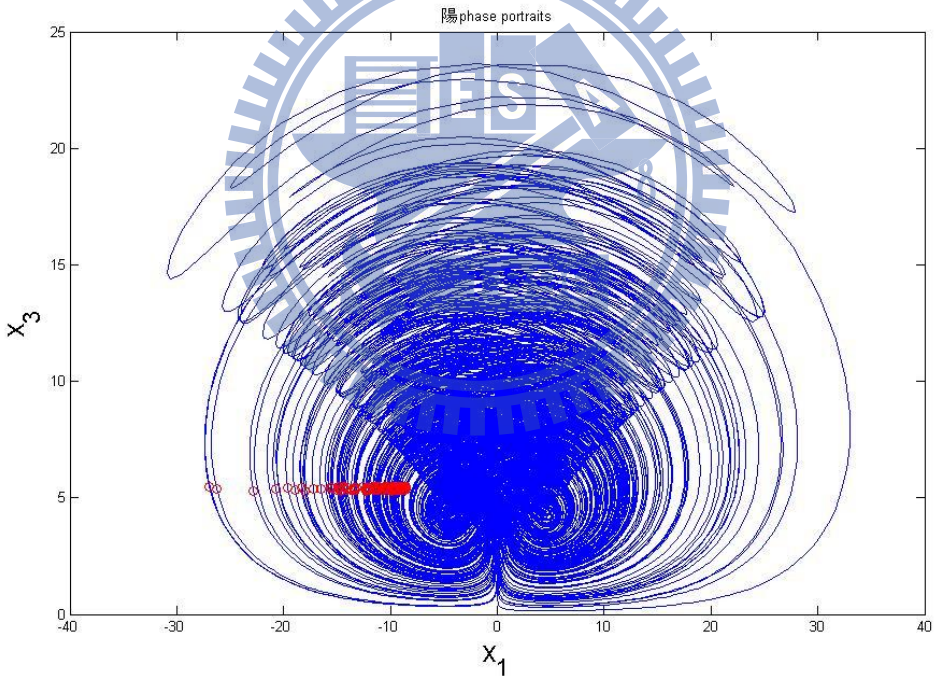
陽phase portraits
25
20
15
10
5
0
-40
-30
-20
-10
0
10
20
30
40
x3
x1

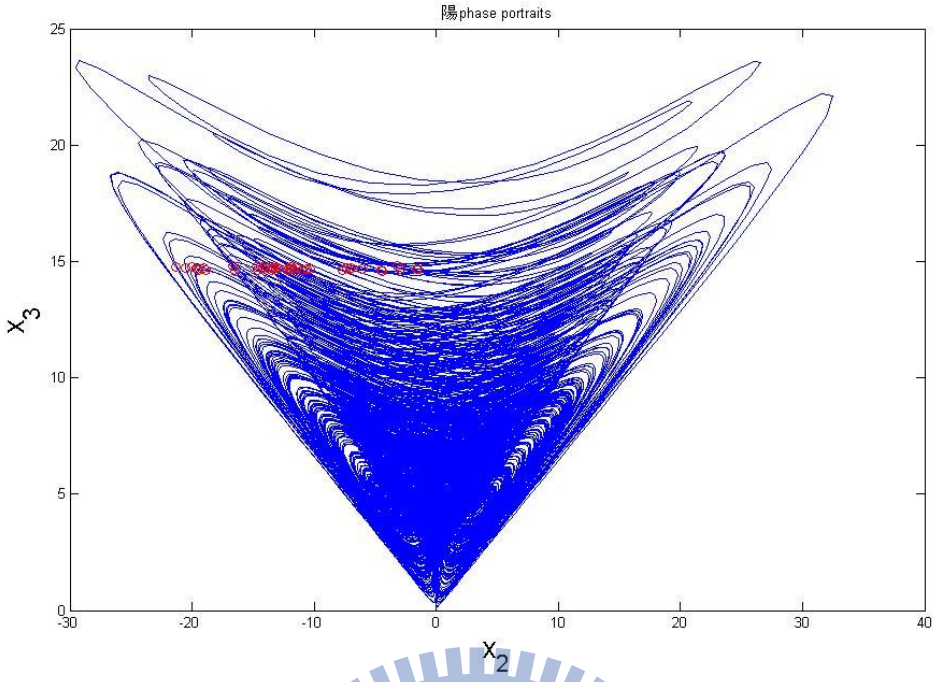

Fig. 2.2 Projections of Phase portraits and Poincaré maps of Yang Chen-Lee chaos with *a*=3.0, *b*=-5.0 and *c*=-1.0.

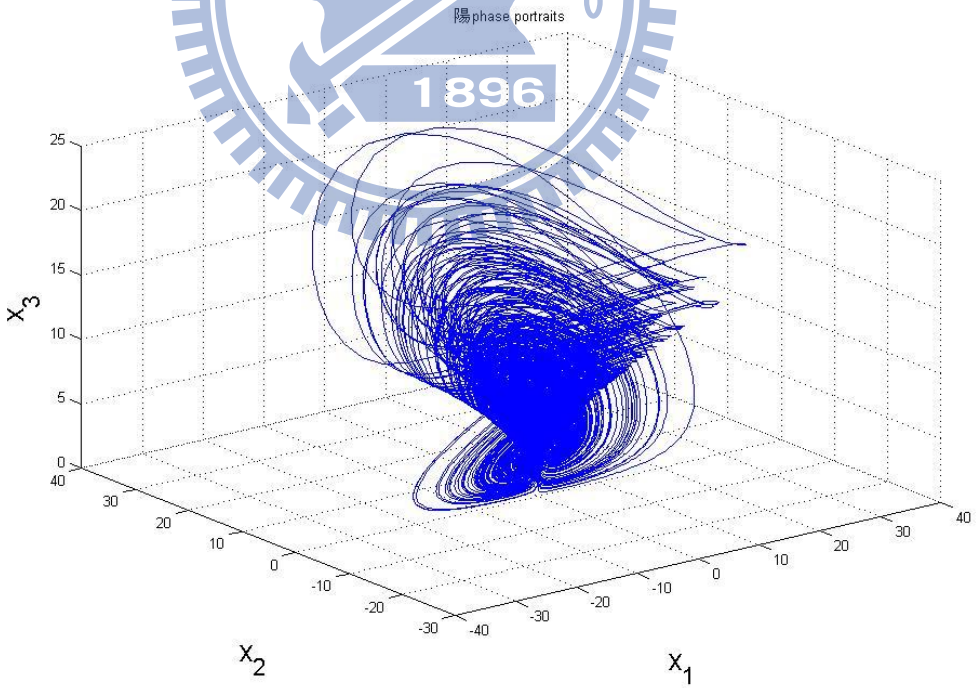

Fig.2.3 3D phase portrait of Yang Chen-Lee chaos with *a*=3.0, *b*=-5.0 and *c*=-1.0.

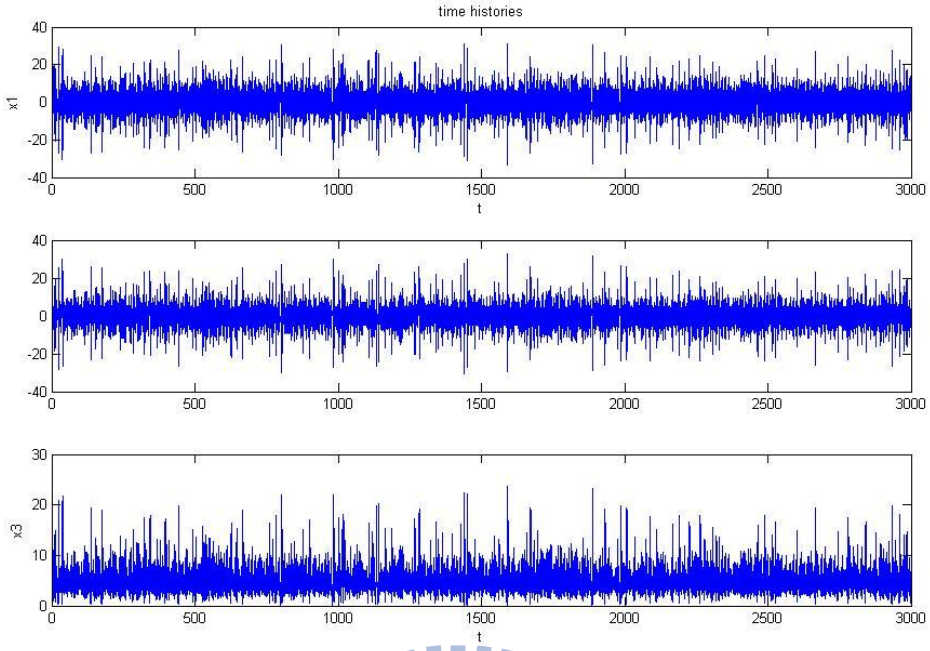

Fig.2.4 Time histories of Yin Chen-Lee chaos for Yin Chen-Lee system with *a*=-3.0, *b*=5.0 and *c*=1.0.

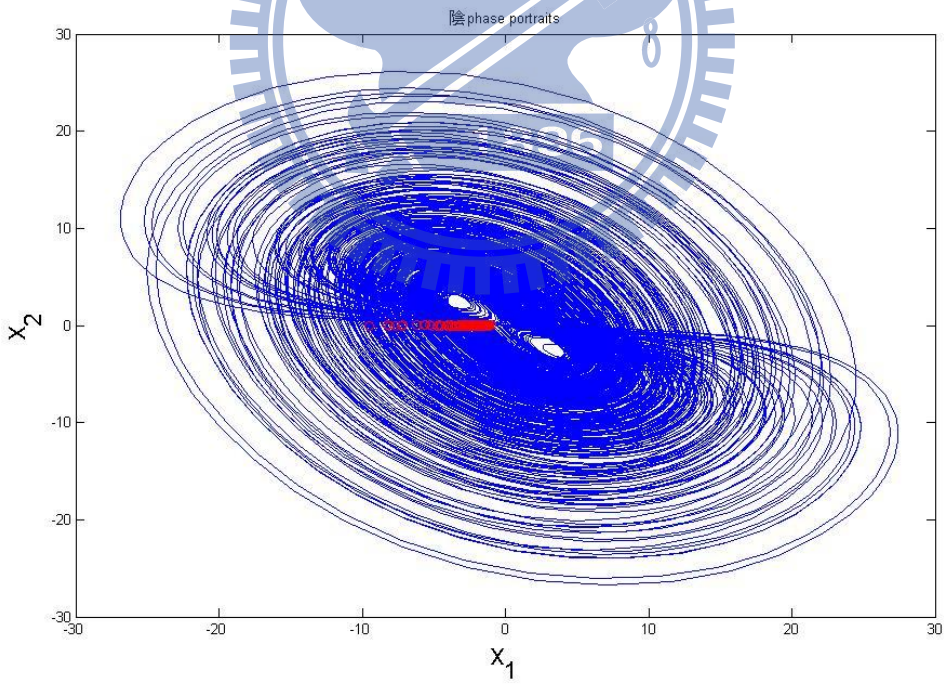

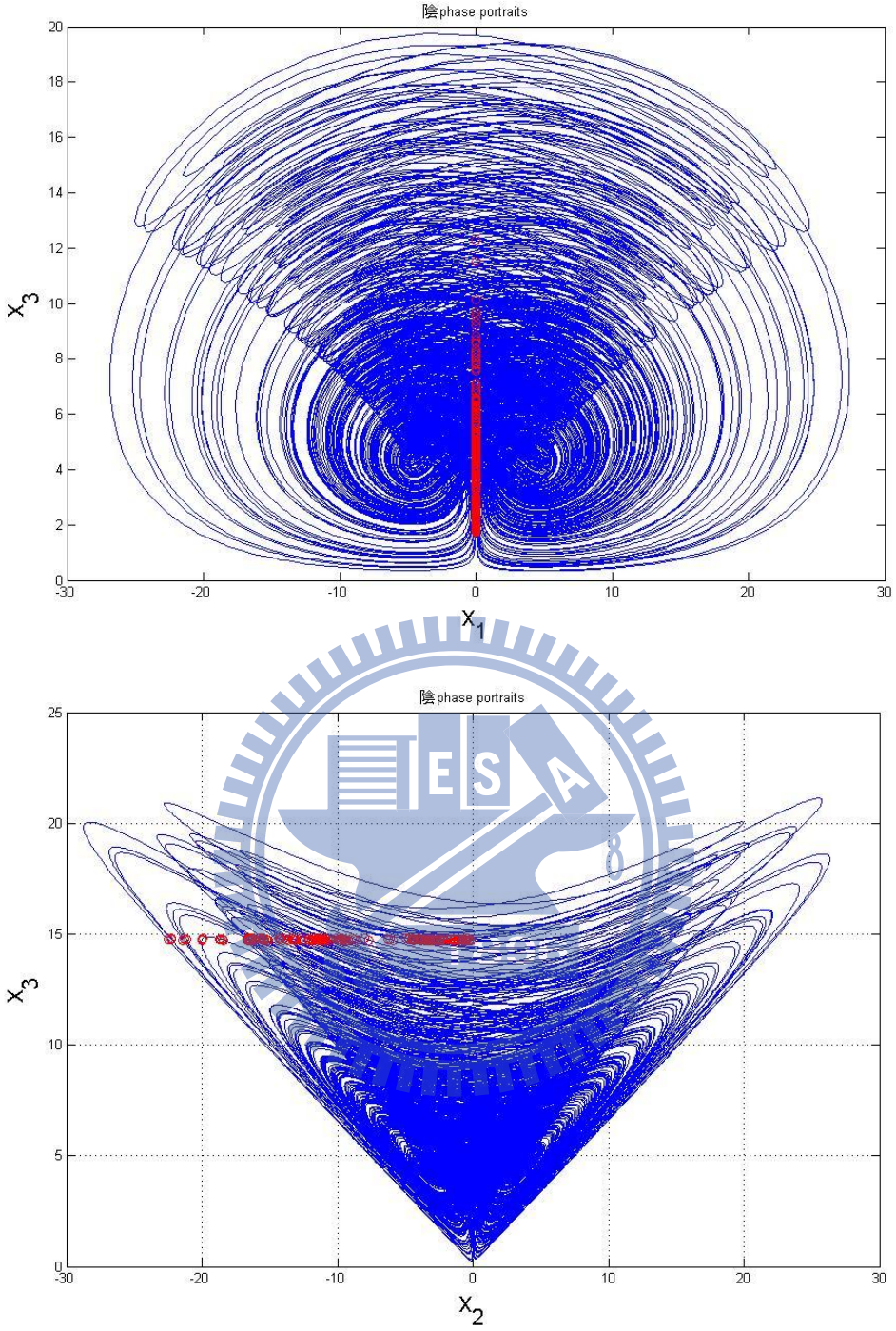

Fig. 2.5 Projections of phase portraits and Poincaré maps of Yin Chen-Lee chaos with a=-3.0, b=5.0 and c=1.0.

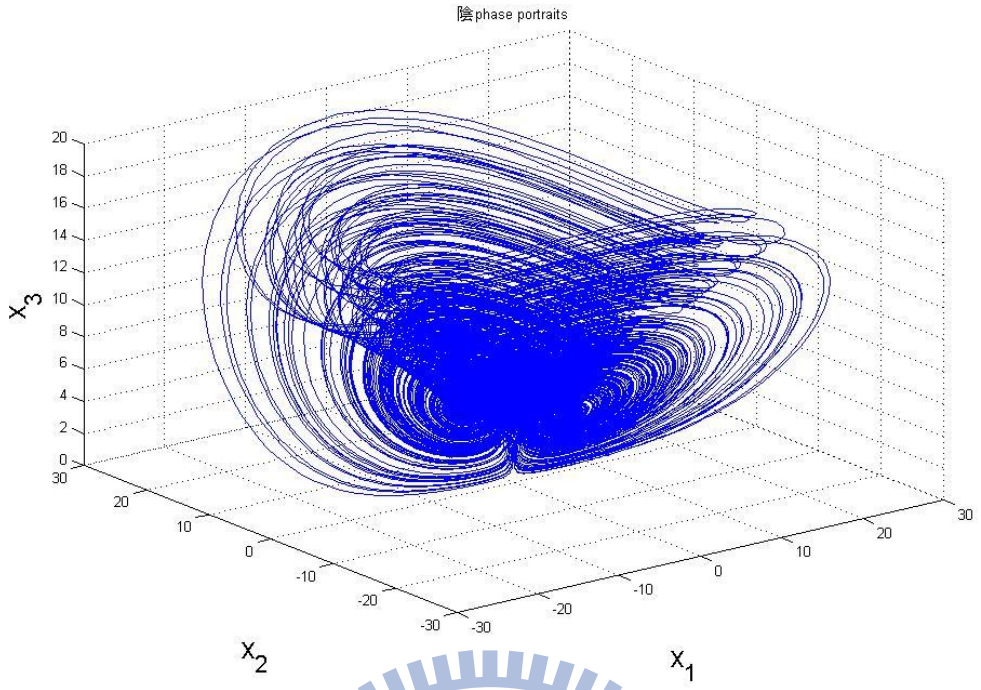

Fig. 2.6 3D phase portrait of Yin Chen-Lee system with *a*=-3.0, *b*=5.0 and *c*=1.0.

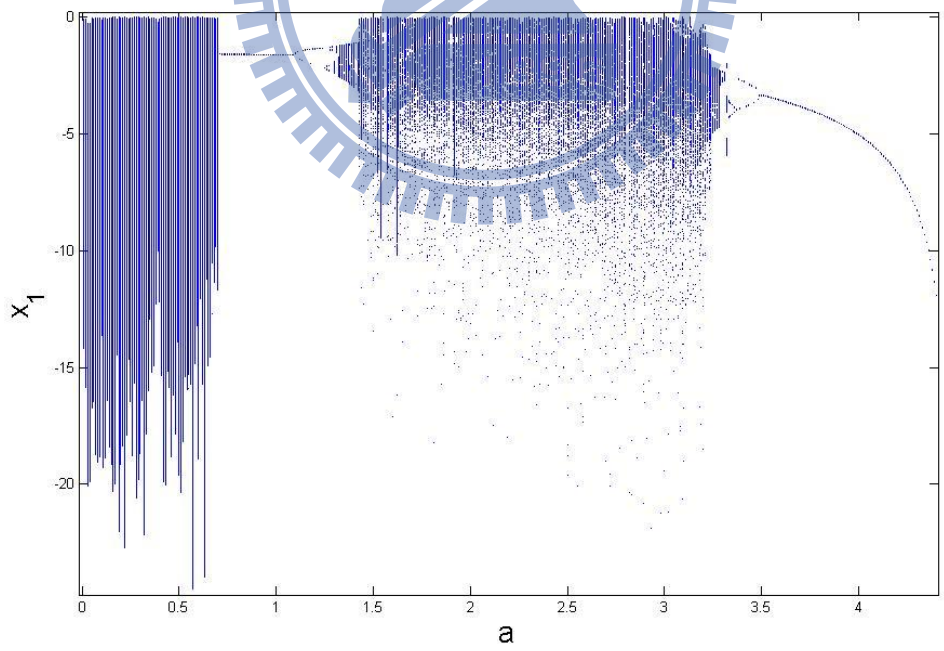

Fig. 2.7 Bifurcation diagram of chaotic Yang Chen-Lee system with *b*=-5.0 and *c*=-1.0.

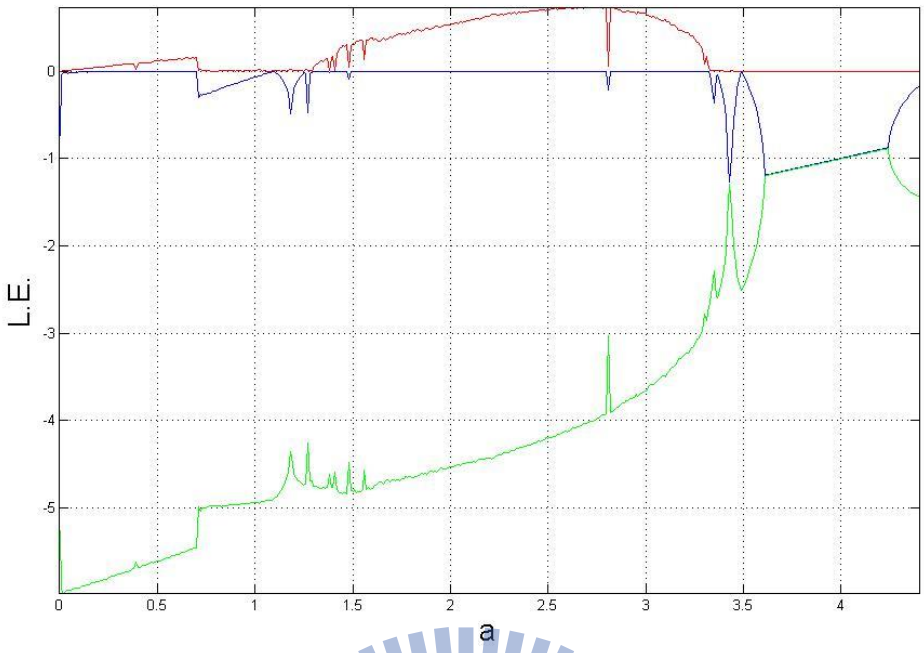

Fig. 2.8 Lyapunov exponents of chaotic Yang Chen-Lee system with *b*=-5.0 and *c*=-1.0.

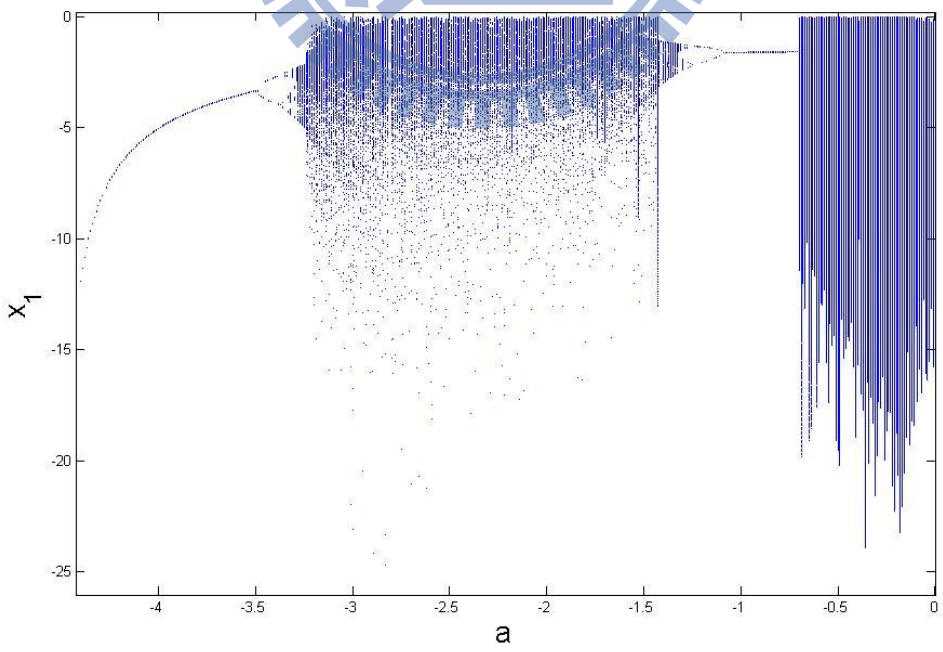

Fig. 2.9 Bifurcation diagram of chaotic Yin Chen-Lee system with *b*=5.0 and *c*=1.0.

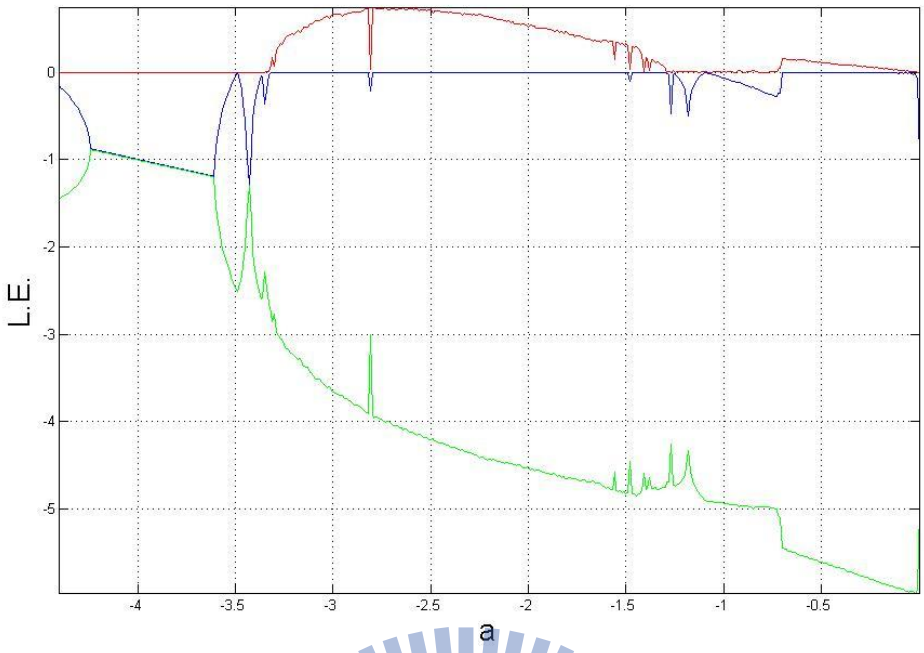

Fig. 2.10 Lyapunov exponents of chaotic Yin Chen-Lee system with *b*=5.0 and *c*=1.0.

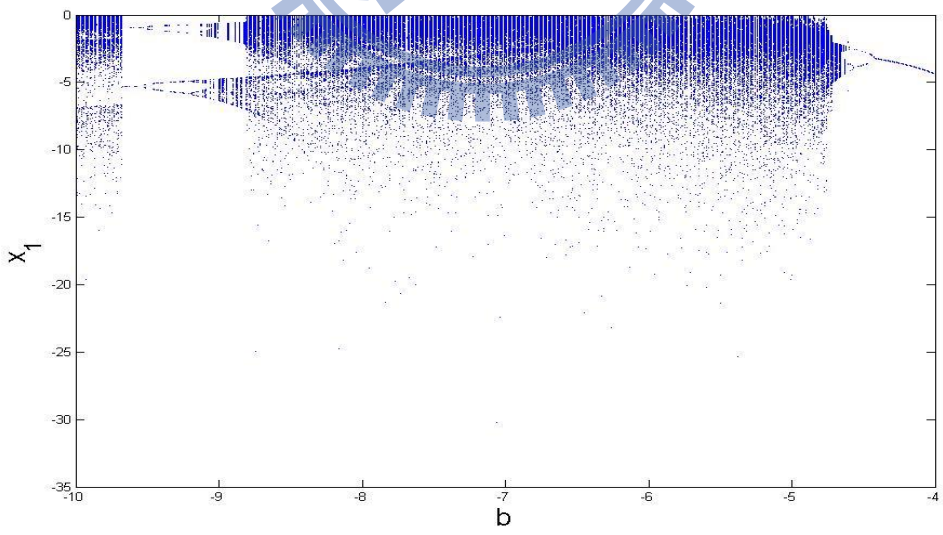

Fig. 2.11 Bifurcation diagram of chaotic Yang Chen-Lee system with *a*=3.0 and *c*=-1.0.

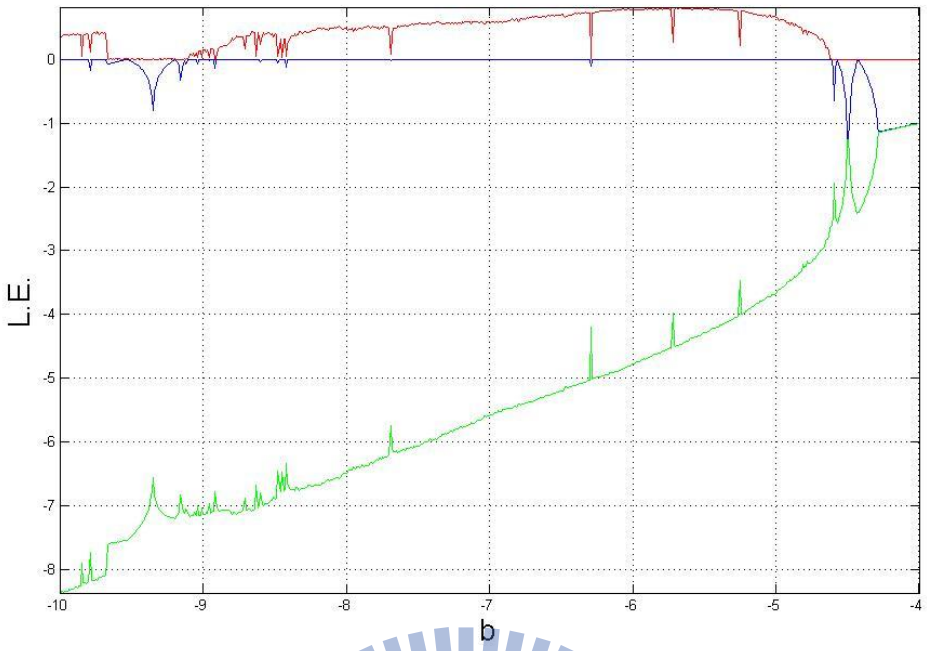

Fig. 2.12 Lyapunov exponents of chaotic Yang Chen-Lee system with *a*=3.0 and *c*=-1.0.

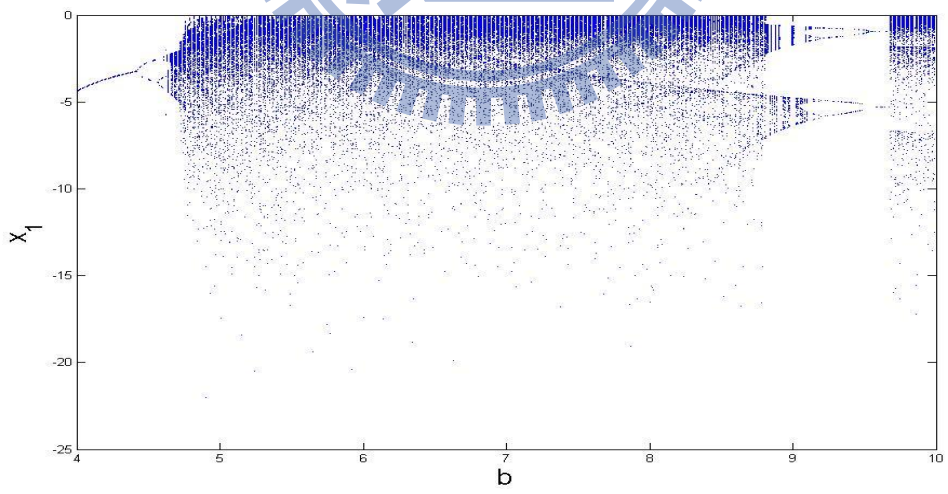

Fig. 2.13 Bifurcation diagram of chaotic Yin Chen-Lee system with *a*=-3.0 and *c*=1.0.

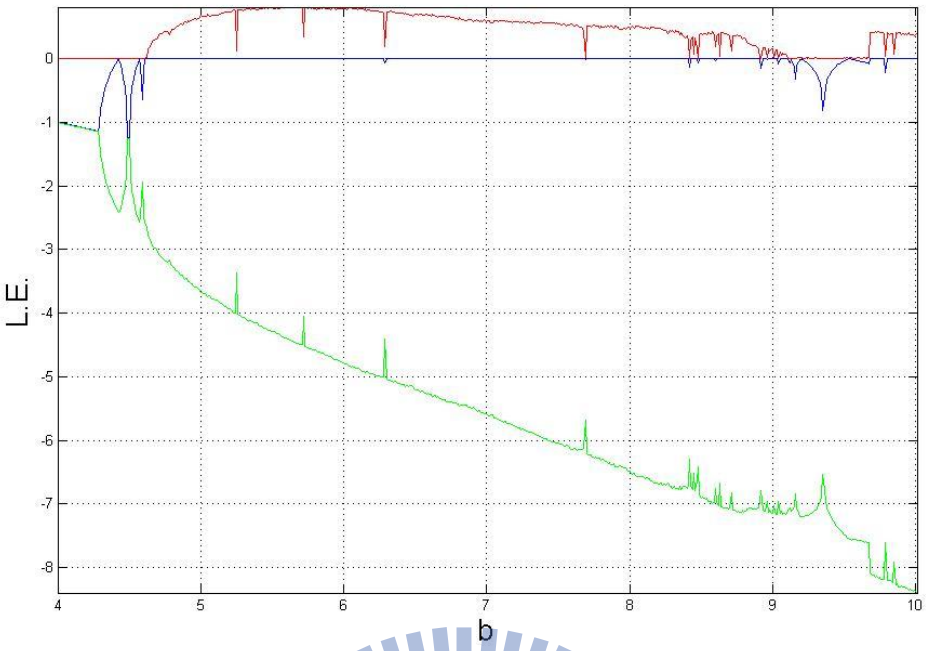

Fig. 2.14 Lyapunov exponents of chaotic Yin Chen-Lee system with *a*=-3.0 and *c*=1.0.

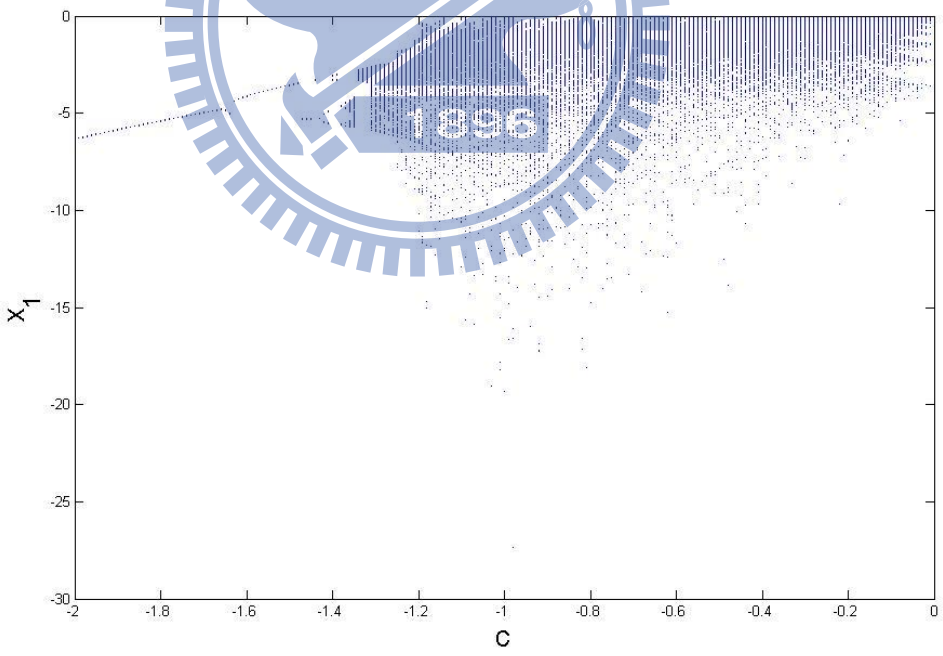

Fig. 2.15 Bifurcation diagram of chaotic Yang Chen-Lee system with *a*=3.0 and *b*=-5.0.

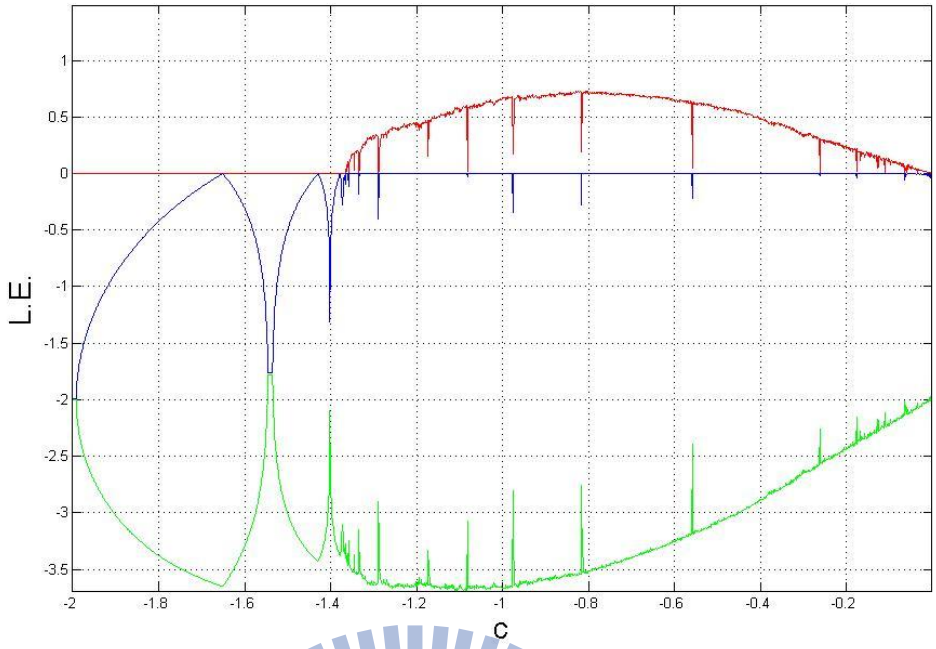

Fig. 2.16 Lyapunov exponents of chaotic Yang Chen-Lee system with *a*=3.0 and *b*=-5.0.

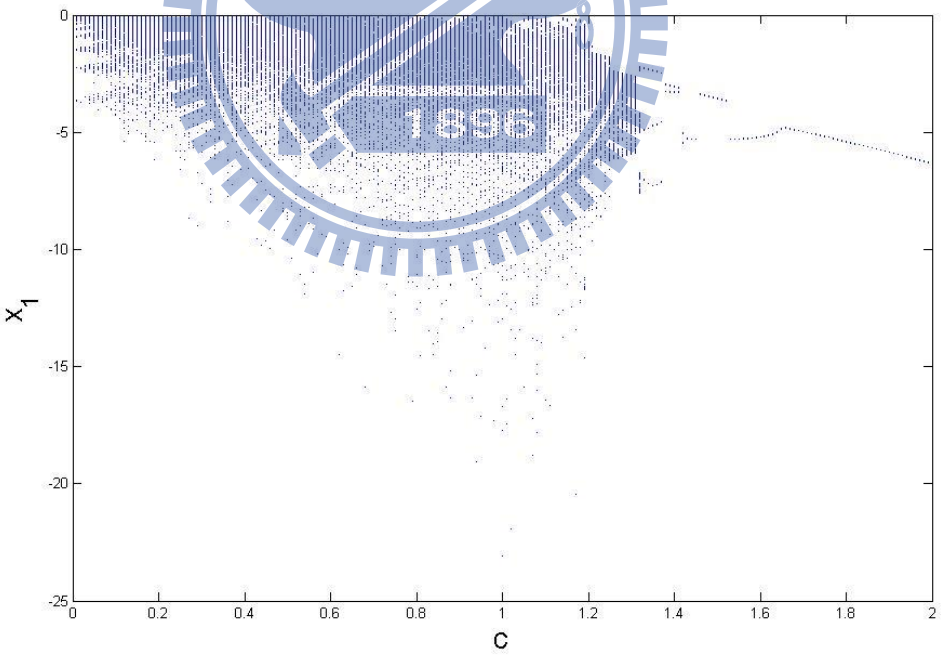

Fig. 2.17 Bifurcation diagram of chaotic Yin Chen-Lee system with *a*=-3.0 and *b*=5.0.

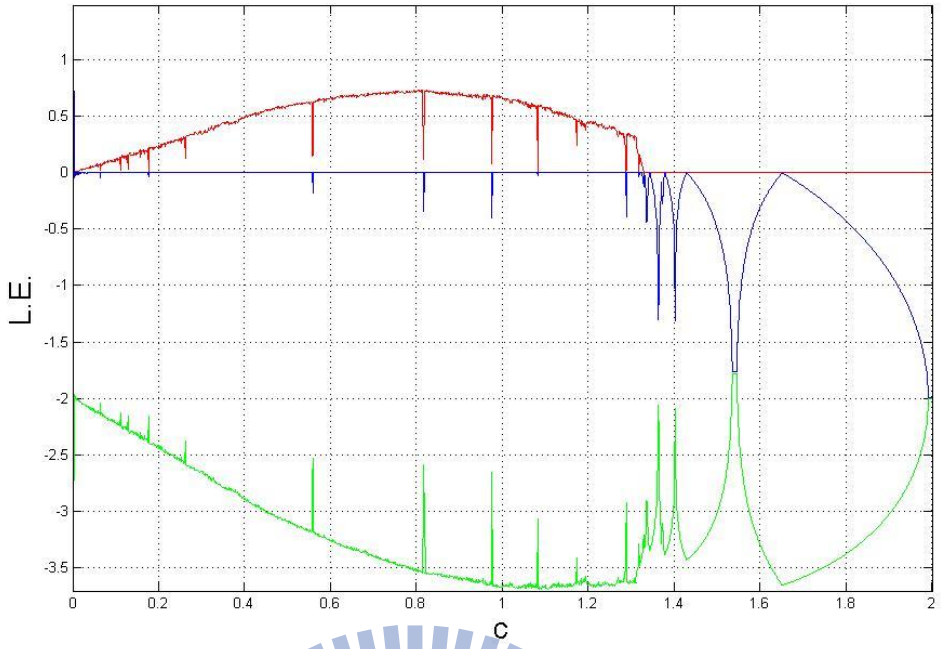

Fig. 2.18 Lyapunov exponents of chaotic Yin Chen-Lee system with *a*=-3.0 and *b*=5.0.

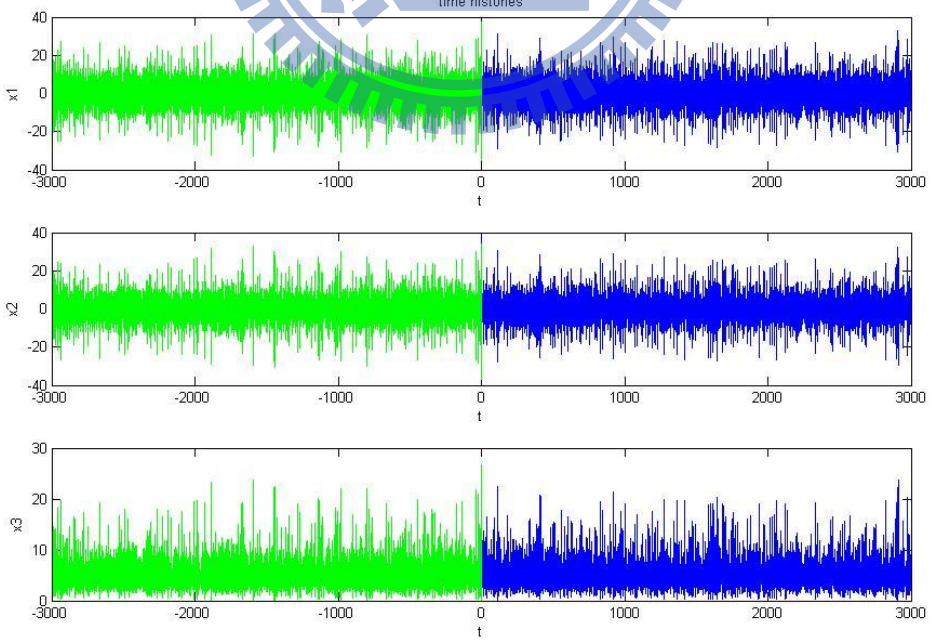

Fig. 2.19 Time histories of Tai Ji Chen-Lee system.

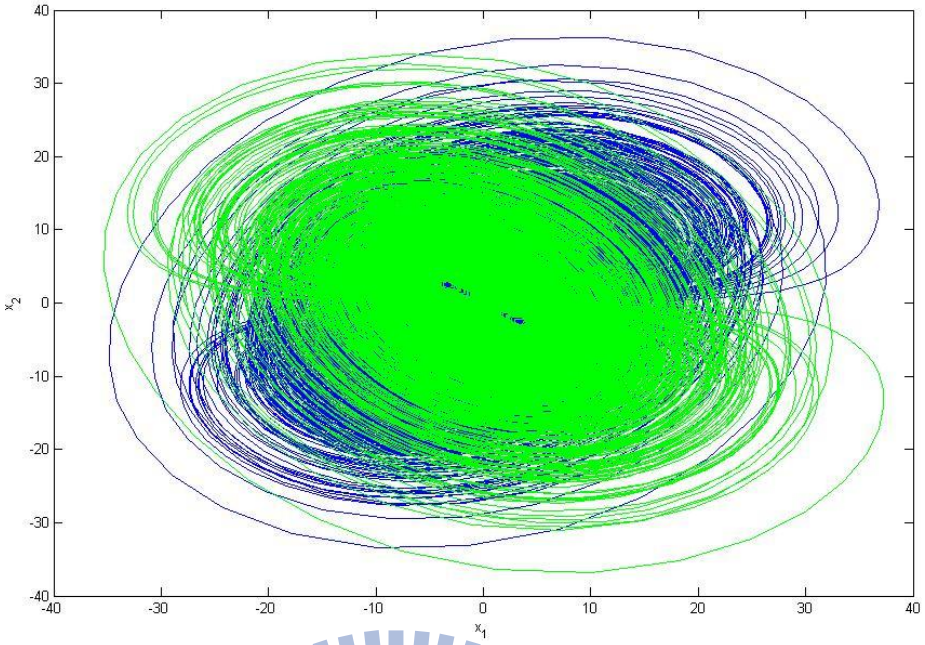
40
30
20
10
0
-10
-20
-30
-40
-40
-30
-20
-10
0
10
20
30
40
x_2
x_1

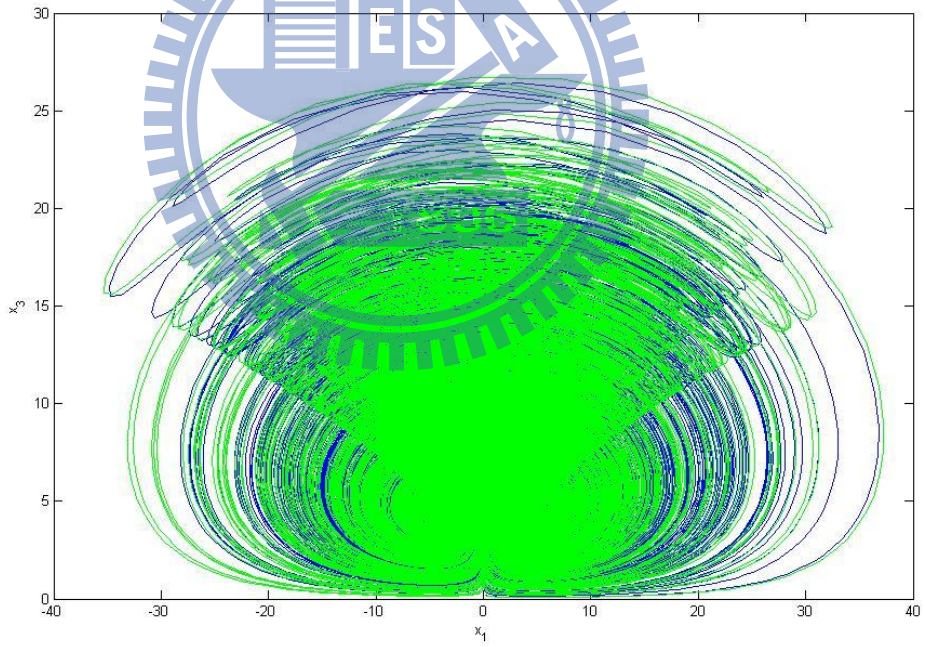
30
25
20
15
10
5
0
-40
-30
-20
-10
0
10
20
30
40
x_3
x_1

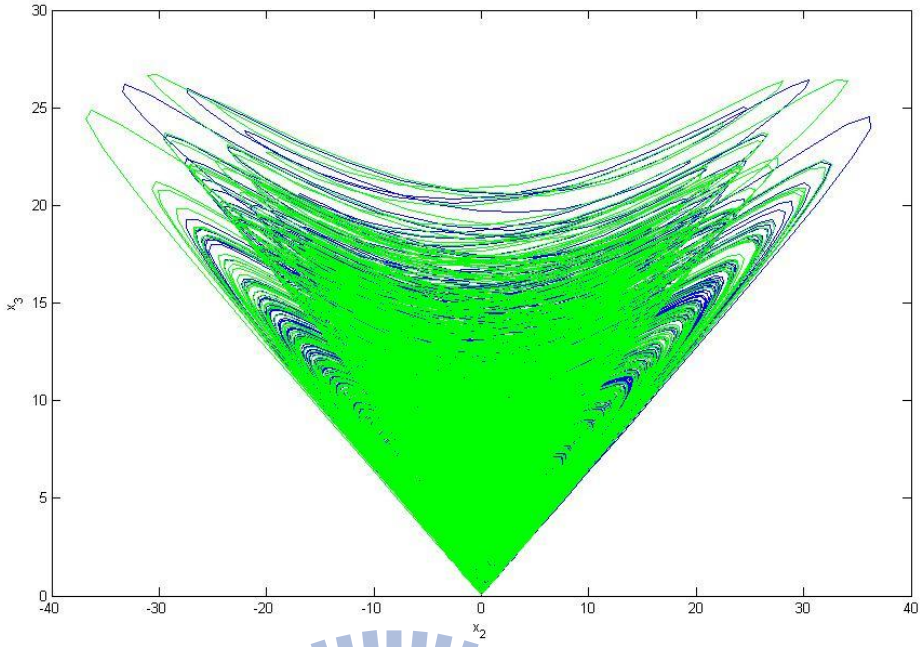

Fig. 2.20 Projections of phase portraits of Tai Ji Chen-Lee system.

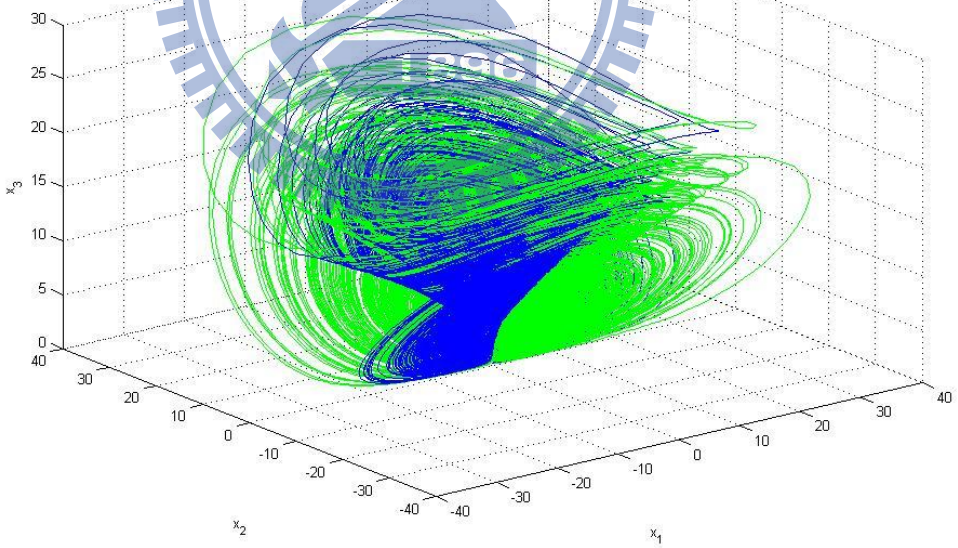

Fig. 2.21 3D phase portrait of Tai Ji Chen-Lee system.

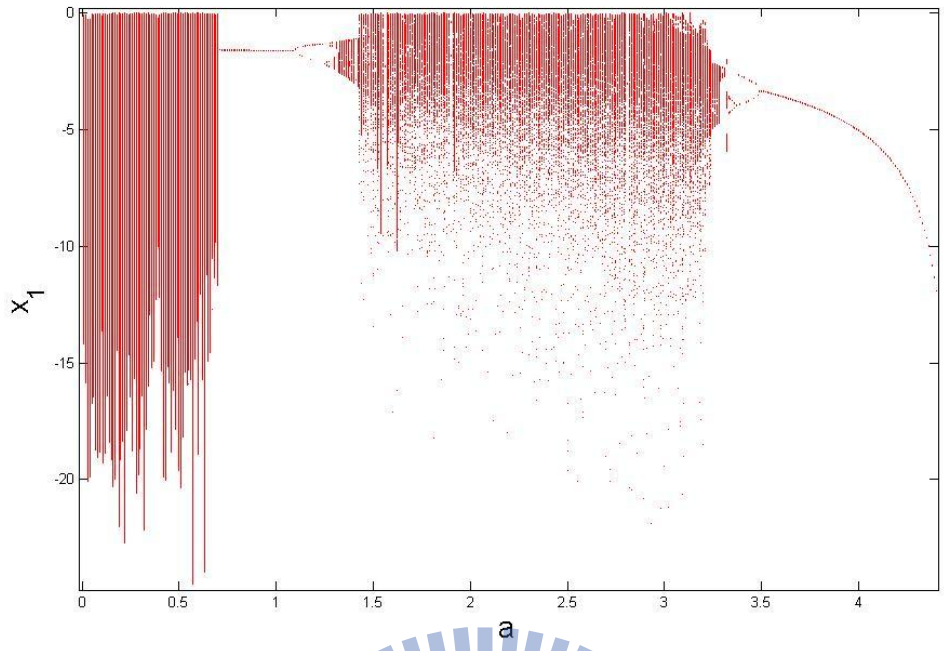

Fig. 2.22 Bifurcation diagram of chaotic Yang Chen-Lee system for varied parameter *a*.

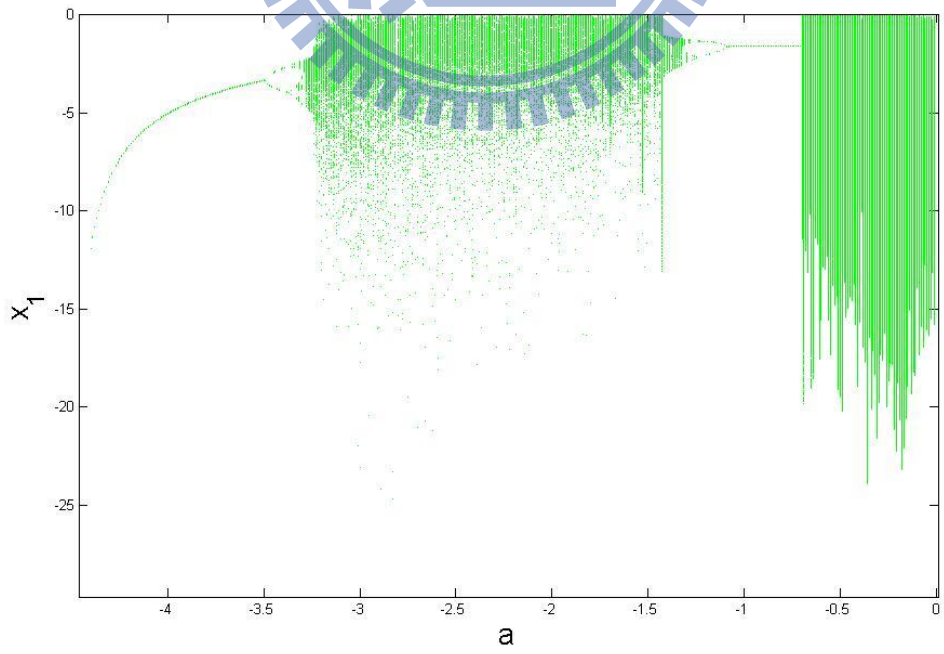

Fig. 2.23 Bifurcation diagram of chaotic Yin Chen-Lee system for varied parameter *a*.

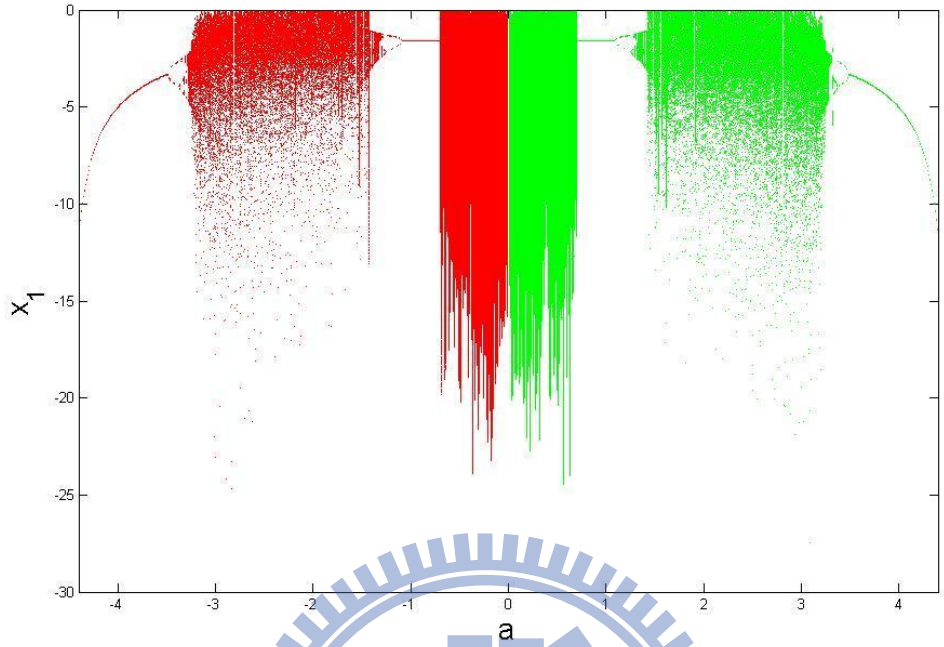

Fig. 2.24 Bifurcation diagram of chaotic Tai Ji Chen-Lee system for varied parameter *a*.

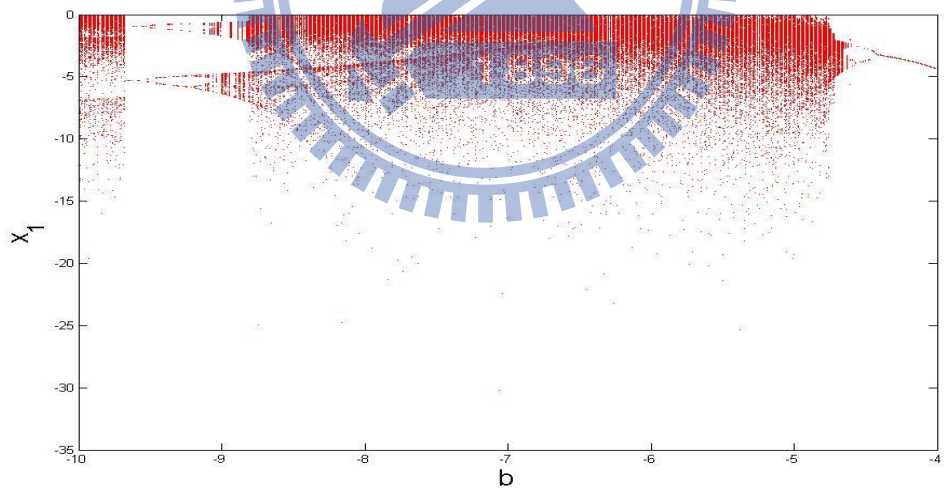

Fig. 2.25 Bifurcation diagram of chaotic Yang Chen-Lee system for varied parameter *b*.

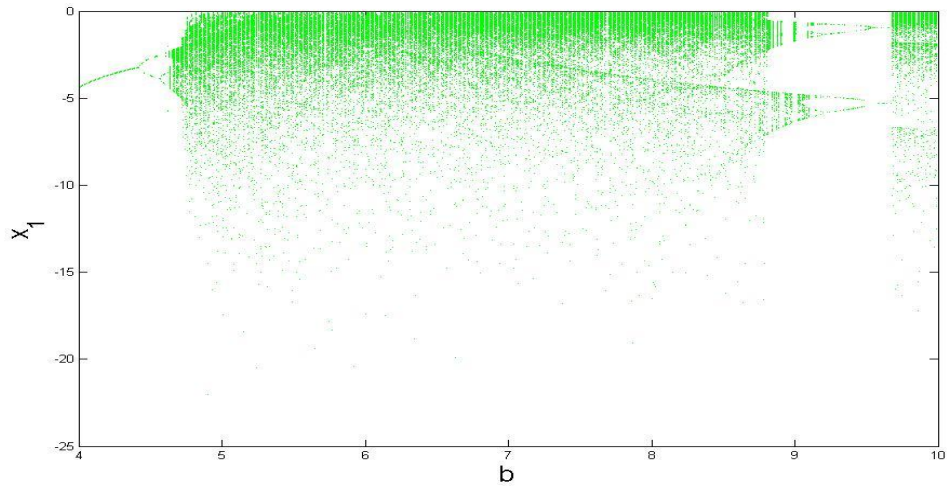

Fig. 2.26 Bifurcation diagram of chaotic Yin Chen-Lee system for varied parameter *b*.

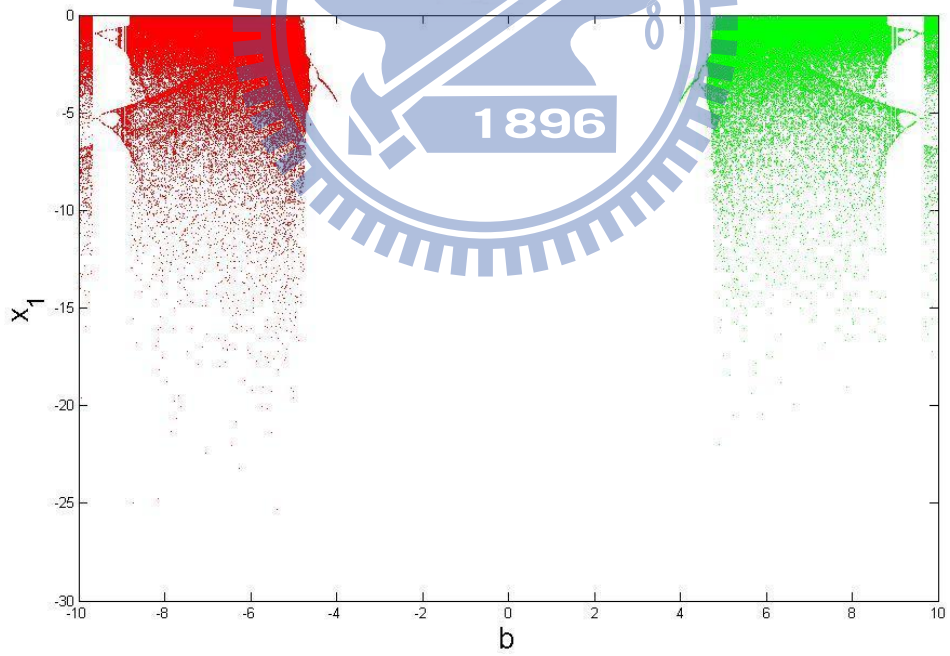

Fig. 2.27 Bifurcation diagram of chaotic Tai Ji Chen-Lee system for varied parameter *b*.

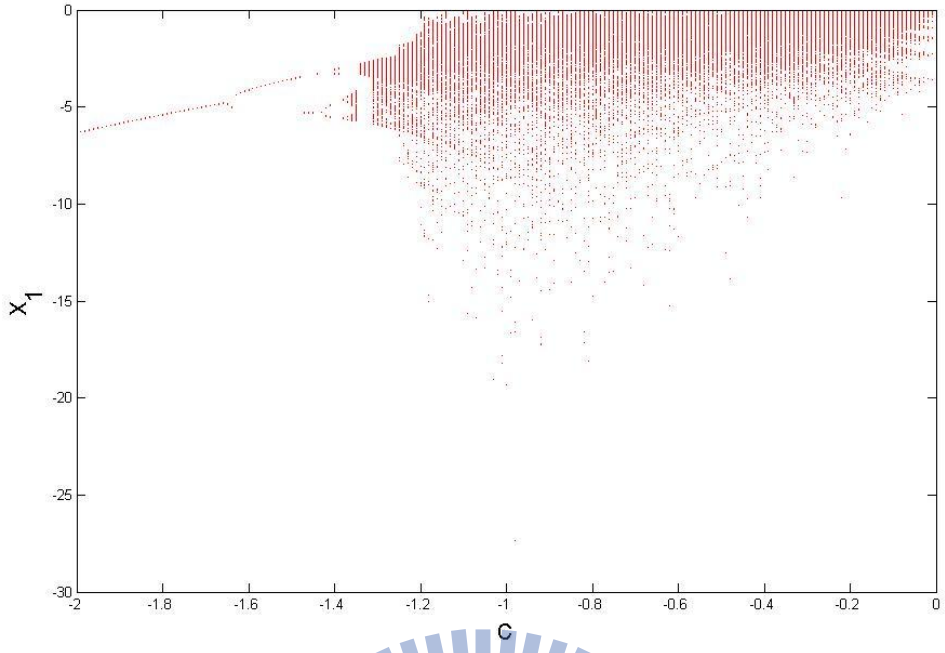

Fig. 2.28 Bifurcation diagram of chaotic Yang Chen-Lee system for varied parameter *c*.

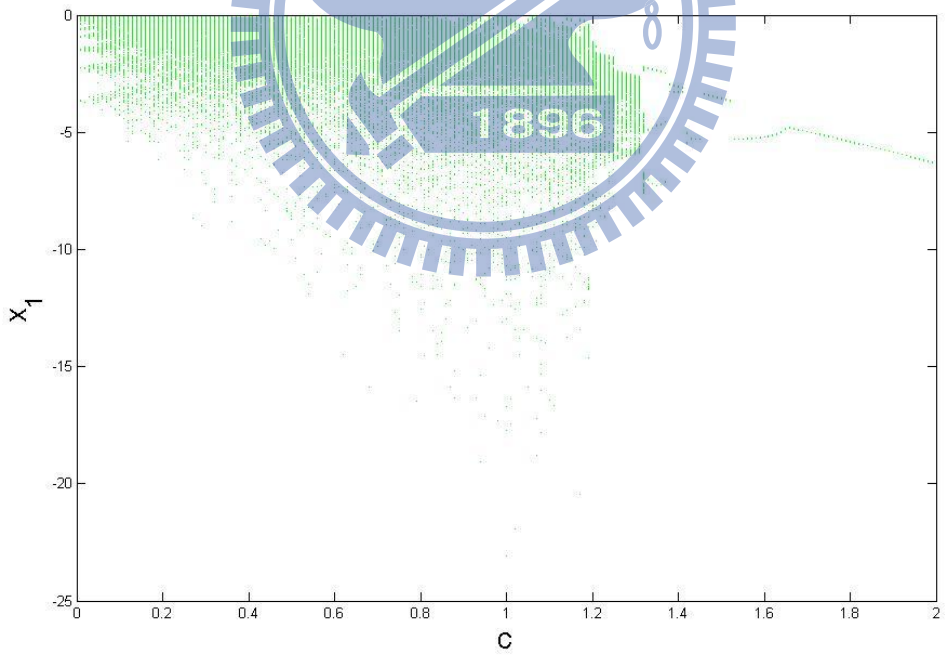

Fig. 2.29 Bifurcation diagram of chaotic Yin Chen-Lee system for varied parameter *c*.

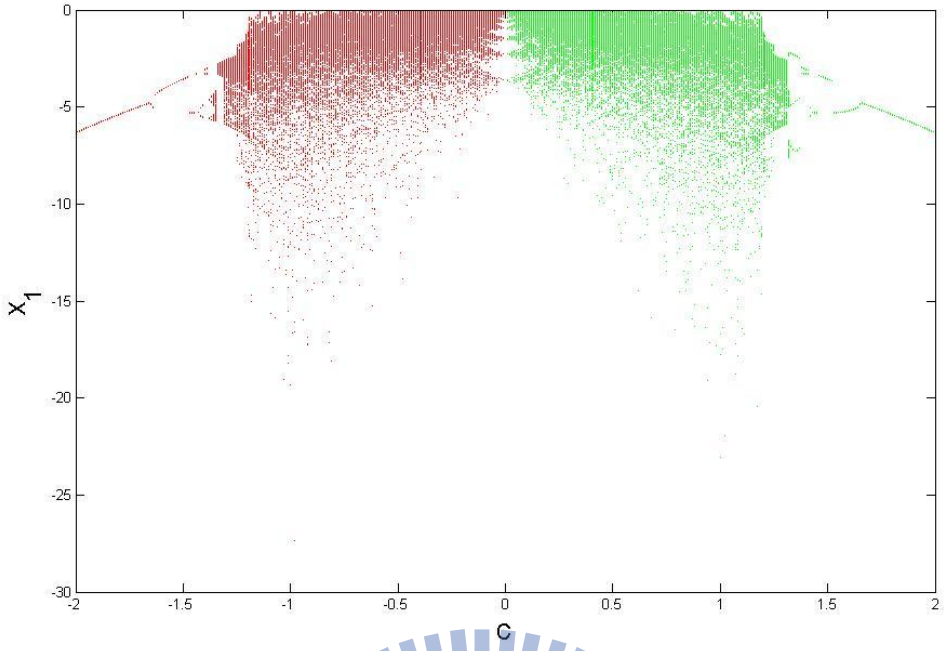

Fig. 2.30 Bifurcation diagram of chaotic Tai Ji Chen-Lee system for varied parameter *c*.

Chapter 3

Multiple Symplectic Derivative Synchronization of Double Ge-Ku - Chen-Lee System with Other Different Systems by Partial Region Stability Theory

3.1 Preliminary

In this research, a new type of synchronization, multiple symplectic derivative synchronization is studied. The symplectic derivative synchronization and double symplectic derivative synchronization are special cases of the multiple symplectic derivative synchronization. There exists a functional relationship between the states of the partners. Numerical simulations are provided to verify the effectiveness of the proposed scheme.

3.2 Strategy of multiple symplectic derivative synchronization

There are two chaotic systems, partner system A and partner system B. The partner A is given by

$$\dot{x} = f(t, x) \tag{3.1}$$

The partner B is given by

$$\dot{y} = g(t, y) \tag{3.2}$$

In order that the error dynamics becomes always positive, the origin of y-coordinate system is translated by a constant positive vector .

Define $e = G - F + K$ as the error state vector, where $G = G(x, y, \cdots, \dot{x}, \dot{y}, \cdots, \ddot{x}, \ddot{y}, \cdots, t)$ and $F = F(x, y, \cdots, \dot{x}, \dot{y}, \cdots, \ddot{x}, \ddot{y}, \cdots, t)$ are two given functions, and K is positive constant vector to keep the error dynamics always in first quadrant.

Then the error vector derivative is obtained:

$$\dot{e}_i = \dot{G}_i - \dot{F}_i - u_i \tag{3.3}$$

where u_i is a component of the control input vector u, $i = 1, 2, \cdots, n$.

The synchronization can be accomplished when $t \to \infty$, the limit of the error vector $e = [e_1, e_2, \cdots, e_n]^T$ approaches to zero:

$$lim_{t\to\infty}\, e = 0 \tag{3.4}$$

3.3 Synchronization by partial region stability theory

Given

$G(x,y,z,\ldots,\dot{x},\dot{y},\dot{z},\ldots\ddot{x},\ddot{y},\ddot{z}\ldots,t)=$

$$\begin{bmatrix} G1 \\ G2 \\ G3 \\ G4 \\ G5 \\ G6 \end{bmatrix} = \begin{bmatrix} x_4 + x_5 - \frac{\dot{x_5}+5x_5+x_1}{x_6} - 3\left(\frac{\dot{x_6}+x_6}{x_4}\right) \\ y_4 + y_5 - \frac{y_6-3y_3-\dot{y_5}}{2} - x_5 - 3.9z_6 \\ -y_3 - \left(\frac{y_5+2y_5-y_6}{3}\right) \\ \dot{y_4} - 2y_6 \\ \ddot{z_6} + \dot{z_4} - 2y_4 + 2y_5 + 2{y_5}^2 \\ z_4 + z_5 + z_6 - 1 + \dot{z_6} - 0.9{z_4}^2 - rz_2 - rz_3 + \dot{z_5} \end{bmatrix} \tag{3.5}$$

$F(x,y,z,\ldots,\dot{x},\dot{y},\dot{z},\ldots\ddot{x},\ddot{y},\ddot{z}\ldots,t)=$

$$F = \begin{bmatrix} F1 \\ F2 \\ F3 \\ F4 \\ F5 \\ F6 \end{bmatrix} = \begin{bmatrix} y_4 + y_5 + y_5^2 - \dot{y_6} \\ \dot{z_4} - y_5 - {y_5}^2 + \dot{y_6} \\ -z_5 - \dot{z_4} + 3.9z_6 \\ \ddot{z_4} + \dot{z_5} + 3.9\dot{z_6} \\ \ddot{y_4} + \ddot{z_6} + z_5 + 3.9z_6 \\ \dot{z_2} - \frac{\dot{z_4}-z_5}{3.9} + z_1 - z_2 \end{bmatrix} \tag{3.6}$$

Six different chaotic systems are used as synchronization examples.

Consider a Double Ge-Ku-Chen-Lee system[13].

$$\begin{cases} \dot{x}_1 = x_2 \\ \dot{x}_2 = -fx_2 - x_1(g(h - {x_1}^2) + kx_3) \\ \dot{x}_3 = -fx_3 - x_3(g(h - {x_3}^2) + lx_1) \\ \dot{x}_4 = -x_5x_6 + 3x_4 \\ \dot{x}_5 = x_4x_6 - 5x_5 + x_1 \\ \dot{x}_6 = (1/3)x_4x_5 - x_6 \end{cases} \tag{3.7}$$

Initial conditions $x_1(0) = 2, x_2(0) = 2.4, x_3(0) = 5, x_4(0) = 0.2, x_5(0) = 0.2$

$x_6(0) = 0.2$, where f=-0.5, g=-1.4, h=1.9, k=-4.5.

The chaotic attractor of the Double Ge-Ku-Chen-Lee system is shown in Figs. 3.1~3.3.

Combining a Sprott N[12] system and Sprott J[12] system by adding $-3y_3$ term in the second equation of Sprott J system,Sprott N-J system is obtained:

$$\begin{cases} \dot{y}_1 = -2y_2 \\ \dot{y}_2 = y_1 + {y_3}^2 \\ \dot{y}_3 = 1 + y_2 - 2y_3 \\ \dot{y}_4 = 2y_6 \\ \dot{y}_5 = -2y_5 + y_6 - 3y_3 \\ \dot{y}_6 = -y_4 + y_5 + {y_5}^2 \end{cases} \tag{3.8}$$

Initial condition is $y_1(0) = 0.3, y_2(0) = 0.3, y_3(0) = 0.3, y_4(0) = 0.3$ $y_5(0) = 0.3, y_6(0) = 0.3$.

The chaotic attractor of the Sprott N-J is show in Figs. 3.4~3.6.

Combining Sprott K[12] system and Sprott L[12] system by adding rz_2, rz_3 two terms in the second equation of sprott L system,Sprott K-L system is obtained:

$$\begin{cases} \dot{z}_1 = z_1 z_2 - z_3 \\ \dot{z}_2 = z_1 - z_2 \\ \dot{z}_3 = z_1 + 0.3z_3 \\ \dot{z}_4 = z_5 + 3.9z_6 \\ \dot{z}_5 = 0.9{z_4}^2 - z_5 + rz_2 + rz_3 \\ \dot{z}_6 = 1 - z_4 \end{cases} \tag{3.9}$$

Initial condition is $z_1(0) = 0.2, z_2(0) = 0.2, z_3(0) = 0.2, z_4(0) = 0.2$ $z_5(0) = 1, z_6(0) = 0.2$ where r=0.041

The chaotic attractor of the Sprott K-L system is shown in Figs. 7~9.

Our goal is to achieve the multiple symplectic derivative synchronization.

Define error function as

$$\boldsymbol{e} = G(x,y,z,\ldots,\dot{x},\ ,\dot{y},\ ,\dot{z},\ldots\ddot{x},\ddot{y},\ddot{z}\ldots,t) - F(x,y,z,\ldots,\dot{x},\ ,\dot{y},\ ,\dot{z},\ldots\ddot{x},\ddot{y},\ddot{z}\ldots,t) + \boldsymbol{K}. \tag{3.10}$$

where $\boldsymbol{K}=[15,10,30,10,20,15]^T$ keep the error dynamics always in first guardant. Our goal is

$$\lim_{t\to\infty} e_i = \lim_{t\to\infty}(G_i - F_i + K_i) = 0, (i = 1,2,3,4,5,6) \tag{3.11}$$

Thus we design the controller as

$$u = \begin{bmatrix} u1 \\ u2 \\ u3 \\ u4 \\ u5 \\ u6 \end{bmatrix} = \begin{bmatrix} e_1 - 2y_6 \\ e_2 + x_2 \\ e_3 - 2y_6 \\ e_4 + z_5 + 3.9z_6 \\ e_5 + y_1 + {y_3}^2 \\ e_6 - 1 + z_4 \end{bmatrix} \tag{3.12}$$

The error dynamics becomes

$$\dot{\boldsymbol{e}} = \dot{\boldsymbol{G}} - \dot{\boldsymbol{F}} - \boldsymbol{u} \tag{3.13}$$

Using partial region stability theory we can choose a Lyapunov function in the form of a positive definite function in first quadrant.

$$V(e) = e_1 + e_2 + e_3 + e_4 + e_5 + e_6 > 0 \tag{3.14}$$

By adding u ,we obtain

$$\dot{V}(e) = -e_1 - e_2 - e_3 - e_4 - e_5 - e_6 < 0 \tag{3.15}$$

which is a negative definite function in first quadrant. The results are shown in Figs. 3.10~3.19.

3.4. Synchronization by traditional method

If the traditional Lyapunov function is used, it means that

$$V(e) = e_1^2 + e_2^2 + e_3^2 + e_4^2 + e_5^2 + e_6^2 \tag{3.16}$$

Its time derivative is

$$\dot{V}(e) = 2(e_1\dot{e}_1 + e_2\dot{e}_2 + e_3\dot{e}_3 + e_4\dot{e}_4 + e_5\dot{e}_5 + e_6\dot{e}_6) \quad (3.17)$$

We want to find *u* in Eq.(3.13) such that

$$\dot{V}(e) = -(e_1^2 + e_2^2 + e_3^2 + e_4^2 + e_5^2 + e_6^2) < 0$$

By traditional method, the controller is designed as

$$u = \begin{bmatrix} u1 \\ u2 \\ u3 \\ u4 \\ u5 \\ u6 \end{bmatrix} = \begin{bmatrix} 0.5e_1 - 2y_6 \\ 0.5e_2 + x_2 \\ 0.5e_3 - 2y_6 \\ 0.5e_4 + z_5 + 3.9z_6 \\ 0.5e_5 + y_1 + {y_3}^2 \\ 0.5e_6 - 1 + z_4 \end{bmatrix} \quad (3.18)$$

Introducing u into Eq.(3.13) where i = 1, 2, ⋯, 6, Eq.(3.17) becomes

$$\dot{V}(e) = -(e_1^2 + e_2^2 + e_3^2 + e_4^2 + e_5^2 + e_6^2)$$

which is a negative definite function in all quadrants. Error states time histories are shown in Figs. 3.20 ~ 3.23.

3.5 Comparison between new strategy and traditional method

From the previous sections, we know that the controllers u of the new strategy and of the traditional method are quite different. Tables and figures for comparing the efficiency of convergence are given as follows. The superioty of new strategy is obvious. The error states of new strategy are much smaller and decay more quickly than that of traditional method.

Table 3.1. Comparison between error data at 60.6~60.70 s after the action of controllers.

e_1		
time	New(10^{-12})	traditional(10^{-5})
60.60	0.9059	0.3960
60.61	0.8971	0.3940
60.62	0.8882	0.3920
60.63	0.8793	0.3901
60.64	0.8704	0.3881
60.65	0.8615	0.3862
60.66	0.8527	0.3843
60.67	0.8438	0.3824
60.68	0.8349	0.3805
60.69	0.8260	0.3786
60.70	0.8171	0.3767

Table3. 2. Comparison between error data at 60.6~60.70 s after the action of controllers.

e_2		
time	New(10^{-12})	traditional(10^{-5})
60.60	0.2824	0.1245
60.61	0.2789	0.1239
60.62	0.2753	0.1233
60.63	0.2718	0.1227
60.64	0.2682	0.1220

60.65	0.2647	0.1214
60.66	0.2629	0.1208
60.67	0.2611	0.1202
60.68	0.2593	0.1196
60.69	0.2576	0.1190
60.70	0.2558	0.1184

.

Table 3.3. Comparison between error data at 60.6~60.70 s after the action of controllers.

	e_3	
time	New(10^{-11})	traditional(10^{-5})
60.60	0.1272	0.5574
60.61	0.1258	0.5546
60.62	0.1243	0.5518
60.63	0.1233	0.5491
60.64	0.1222	0.5463
60.65	0.1211	0.5436
60.66	0.1201	0.5409
60.67	0.1190	0.5382
60.68	0.1180	0.5355
60.69	0.1169	0.5328
60.70	0.1158	0.5302

Table 3.4. Comparison between error data at 60.6~60.70 s after the action of controllers.

e_4		
time	New(10^{-12})	traditional(10^{-5})
60.60	0.7390	0.3227
60.61	0.7319	0.3211
60.62	0.7248	0.3195
60.63	0.7176	0.3179
60.64	0.7105	0.3163
60.65	0.7034	0.3148
60.66	0.6963	0.3132
60.67	0.6892	0.3116
60.68	0.6821	0.3101
60.69	0.6750	0.3085
60.70	0.6679	0.3070

Table 3.5. Comparison between error data at 60.6~60.70 s after the action of controllers.

e_5		
time	New(10^{-11})	traditional(10^{-5})
60.60	0.1304	0.5700
60.61	0.1290	0.5672
60.62	0.1275	0.5643
60.63	0.1261	0.5615
60.64	0.1247	0.5587

60.65	0.1236	0.5559
60.66	0.1226	0.5532
60.67	0.1215	0.5504
60.68	0.1204	0.5477
60.69	0.1194	0.5449
60.70	0.1183	0.5422

Table 3.6. Comparison between error data at 60.6~60.70 s after the action of controllers.

	e_6	
time	New(10^{-12})	traditional(10^{-5})
60.60	0.9948	0.4366
60.61	0.9841	0.4344
60.62	0.9734	0.4323
60.63	0.9646	0.4301
60.64	0.9557	0.4280
60.65	0.9468	0.4258
60.66	0.9379	0.4237
60.67	0.9290	0.4216
60.68	0.9202	0.4195
60.69	0.9113	0.4174
60.70	0.9024	0.4153

.

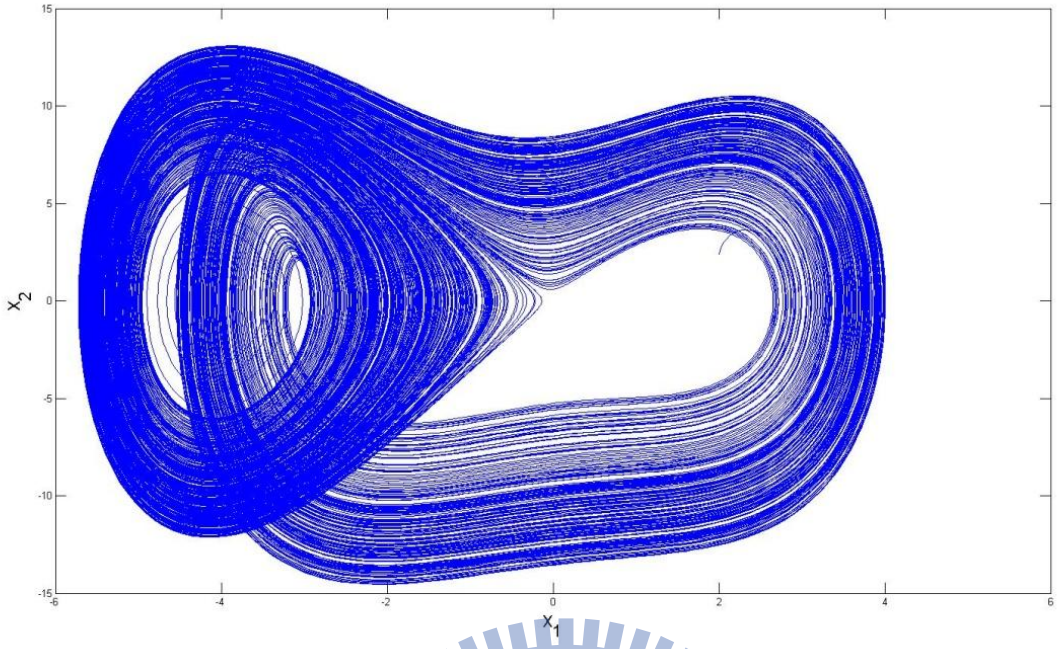

Fig.3.1 Phase portrait of the Double Ge-Ku-Chen-Lee system.

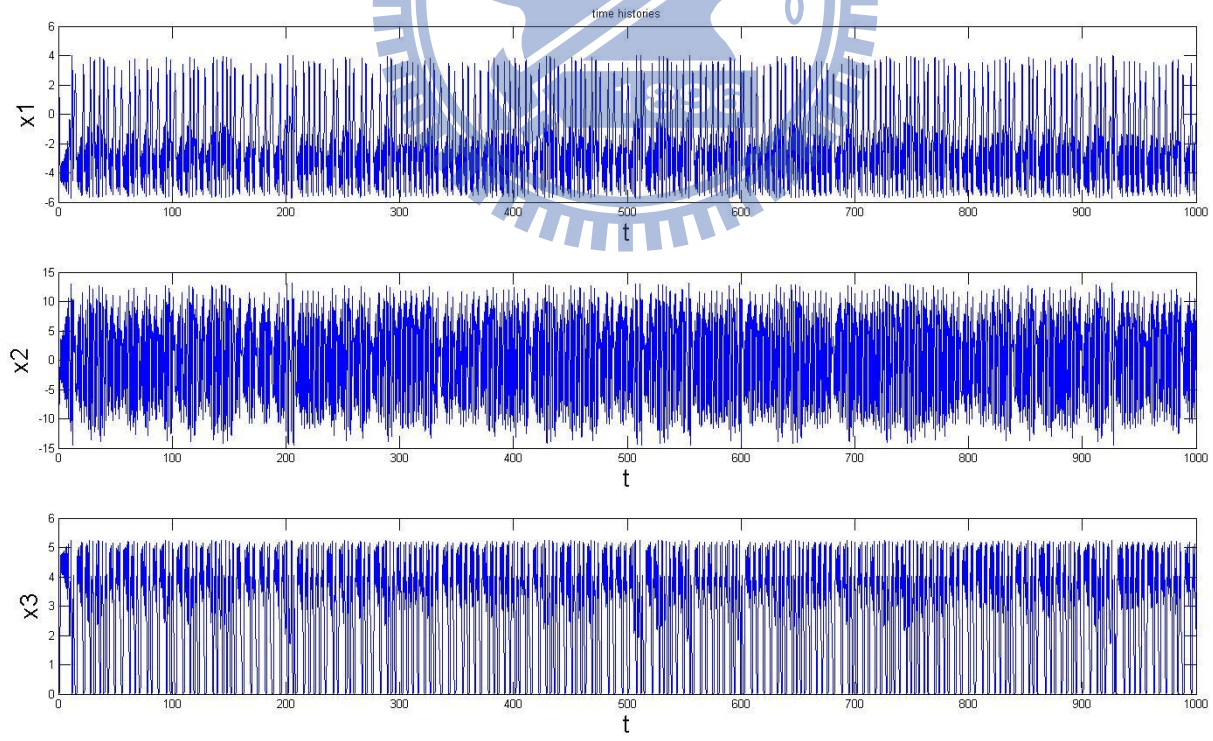

Fig.3.2 Time histories of the Double Ge-Ku-Chen-Lee system.

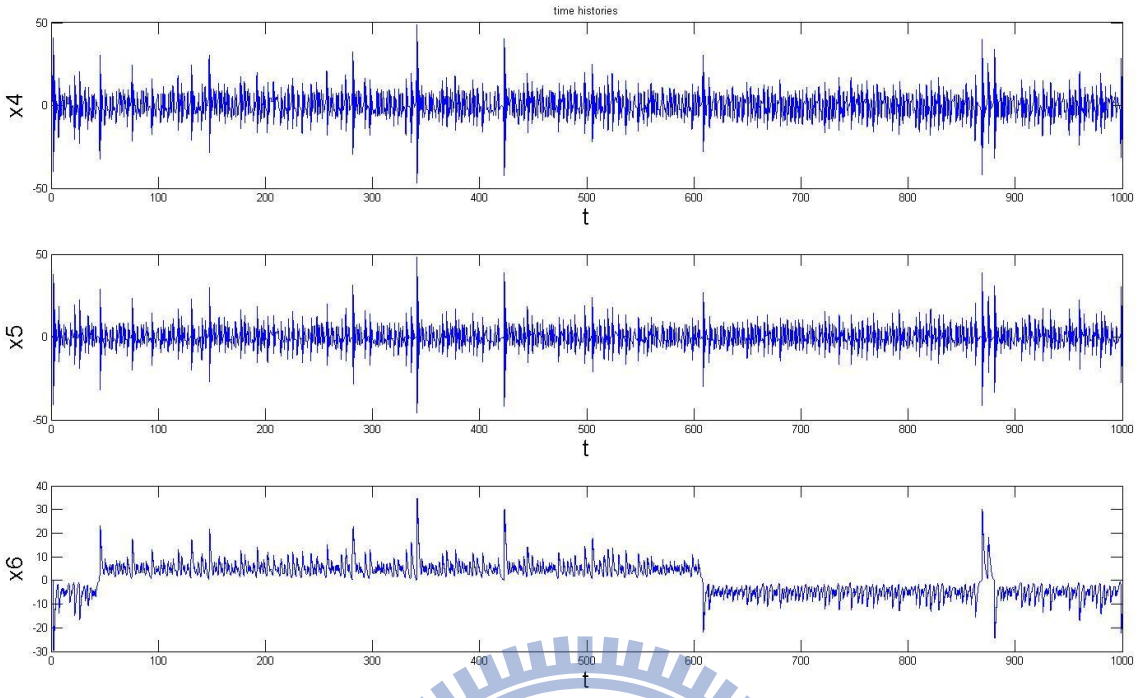

Fig.3.3 Time histories of the Double Ge-Ku-Chen-Lee system.

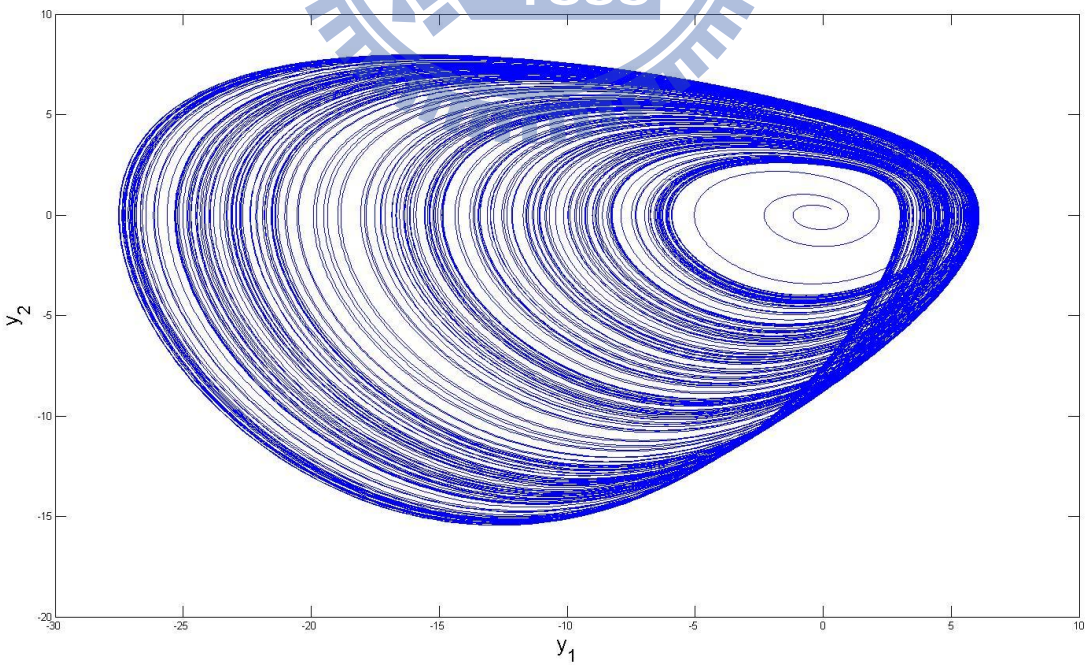

Fig.3.4 Phase portrait of the Sprott N-J system.

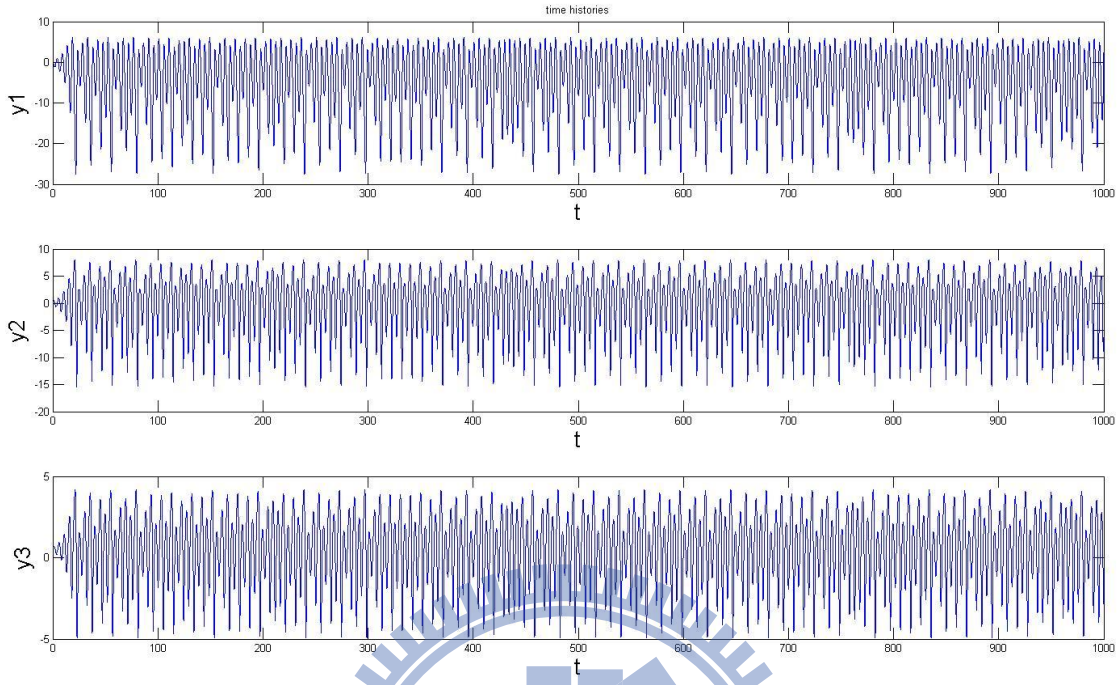

Fig.3.5 Time histories of the Sprott N-J system.

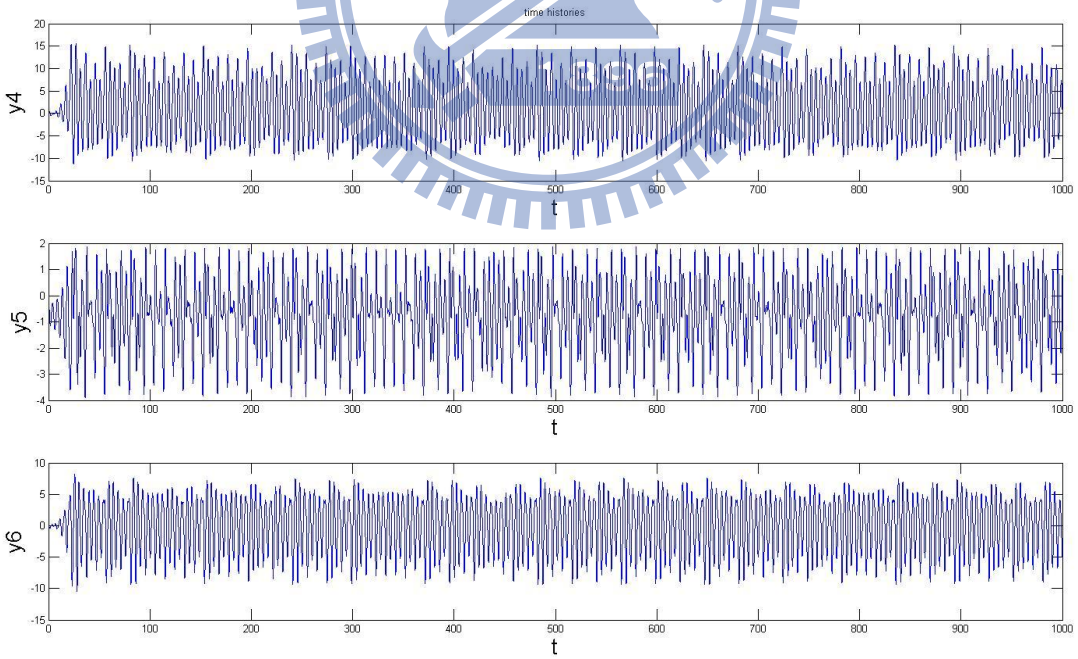

Fig.3.6 Time histories of the Sprott N-J system.

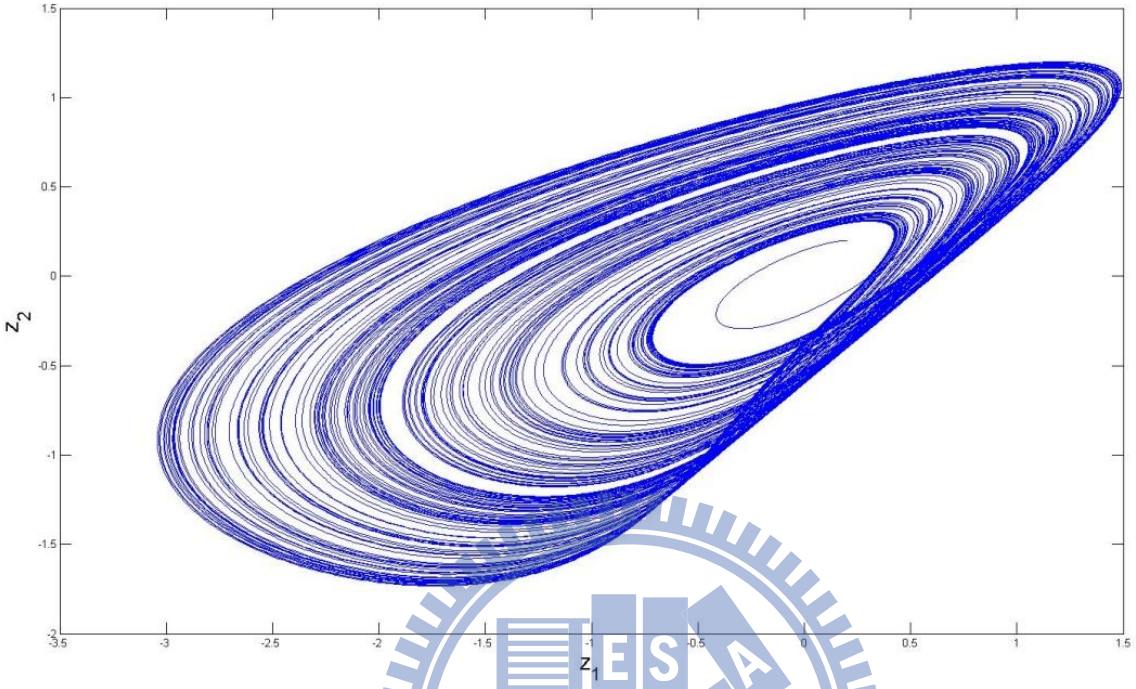

Fig.3.7 Phase portrait of the Sprott K-L system.

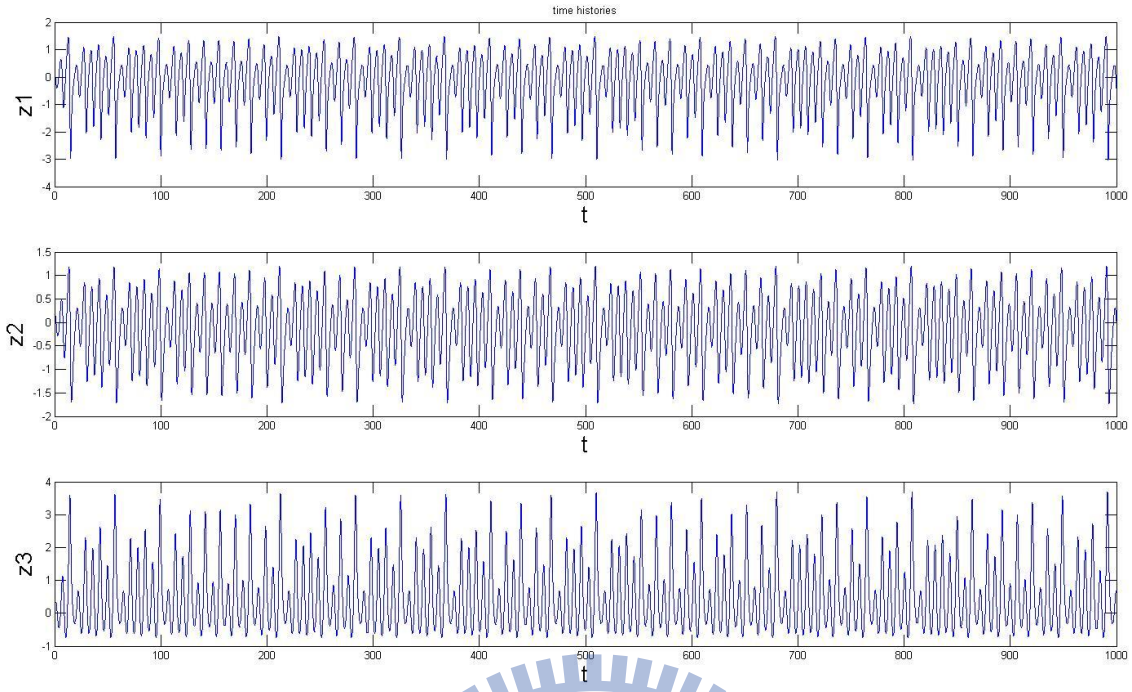

Fig.3.8 Time histories of the Sprott K-L system.

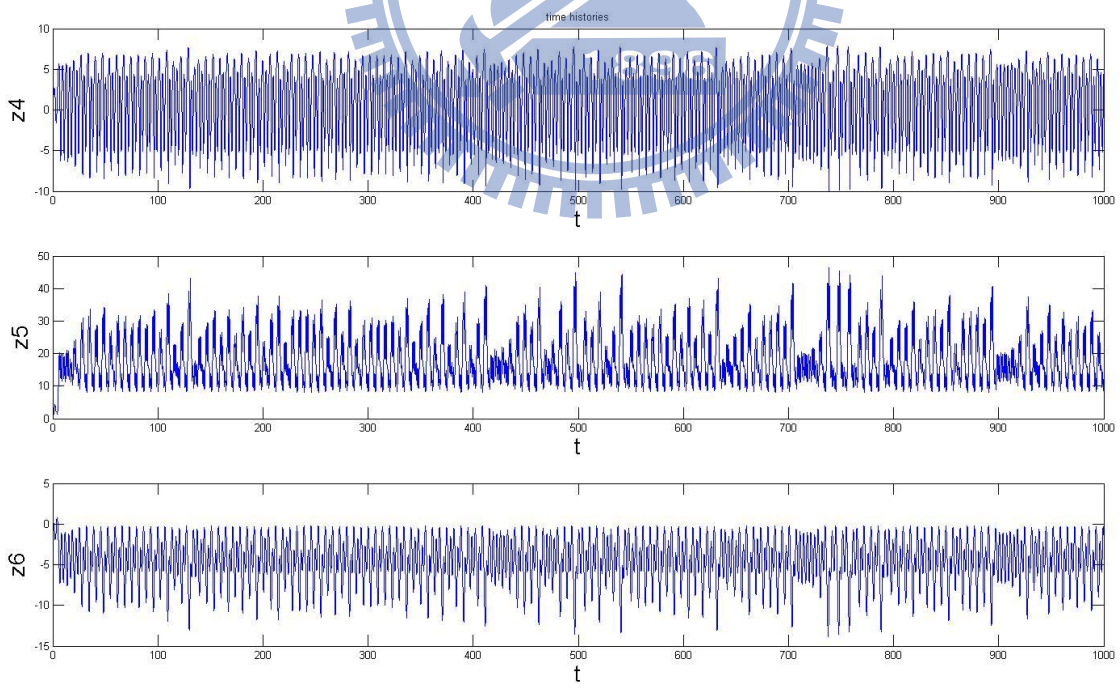

Fig.3.9 Time histories of the Sprott K-L system

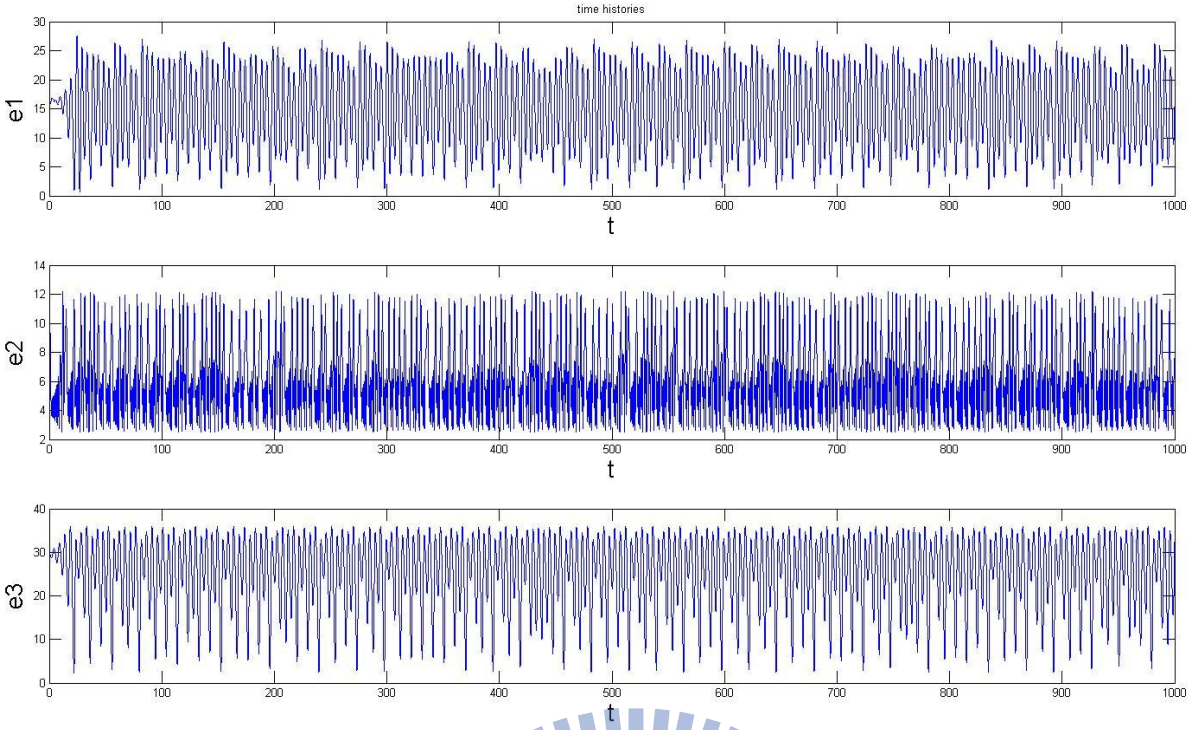

Fig. 3.10 Time histories of e_1, e_2, e_3 before control.

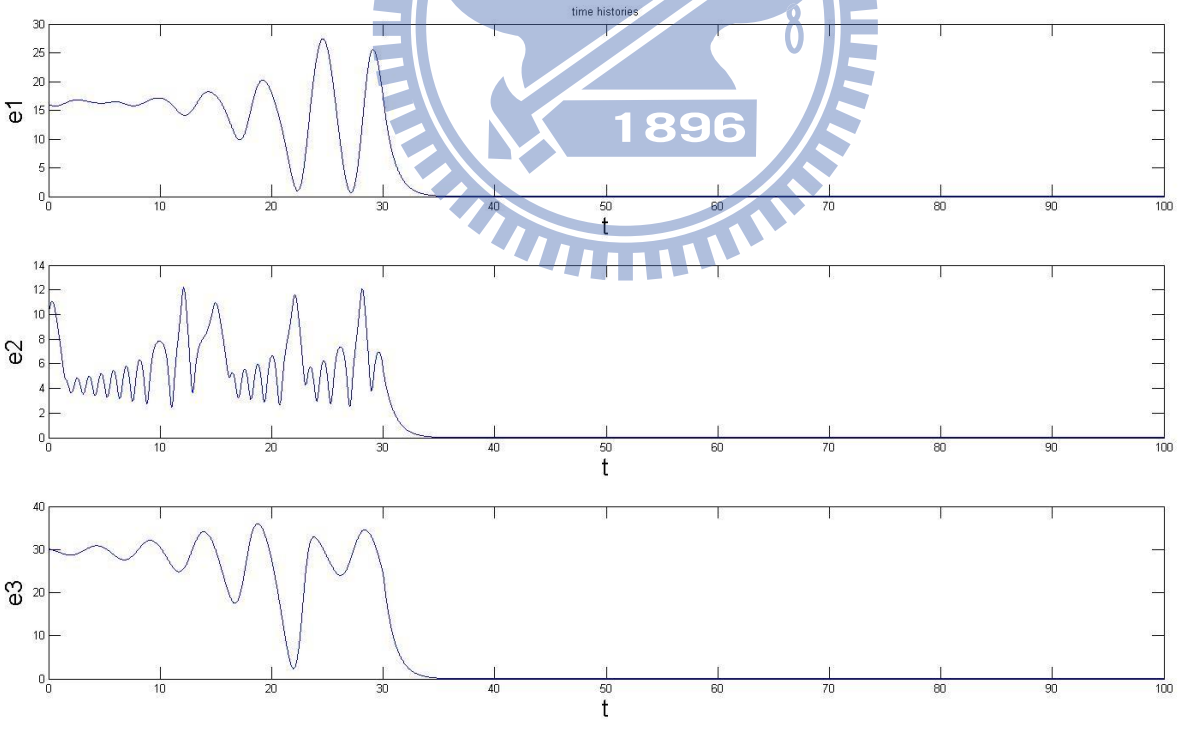

Fig. 3.11 Time histories of e_1, e_2, e_3 before and after control.

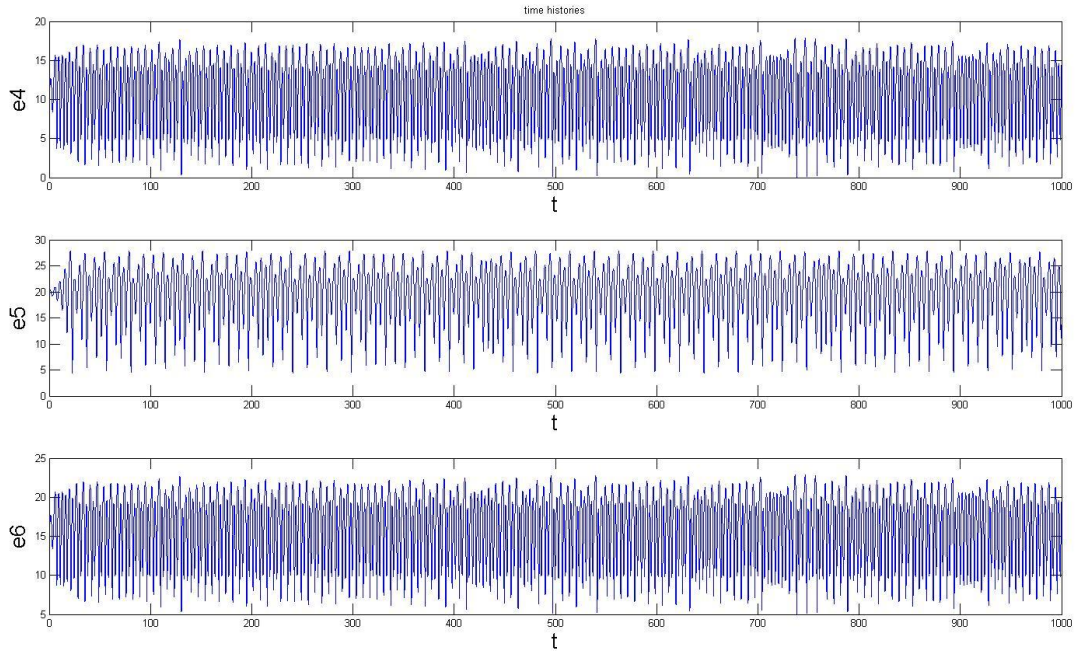

Fig. 3.12 Time histories of e_4,e_5,e_6 before control.

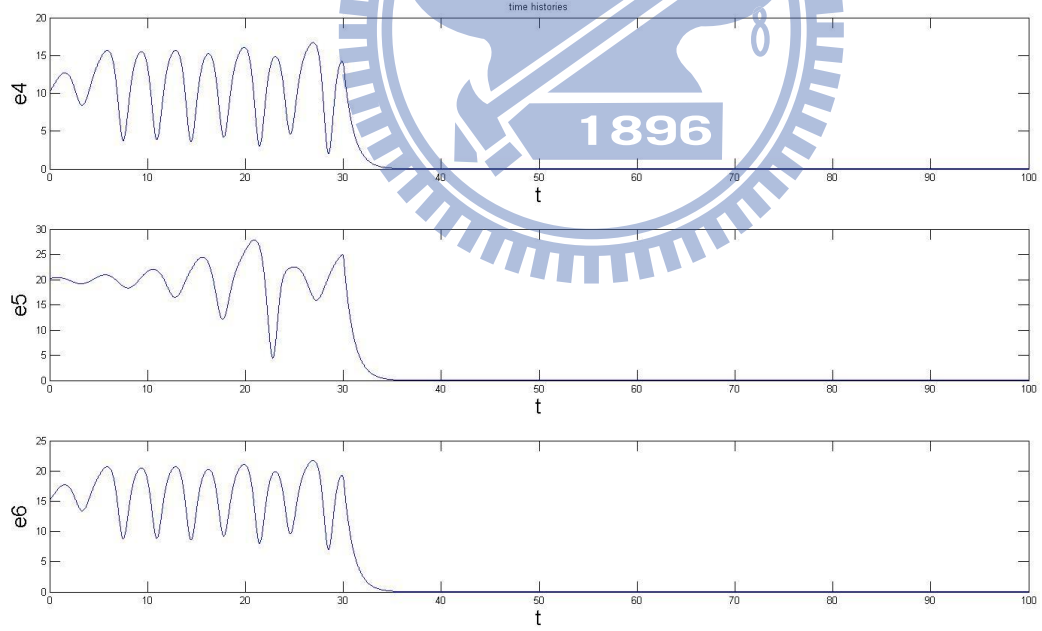

Fig. 3.13 Time histories of e_4,e_5,e_6 before and after control.

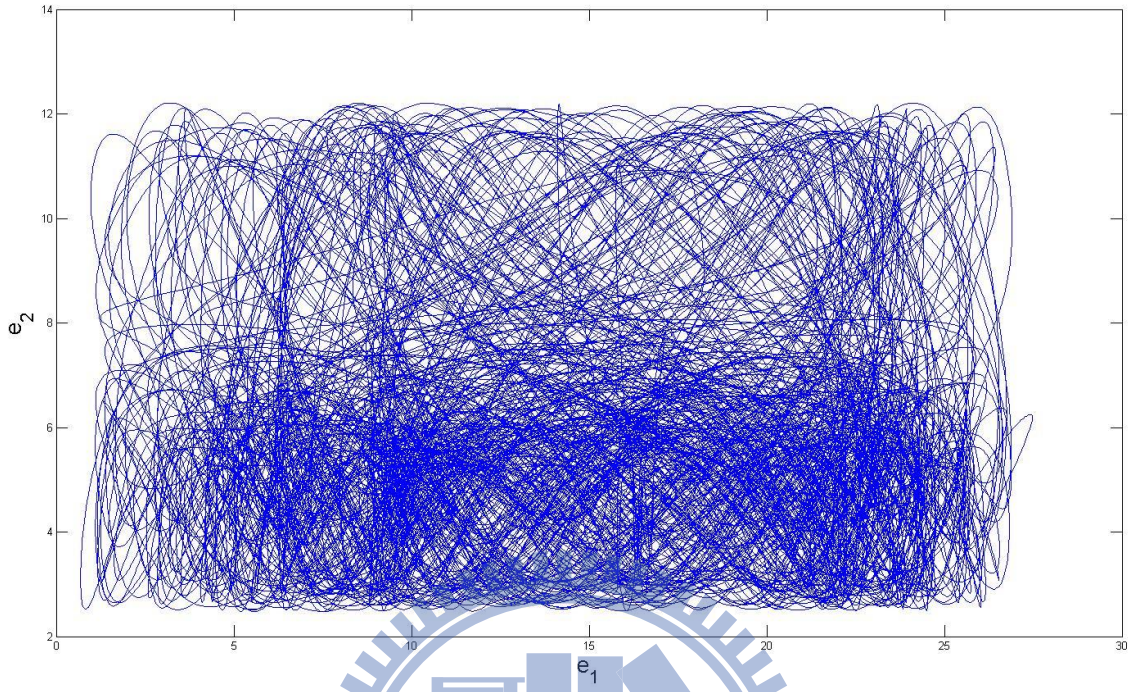

Fig. 3.14 Phase portrait of e_1, e_2 before control.

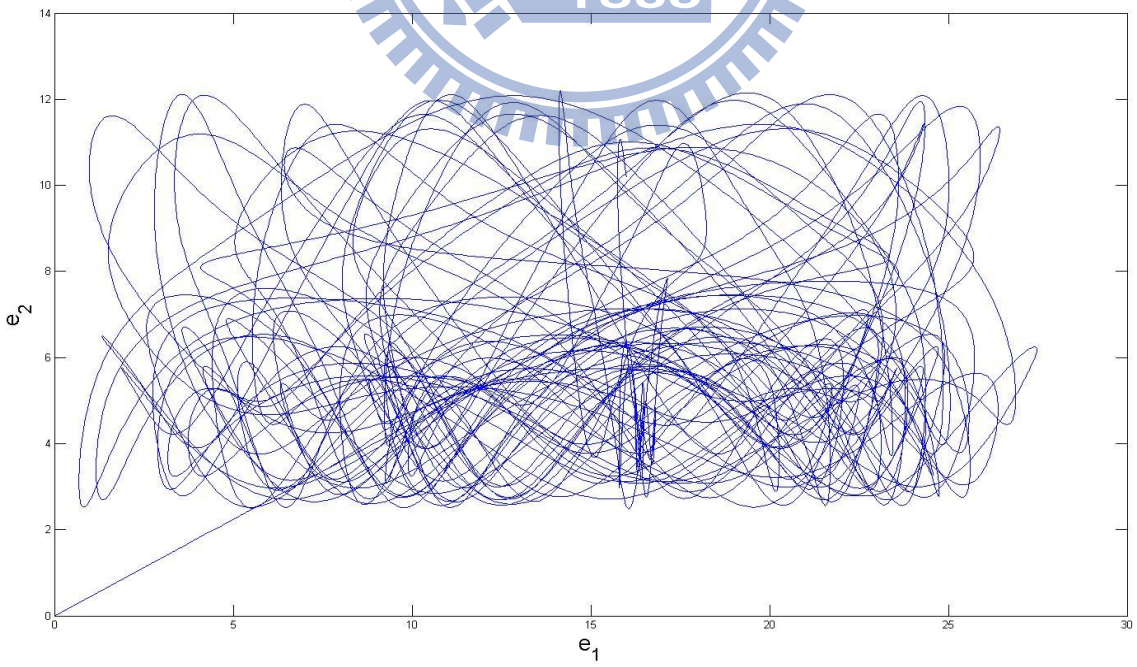

Fig. 3.15 Phase portrait of e_1, e_2 before and after control.

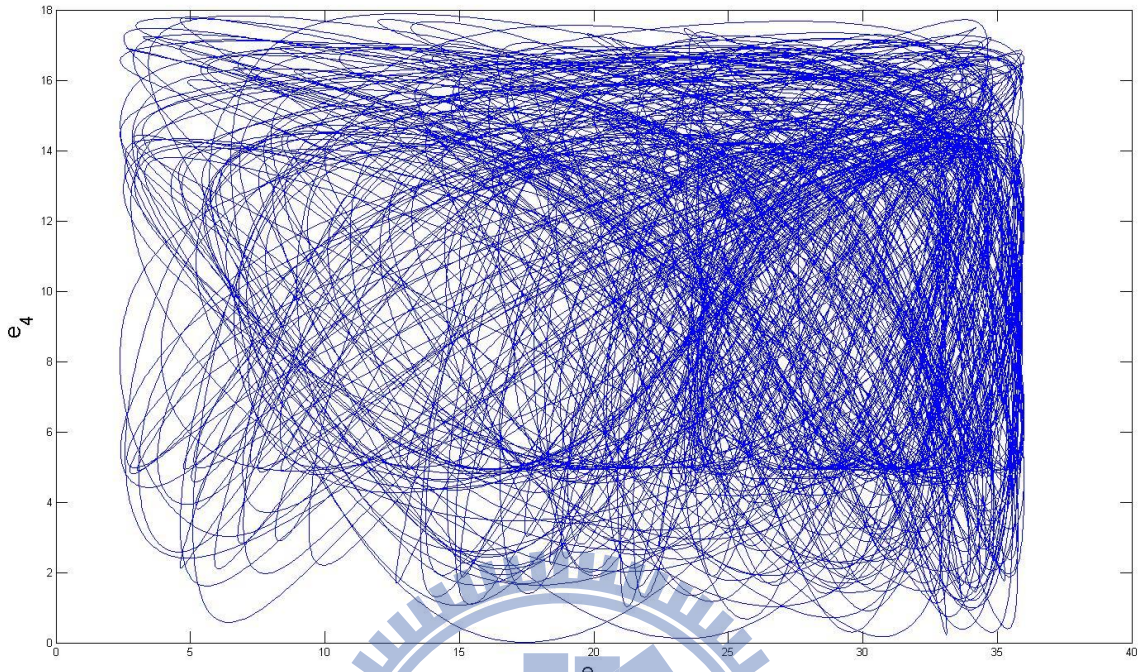

Fig. 3.16 Phase portrait of e_3, e_4 before control.

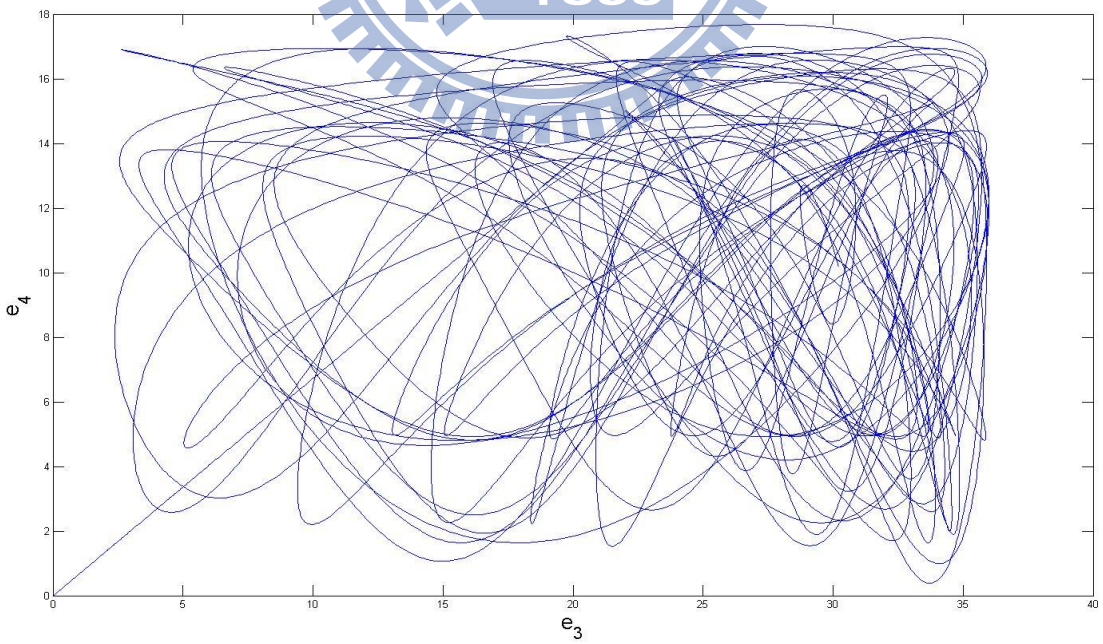

Fig. 3.17 Phase portrait of e_3, e_4 before and after control.

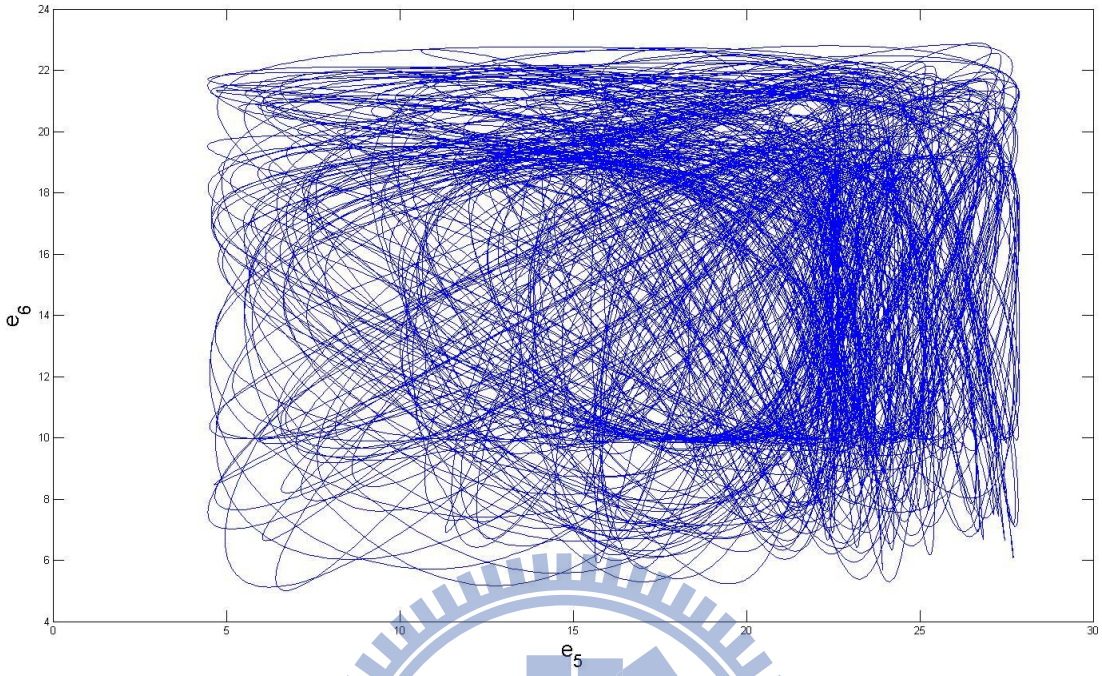

Fig. 3.18 Phase portrait of e_5, e_6 before control.

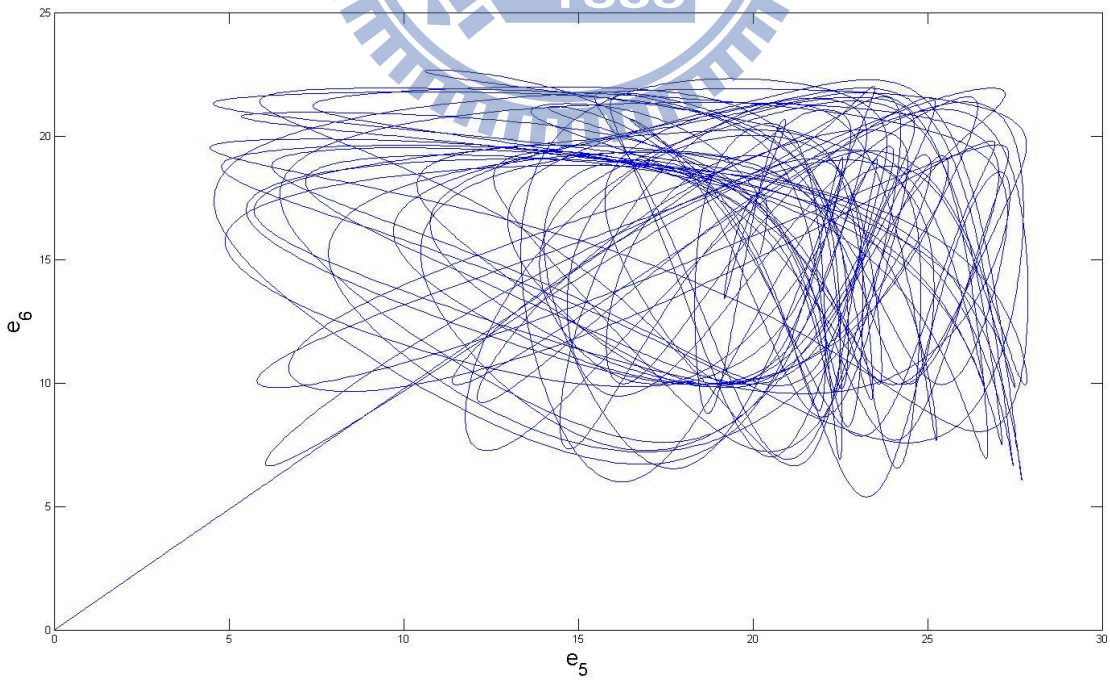

Fig. 3.19 Phase portrait of e_5, e_6 before and after control.

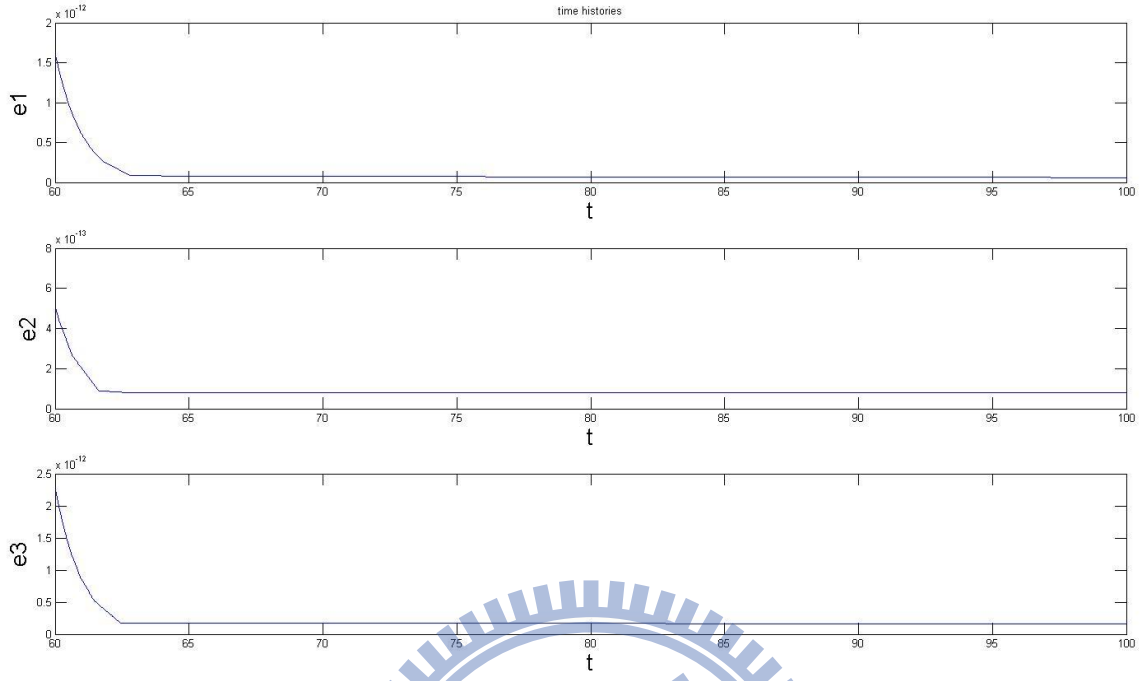

Fig.3.20 Time histories of e_1, e_2, e_3 for new strategy controller design method.

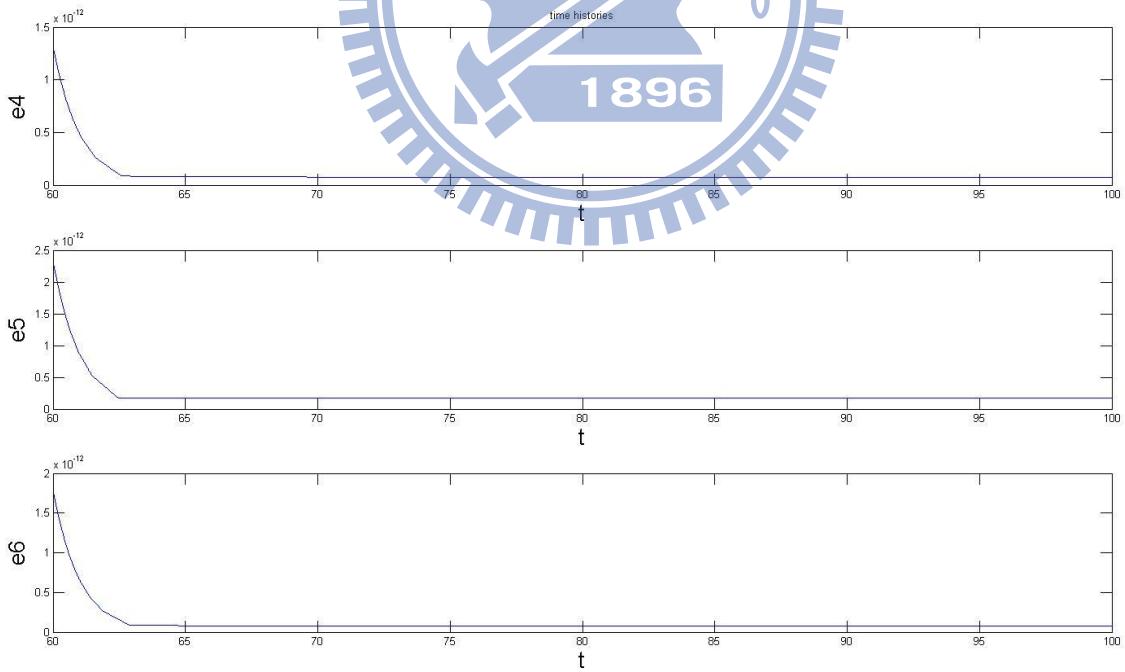

Fig.3.21 Time histories of e_4, e_5, e_6 for new strategy controller design method.

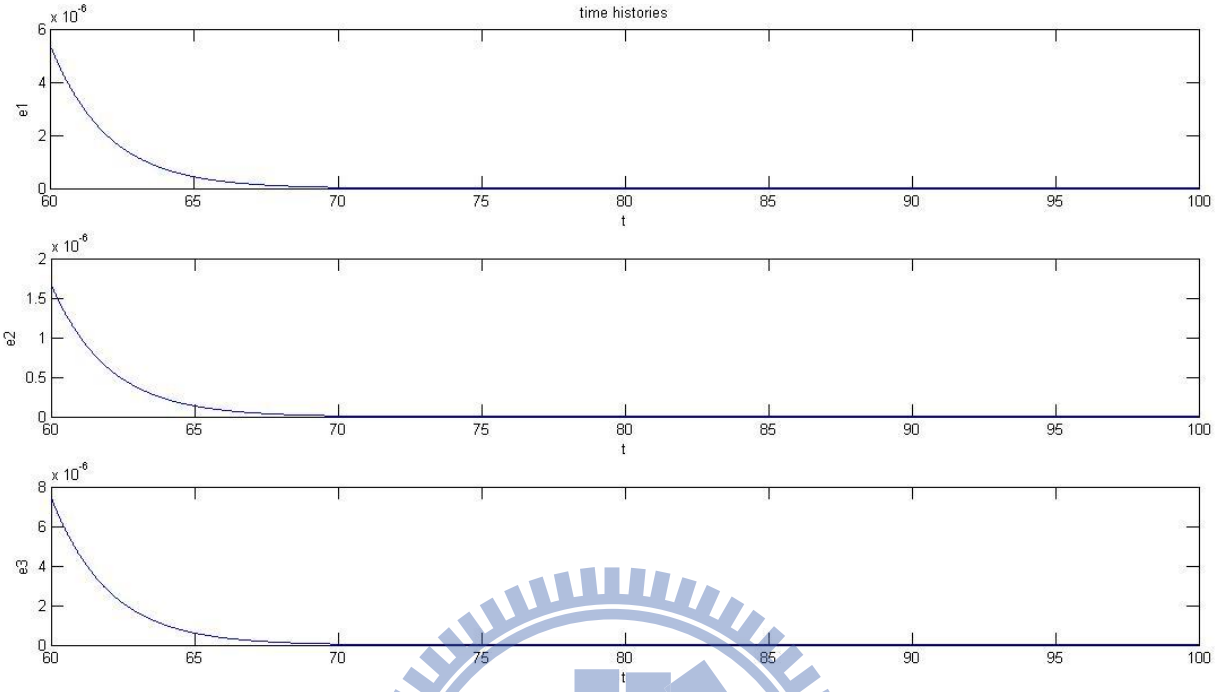

Fig3.22. Time histories of e_1, e_2, e_3 of using traditional controller design method.

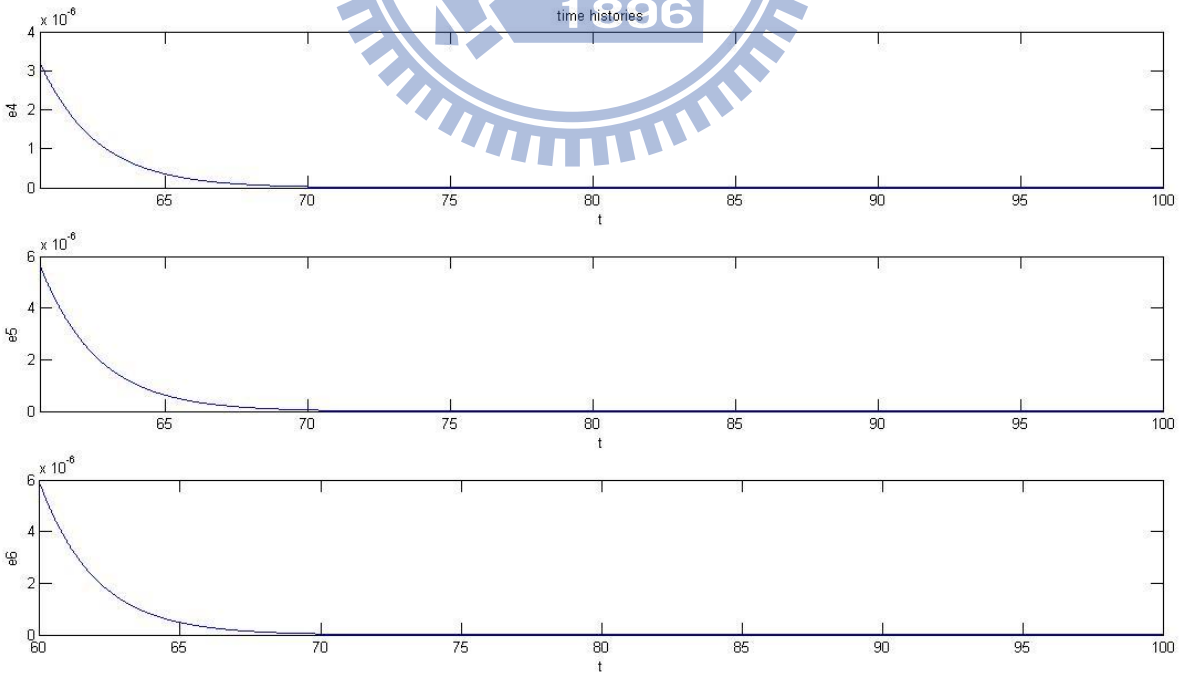

Fig3.23. Time histories of e_4, e_5, e_6 of using traditional controller design method.

Chapter 4

Multiple Symplectic Derivative Synchronization of Chen-Lee System and Sprott N System with Variable Time Scale by Partial Region Stability Theory

4.1 Preliminary

In this research, a new strategy to achieve multiple symplectic derivative synchronization with variable time scale, is obtained with the state variables of the **o**riginal system and of another different order system as constituents of the functional relation of "partners".

4.2 Synchronization by partial region stability theory

Given

$G(x,y,\ldots,\dot{x},\dot{y},\ldots\ddot{x},\ddot{y},\ldots,t,\tau)=$

$$\begin{cases} G_1 = x_1 y_1 \\ G_2 = -2y_2 + y_3 \\ G_3 = y_1 y_3 \end{cases} \tag{4.1}$$

$F(x,y,\ldots,\dot{x},\dot{y},\ldots\ddot{x},\ddot{y},\ldots,t,\tau)=$

$$\begin{cases} F_1 = x_3 + (-x_2 x_3 + 3x_1)(-2y_2) \\ F_2 = \frac{-\frac{dy_3}{d\tau}+1+y_2}{2} \\ F_3 = -2y_2 y_3 - y_2 \end{cases} \tag{4.2}$$

Two different chaotic systems are used as synchronization examples.

Consider a Chen-Lee system[13].

$$\begin{cases} \dot{x}_1 = -x_2 x_3 + 3x_1 \\ \dot{x}_2 = x_1 x_3 - 5x_2 \\ \dot{x}_3 = \frac{1}{3}(x_1 x_2) - x3 \end{cases} \tag{4.3}$$

The chaotic attractor of Chen-Lee system is shown in Figs.4.1~4.3.

Consider a Sprott N system[12].

$$\begin{cases} \frac{dy_1}{d\tau} = -2y_2 \\ \frac{dy_2}{d\tau} = y_1 + {y_3}^2 \\ \frac{dy_3}{d\tau} = 1 + y_2 - 2y_3 \end{cases} \tag{4.4}$$

Initial conditions $x_1(0) = 5, x_2(0) = 0.2, x_3(0) = 0.2, y_1(0) = 0.3, y_2(0) = 0.3$ $y_3(0) = 0.3$. where $\tau = t + sint$. The chaotic attractor of Sprott N is shown in Figs. 4.4~4.6.

Our goal is to achieve the multiple symplectic derivative synchronization with variable time scale.

$$G(x, y, z, \dot{x}, \dot{y}, \dot{z}, \ddot{x}, \ddot{y}, \ddot{z}, t, \tau) = F(x, y, z, \dot{x}, \dot{y}, \dot{z}, \ddot{x}, \ddot{y}, \ddot{z}, t, \tau) \tag{4.5}$$

The error state vector is

$$e = G(x,y,z,\ldots,\dot{x},\dot{y},\dot{z},\ldots\ddot{x},\ddot{y},\ddot{z}\ldots,t,\tau) - F(x,y,z,\ldots,\dot{x},\dot{y},\dot{z},\ldots\ddot{x},\ddot{y},\ddot{z}\ldots,t,\tau) + \boldsymbol{K}. \tag{4.6}$$

where $\boldsymbol{K}=[30,-130,20]^T$ such that error dynamics always exists in fourth quadrant as shown in Figs. 4.7~4.9.

Our goal is

$$\lim_{t\to\infty} e_i = \lim_{t\to\infty}(G_i - F_i + K_i) = 0, (i = 1,2,3) \tag{4.7}$$

A positive definite Lyapunov function in fourth octant is given as

$$V(e) = e_1 - e_2 + e_3 > 0 \tag{4.8}$$

The error dynamics becomes

$$\dot{\boldsymbol{e}} = \dot{\boldsymbol{G}} - \dot{\boldsymbol{F}} - \boldsymbol{u} \tag{4.9}$$

The controller u can be selected as

$$\boldsymbol{u} = \begin{bmatrix} u_1 \\ u_2 \\ u_3 \end{bmatrix} = \begin{bmatrix} \frac{1}{3}x_1x_2 - x_3 + e1 \\ (8y_3 - 4) + e2 \\ (y_1 + {y_3}^2) + e3 \end{bmatrix} \tag{4.10}$$

such that

$$\dot{V}(e) = \dot{V}(e) = -e_1 + e_2 - e_3 < 0 \tag{4.11}$$

Error states versus time and time histories are shown in Figs. 4.10~4.12,where the sign rule of the quadrants are shown as following in Table4.1 and Fig.4.13.

Table 4.1. The sign rule of eight quadrants

Quadrant Number	Sign Rule
I	$(+,+,+)$
II	$(-,+,+)$
III	$(-,-,+)$
IV	$(+,-,+)$
V	$(+,+,-)$
VI	$(-,+,-)$
VII	$(-,-,-)$
VIII	$(+,-,-)$

4.3 Synchronization by traditional method

If the traditional Lyapunov function is used, it means that

$$V(e) = e_1^2 + e_2^2 + e_3^2 \tag{4.12}$$

Its time derivative is

$$\dot{V}(e) = 2(e_1\dot{e}_1 + e_2\dot{e}_2 + e_3\dot{e}_3) \tag{4.13}$$

We want to find u in Eg.(13) such that

$$\dot{V}(e) = -(e_1^2 + e_2^2 + e_3^2) < 0 \tag{4.14}$$

By traditional method, the controller is designed as

$$\boldsymbol{u} = \begin{bmatrix} u_1 \\ u_2 \\ u_3 \end{bmatrix} = \begin{bmatrix} \frac{1}{3}x_1x_2 - x_3 + 0.5e1 \\ (8y_3 - 4) + 0.5e2 \\ (y_1 + {y_3}^2) + 0.5e3 \end{bmatrix} \tag{4.15}$$

Introduce *u* into Eq.(9) where *i* = 1, 2, 3, Eq.(13) becomes

$$\dot{V}(e) = -(e_1^2 + e_2^2 + e_3^2)$$

which is a negative definite function in all quadrants. Error states time histories are shown in Figs. 4.14~4.16.

4.4 Comparison between new strategy and traditional method

From the previous sections, we know that the controllers u of the new strategy and of the traditional method are different. Tables (Tables. 4.2~ 4.4) and figures (Fig. 4.17and Fig. 4.18) for comparing the efficiency of convergence are given as follows. The superioty of new strategy is obvious. The error states of new strategy are much smaller and decay more quickly than that of traditional method.

Table 4.2. Comparison between error data at 99.6~99.70 s after the action of controllers.

e_1		
time	new method($\times 10^{-13}$)	traditional method($\times 10^{-9}$)
99.60	0.9237	0.4436
99.61	0.9237	0.4414
99.62	0.9237	0.4392
99.63	0.9237	0.4370
99.64	0.9237	0.4349
99.65	0.9237	0.4327
99.66	0.9237	0.4305
99.67	0.9237	0.4284
99.68	0.9237	0.4263
99.69	0.9237	0.4241
99.70	0.9237	0.4220

Table 4.3. Comparison between error data at 99.6~99.70 s after the action of controllers.

e_2		
time	new method($\times 10^{-11}$)	traditional method($\times 10^{-8}$)
99.60	-0.1364	-0.2088
99.61	-0.1364	-0.2077
99.62	-0.1364	-0.2067
99.63	-0.1364	-0. 2057

99.64	-0.1364	-0.2047
99.65	-0.1364	-0.2036
99.66	-0.1364	-0.2026
99.67	-0.1364	-0.2016
99.68	-0.1364	-0.2006
99.69	-0.1364	-0.1996
99.70	-0.1364	-0.1986

Table 4.4. Comparison between error data at 99.6~99.70 s after the action of controllers.

e_3		
time	new method($\times 10^{-12}$)	traditional method($\times 10^{-9}$)
99.60	0.1492	0.2398
99.61	0.1492	0.2386
99.62	0.1492	0.2374
99.63	0.1492	0.2363
99.64	0.1492	0.2351
99.65	0.1492	0.2339
99.66	0.1492	0.2327
99.67	0.1492	0.2316
99.68	0.1492	0.2304
99.69	0.1492	0.2293
99.70	0.1492	0.2281

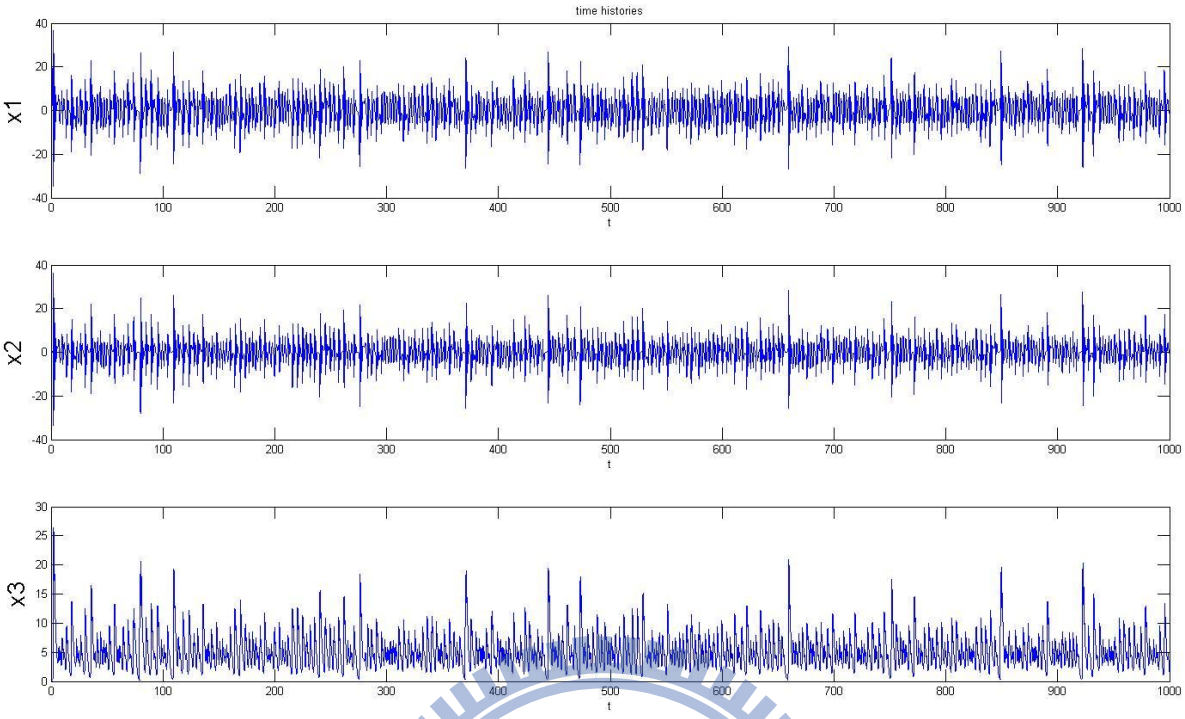

Fig.4.1 Time histories of the Chen-Lee system.

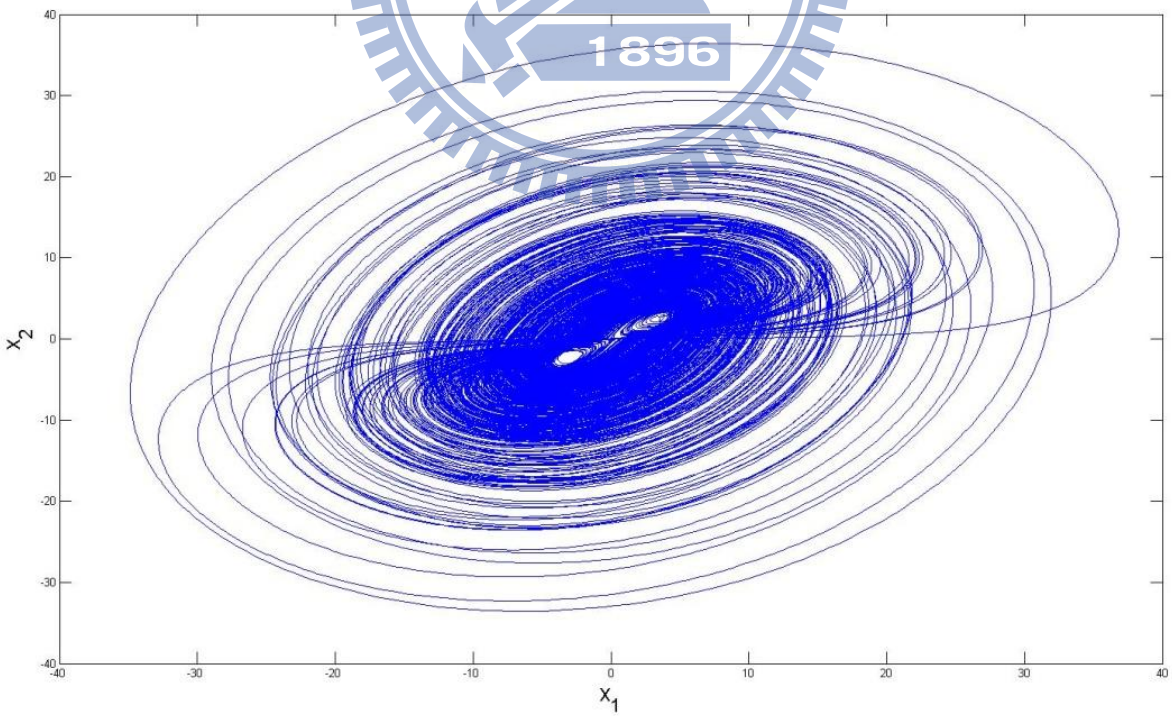

Fig.4.2 Phase portrait of the Chen-Lee system.

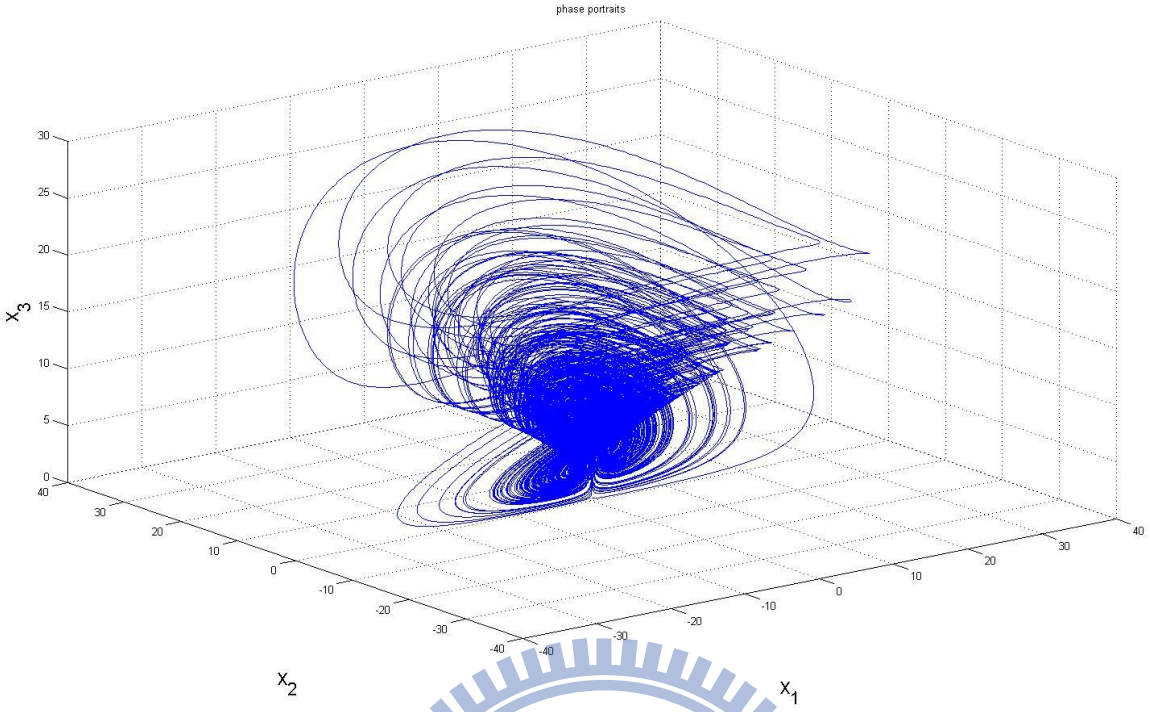

Fig.4.3 Phase portrait of the Chen-Lee system.

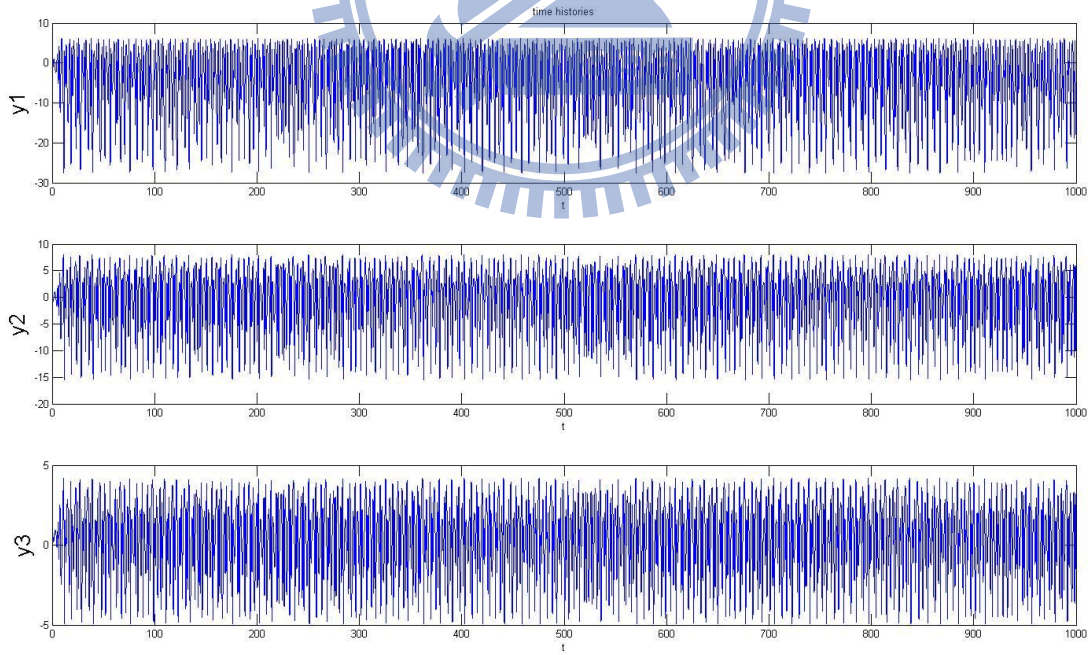

Fig.4.4 Time histories of the Sprott N system.

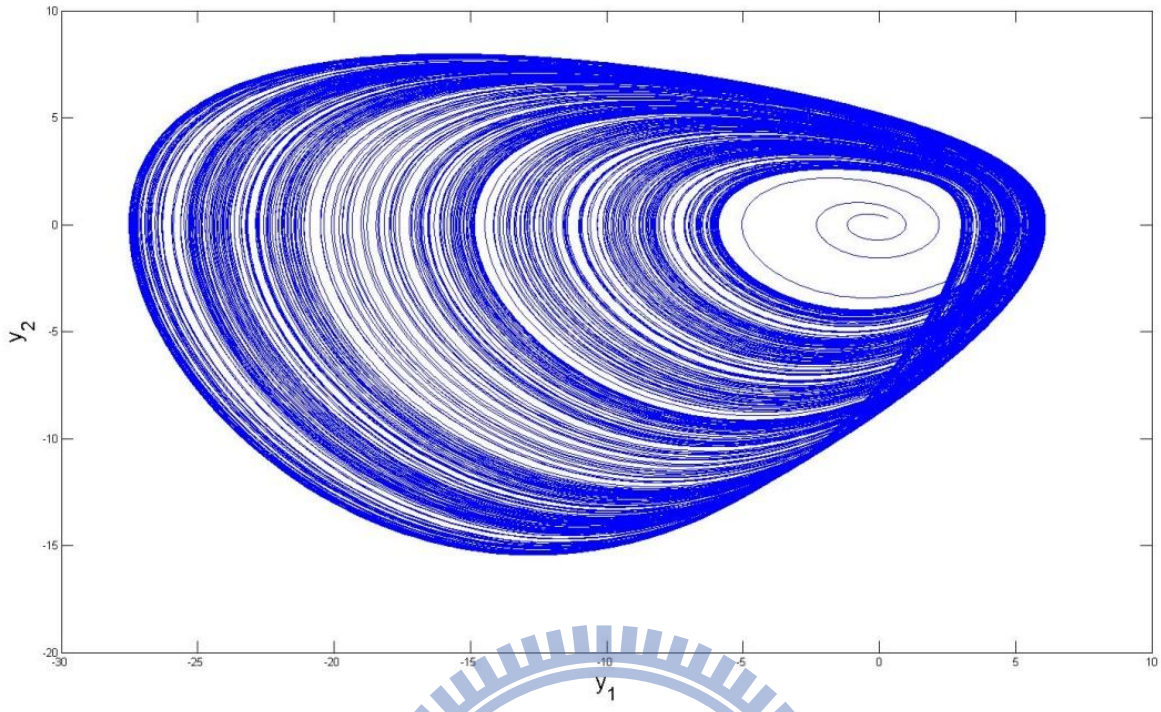

Fig.4.5 Phase portrait of the Sprott N system.

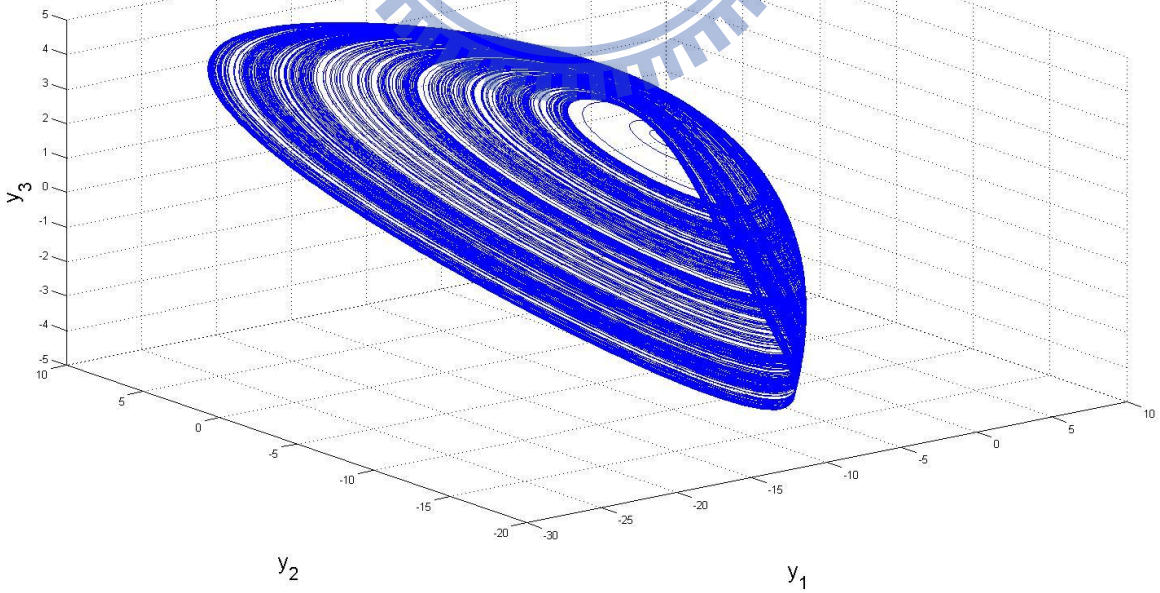

Fig.4.6 Phase portrait of the Sprott N system.

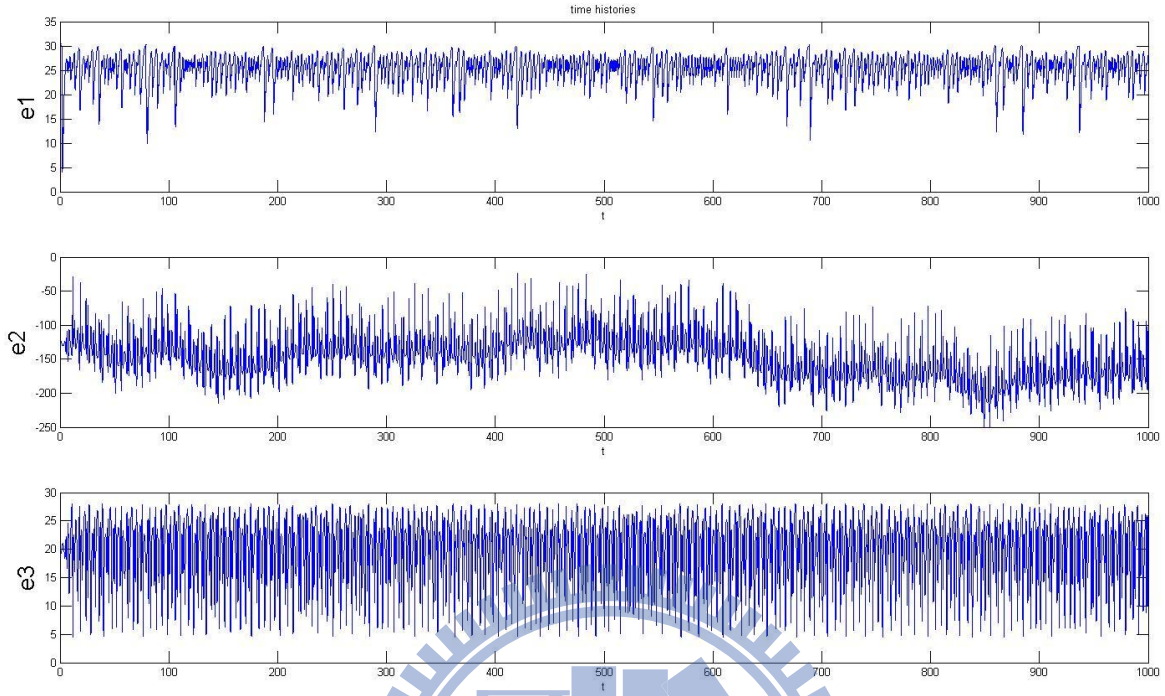

Fig. 4.7 Time histories of e_1, e_2, e_3 before control.

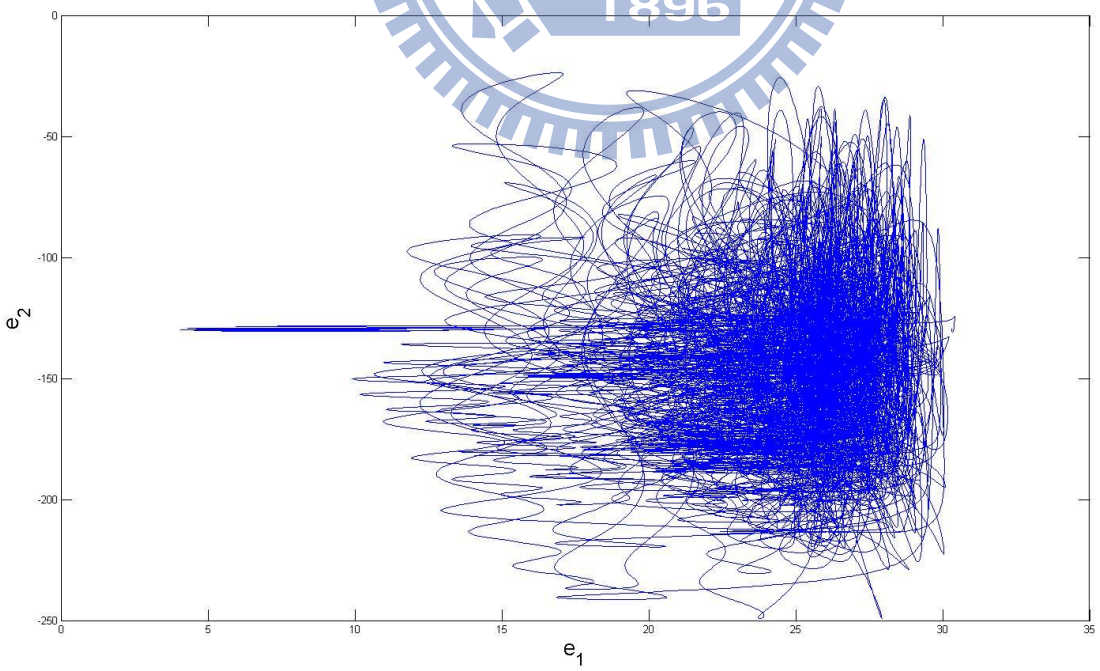

Fig.4.8 Phase portrait of e_1, e_2 before control.

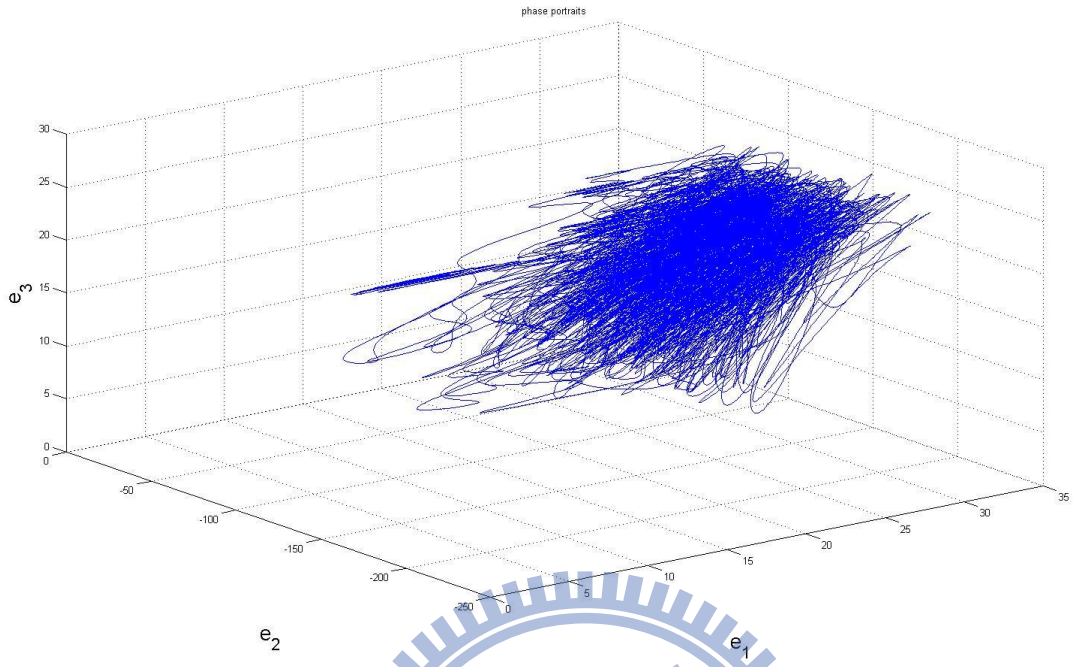

Fig. 4.9 Phase portrait of e_1, e_2, e_3 before control.

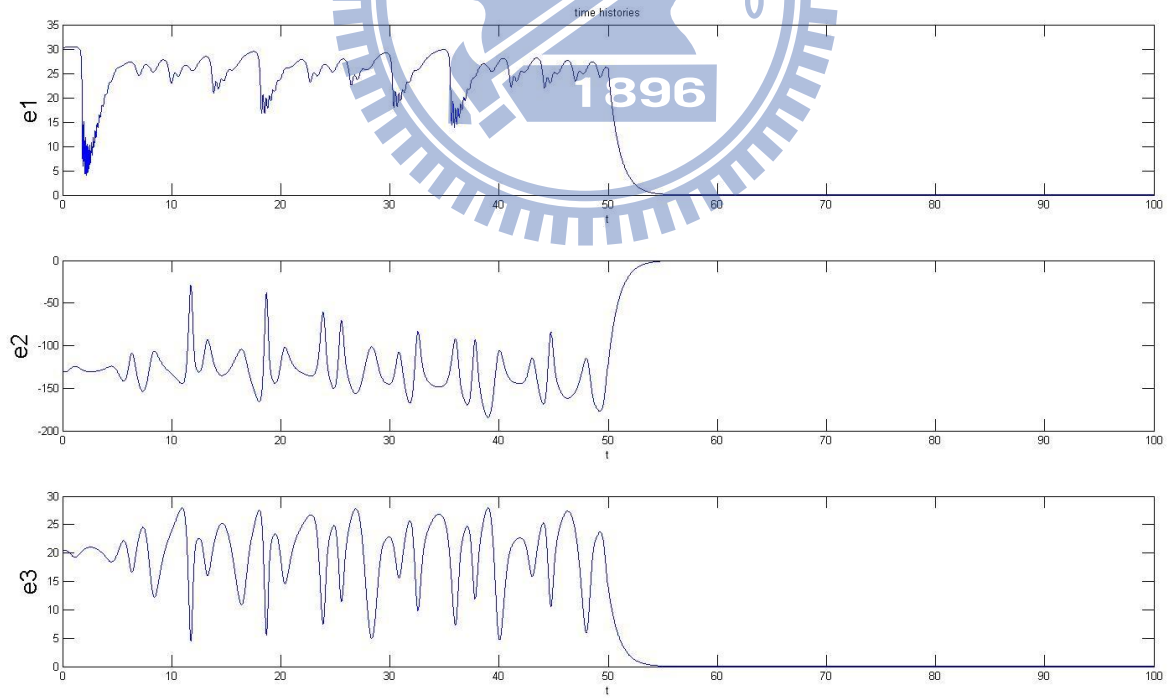

Fig. 4.10 Time histories of e_1, e_2, e_3 before and after control.

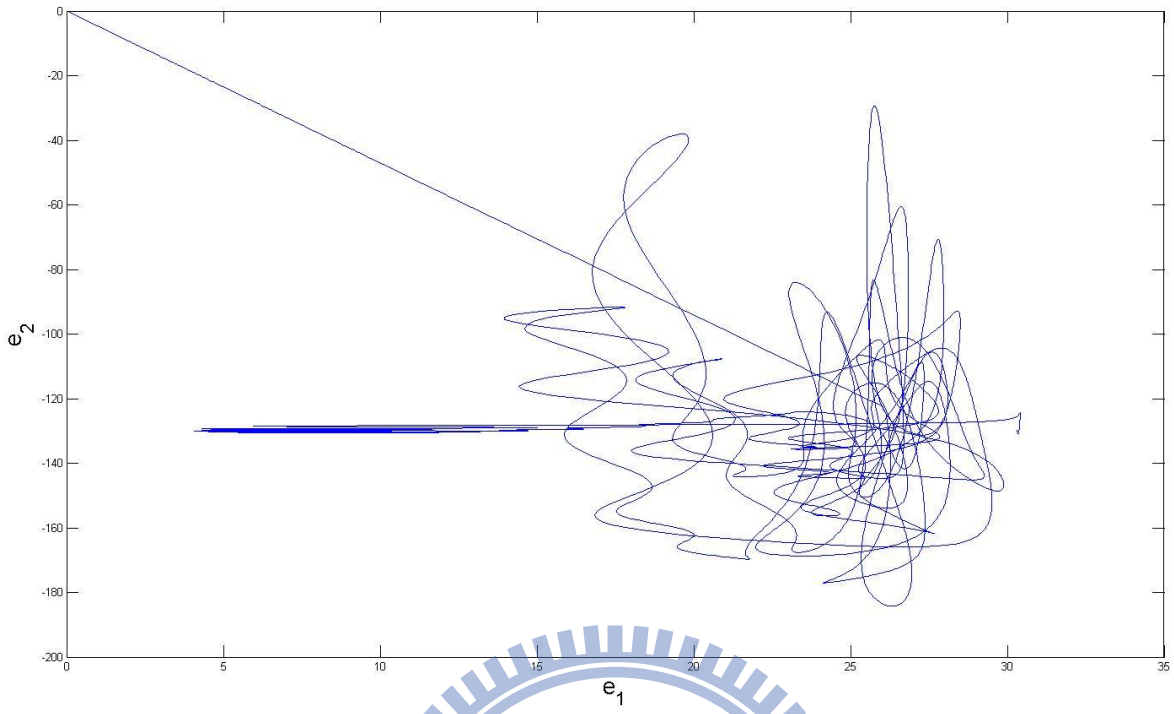

Fig. 4.11 Phase portrait of e_1, e_2 before and after control.

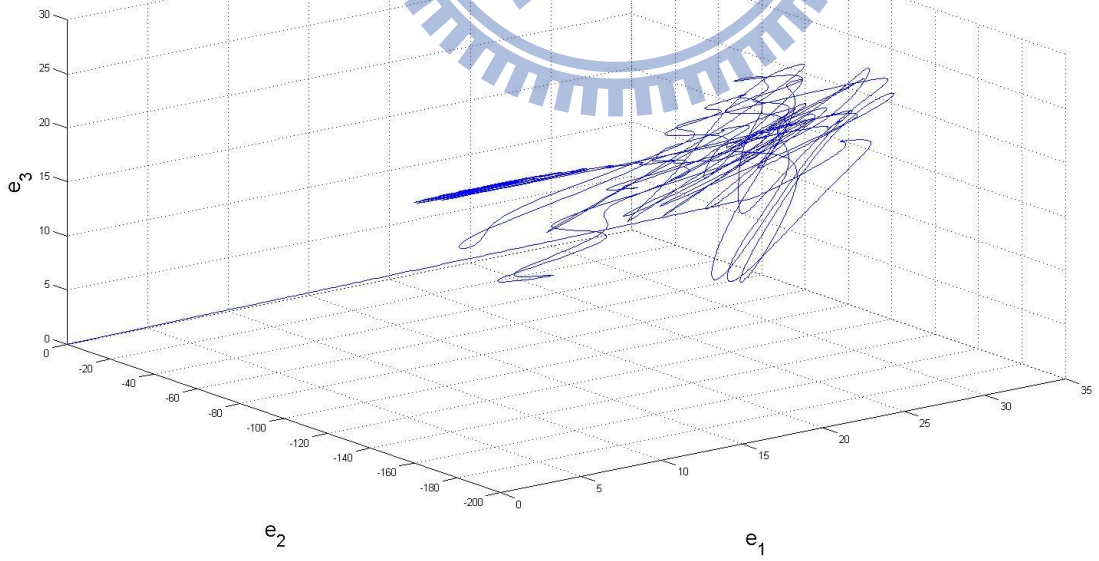

Fig. 4.12 Phase portrait of e_1, e_2, e_3 before and after control.

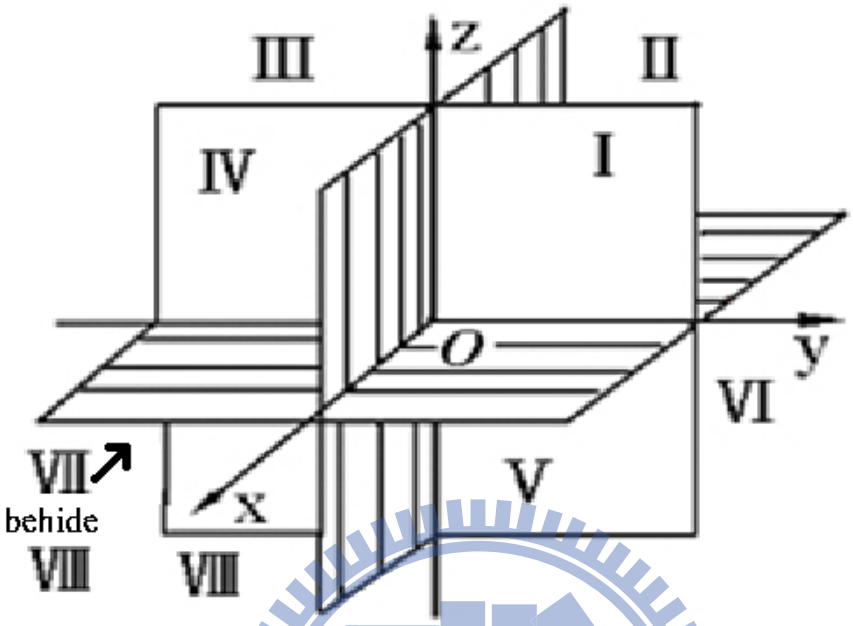

Fig. 4.13 Definitions of the eight quadrants.

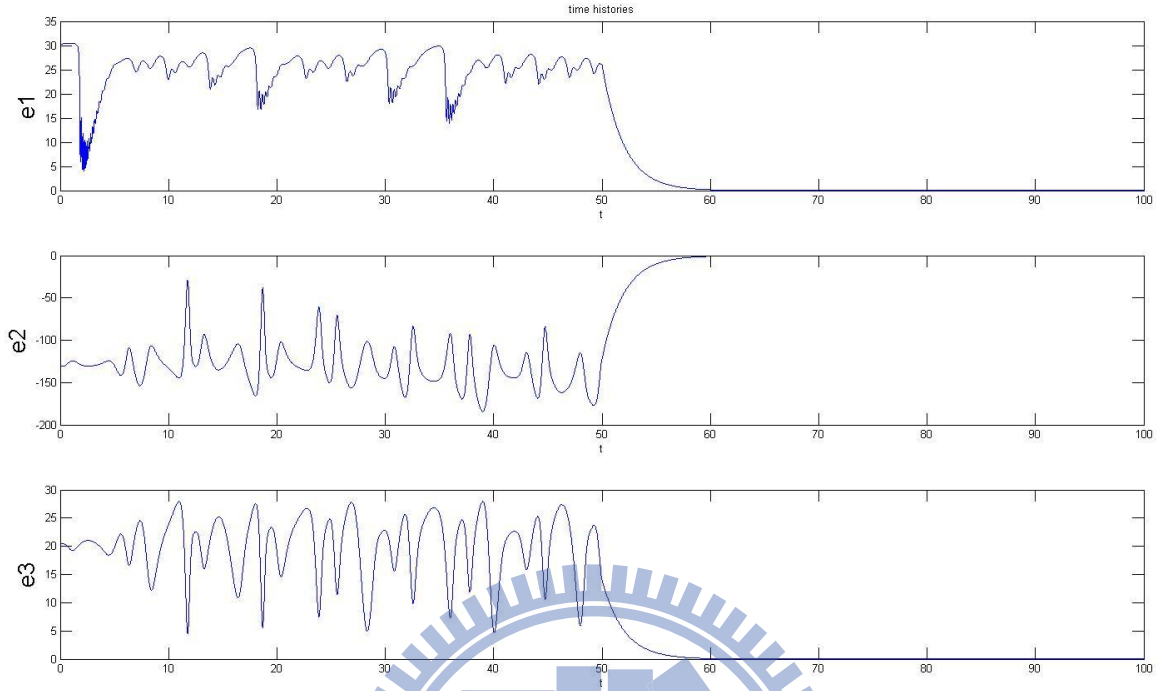

Fig. 4.14 Time histories of error function after synchronization for traditional method.

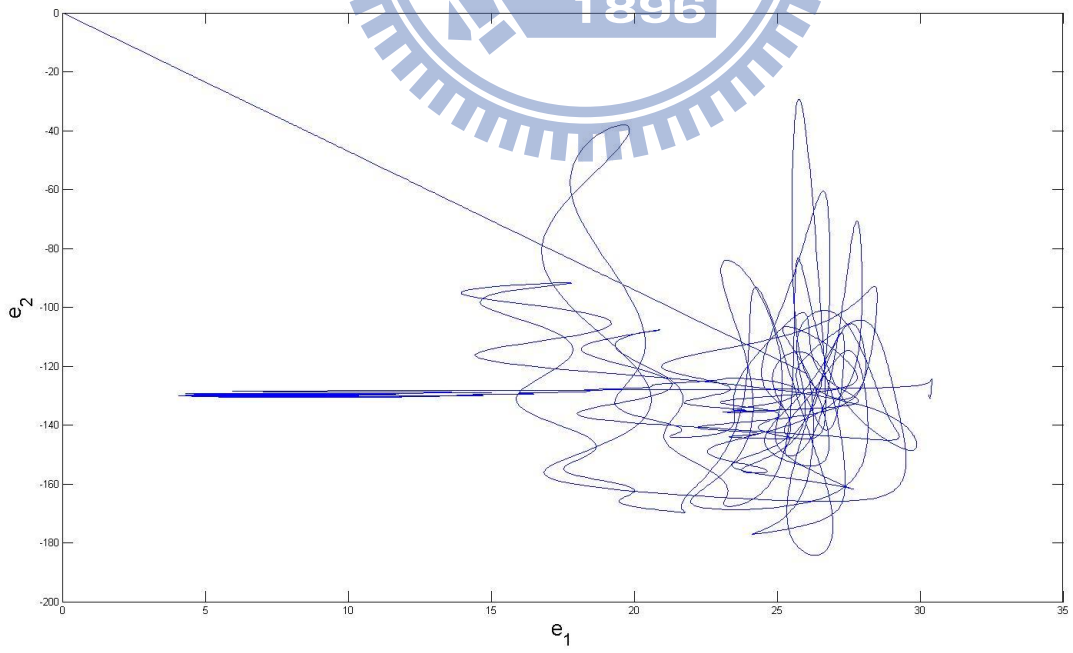

Fig. 4.15 Phase portrait of error function after synchronization for traditional method.

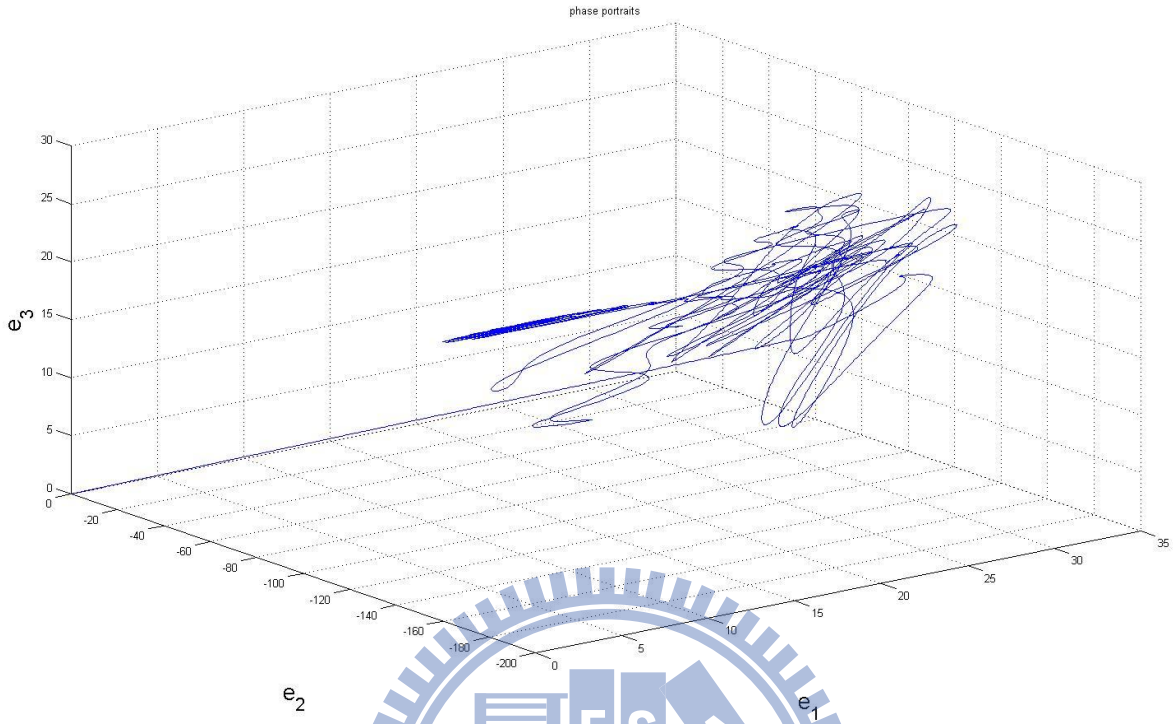

Fig. 4.16 Phase portrait of error function after synchronization for traditional method.

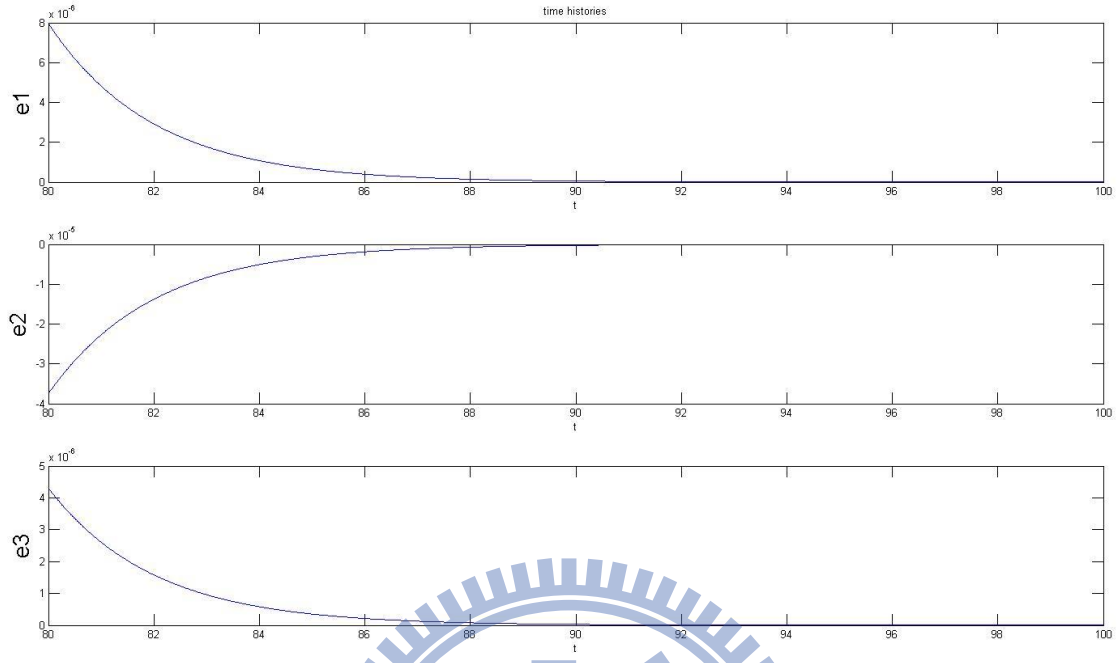

Fig. 4.17 Time histories of error function after synchronization for traditional method.

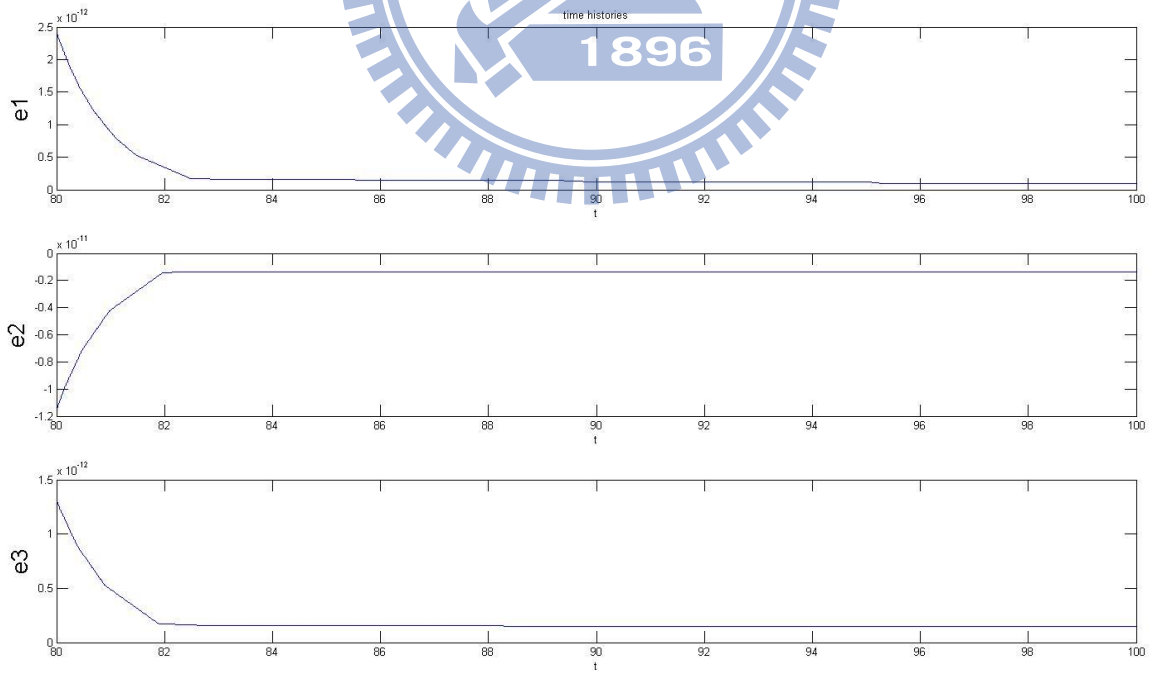

Fig. 4.18 Time histories of error function after synchronization for new strategy.

Chapter 5

Kun-Zhen Hexagram Multiple Symplectic Derivative Chaos Synchronization by Partial Region Stability Theory

5.1. Preliminary

The Book of Changes is fundamental in Chinese philosophy. Kun Trigram and Zhen Trigram are two of Eight Trigrams. When the Eight Trigrams, each containing three lines, multiply themselves to become sixty-four hexagrams, they are taken to represent all possible forms of change. New strategy to achieve multiple symplectic derivative synchronization is presented. Furthermore, by Chinese philosophy, Tai Ji chaos, i.e. Great One chaos, consists of Yin chaos and Yang chaos. Finally, combining Kun trigram in upper place and Zhen trigram in lower place can get Kun-Zhen hexagram. Kun-Zhen hexagram can be annotated by chaos and its synchronization.

Trigram has three parts, upper, central, and low. The three parts of Kun trigram and Zhen trigram, a part of the eight trigrams, both represent three different chaos systems separately, and they are used to complete a two times multiple synplectic derivative synchronization by partial region stability theory.

Hexagram has two parts, upper, and low. The Kun-Zhen Hexagram is used for multiple synplectic derivative synchronization by partial region stability theory. $G(x, y, z, \cdots, \dot{x}, \dot{y}, \dot{z}, \cdots, t) = F(x, y, z, \cdots, \dot{x}, \dot{y}, \dot{z}, \cdots, t)$, is a more general form of

symplectic synchronization. A new chaos control strategy by GYC (Ge-Yao-Chen) partial region stability theory is used in this chapter.

This chapter is presented as follows. In Section 2, systems used in this paper are shown and the Yang (normal) and Yin (historical) systems for Chen-lee System, Spott N system, and Spott K system are synchronized. In Section 3, the Kun trigram multiple symplectic derivative synchronization is presented by GYC partial region stability theory. In Section 4, the Zhen trigram multiple symplectic derivative synchronization is proposed. In Section 5, Kun-Zhen hexagram multiple symplectic derivative synchronization by partial region stability Theory.

5.2. Yin system and Yang system

Chen-Lee system for time interval $0 \to +\infty$ is called Yang Chen-Lee system:

$$\begin{cases} \dot{x}_1(t) = -x_2(t)x_3(t) + 3x_1(t) \\ \dot{x}_2(t) = x_1(t)x_3(t) - 5x_2(t) \\ \dot{x}_3(t) = \frac{1}{3}x_1(t)x_2(t) - x_3(t) \end{cases} \tag{5.1}$$

Initial conditions $x_1(0) = 0.2, x_2(0) = 0.2, x_3(0) = 0.2,$. The chaos of Yang Chen-Lee is shown in Figs. 5.1~5.2.

By replacing variable $(x_1(t), x_2(t), x_3(t), t)$ with $(x_4(-t), x_5(-t), x_6(-t), -t)$ in Eq. (5.1) to study the past $(\mathrm{t}: 0 \to -\infty)$ of the system, Yin Chen-Lee system is described as follows:

$$\begin{cases} \dot{x}_4(-t) = -x_5(-t)x_6(-t) + 3x_4(-t) \\ \dot{x}_5(-t) = x_4(-t)x_6(-t) - 5x_5(-t) \\ \dot{x}_6(-t) = \frac{1}{3}x_4(-t)x_5(-t) - x_6(-t) \end{cases} \tag{5.2}$$

Initial conditions $\mathrm{x}_4(0) = 0.2, \mathrm{x}_5(0) = 0.2, \mathrm{x}_6(0) = 0.2,$. The chaos of Yin Chen-Lee is shown in Figs. 5.3~5.4.

Set the Yin Chen-Lee system be

$$\begin{cases} \dot{x}_4(-t) = -x_5(-t)x_6(-t) + 3x_4(-t) & + k(x_1 - x_4) \\ \dot{x}_5(-t) = x_4(-t)x_6(-t) - 5x_5(-t) & + k(x_2 - x_5) \\ \dot{x}_6(-t) = \frac{1}{3}x_4(-t)x_5(-t) - x6(-t) & + k(x_3 - x_6) \end{cases} \quad (5.3)$$

where x_1, x_2, and x_3 are states of Eq. (5.1), k is a positive constant, 50.

The states of linear feedback synchronization for Yang Chen-Lee system and Yin Chen-Lee system are shown in Fig. 5.5.

Sprott N system for time interval $0 \to +\infty$ is called Yang Sprott N system:

$$\begin{cases} \dot{y}_1(t) = -2y_2(t) \\ y_2(t) = y_1(t) + y_3(t)^2 \\ \dot{y}_3(t) = 1 + y_2(t) - 2y_3(t) \end{cases} \quad (5.4)$$

Initial conditions $y_1(0) = 0.3, y_2(0) = 0.3, \text{and } y_3(0) = 0.3$. The chaotic of Yang Sprott N is shown in Figs. 5.6~5.7.

By replacing variable $(y_1(t), y_2(t), y_3(t), t)$ with $(y_4(-t), y_5(-t), y_6(-t), -t)$ in Eq. (5.4) to study the past $(-t: 0 \to -\infty)$ of the system, Yin Sprott N system is described as follows:

$$\begin{cases} \dot{y}_4(-t) = -2y_5(-t) \\ y_5(-t) = y_4(-t) + y_6(-t)^2 \\ \dot{y}_6(-t) = 1 + y_5(-t) - 2y_6(-t) \end{cases} \quad (5.5)$$

Initial conditions $y_4(0) = 0.3, y_5(0) = 0.3, y_6(0) = 0.3,$. The chaotic of Yin Sprott N is shown in Figs. 5.8~5.9.

Set the Yin Sprott N system be

$$\begin{cases} \dot{y}_4(-t) = -2y_5(-t) & + k(y_1 - y_4) \\ y_5(-t) = y_4(-t) + y_6(-t)^2 & + k(y_2 - y_5) \\ \dot{y}_6(-t) = 1 + y_5(-t) - 2y_6(-t) & + k(y_3 - y_6) \end{cases} \quad (5.6)$$

where y_1, y_2, and y_3 are states of Eq. (5.4), k is a positive constant, 50.

The states of linear feedback synchronization for Yang Sprott N system and Yin Sprott N system are shown in Fig. 5.10.

Sprott K system for time interval $0 \to +\infty$ is called Yang Sprott K system:

$$\begin{cases} \dot{z}_1(t) = z_1(t)z_2(t) - z_3(t) \\ \dot{z}_2(t) = z_1(t) - z_2(t) \\ \dot{z}_3(t) = z_1(t) + 0.3z_3(t) \end{cases} \tag{5.7}$$

Initial conditions $z_1(0) = 0.2, z_2(0) = 0.2, z_3(0) = 0.2,$. The chaotic of Yang Sprott K is shown in Figs. 5.11~5.12.

By replacing variable $(z_1(t), z_2(t), z_3(t), t)$ with $(z_4(-t), z_5(-t), z_6(-t), -t)$ in Eq. (5.7) to study the past $(t: 0 \to -\infty)$ of the system, Yin Sprott K system is described as follows:

$$\begin{cases} \dot{z}_4(-t) = z_4(-t)z_5(-t) - z_6(-t) \\ \dot{z}_5(-t) = z_4(-t) - z_5(-t) \\ \dot{z}_6(-t) = z_4(-t) + 0.3z_6(-t) \end{cases} \tag{5.8}$$

Initial conditions $z_4(0) = 0.2, z_5(0) = 0.2, z_6(0) = 0.2,$. The chaotic of Yin Sprott K is shown in Figs. 5.13~5.14.

Set the Yin Sprott K system be

$$\begin{cases} \dot{z}_4(-t) = z_4(-t)z_5(-t) - z_6(-t) & + k(z_1 - z_4) \\ \dot{z}_5(-t) = z_4(-t) - z_5(-t) & + k(z_2 - z_5) \\ \dot{z}_6(-t) = z_4(-t) + 0.3z_6(-t) & + k(z_3 - z_6) \end{cases} \tag{5.9}$$

where z_1, z_2, and z_3 are states of Eq. (5.7), k is a positive constant, 50.

The states of linear feedback synchronization for Yang Sprott K system and Yin Sprott K system are shown in Fig. 5.15.

The chaotic attractor of Tai Ji Sportt N system and Tai Ji Sportt K system, the combination of Yang and Yin systems, is shown in Figs. 5.16~5.19.

5.3. Kun Trigram Synchronization

Kun Trigram

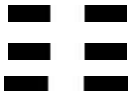

$t \to -\infty \longleftarrow 0 \longrightarrow t \to \infty$ Chen-Lee

$t \to -\infty \longleftarrow 0 \longrightarrow t \to \infty$ Sprott N

$t \to -\infty \longleftarrow 0 \longrightarrow t \to \infty$ Sprott K

Yang Chen-Lee and Yang Sprott N chaotic systems are used as synchronization.

Given

$G(x,y,z,\ldots,\dot{x},\dot{y},\dot{z},\ldots\ddot{x},\ddot{y},\ddot{z}\ldots,t)$:

$$\begin{cases} G_1 = y_1 - x_2 - x_1\dot{x}_3 \\ G_2 = \dot{y}_2 - \dot{x}_1 + 3x_1 \\ G_3 = y_3 - x_3 - \dot{x}_3 \end{cases} \tag{5.10}$$

$F(x,y,z,\ldots,\dot{x},\dot{y},\dot{z},\ldots\ddot{x},\ddot{y},\ddot{z}\ldots,t)$:

$$\begin{cases} F_1 = 0.2\dot{x}_2 + 1.2x_1x_3 - \frac{1}{3}x_1^2x_2 \\ F_2 = -x_2x_3 \\ F_3 = -\frac{1}{2}y_1 - \frac{1}{3}x_1x_2 \end{cases} \tag{5.11}$$

Our goal is to achieve the multiple symplectic derivative synchronization.

Define error function as

$$e = G(x,y,z,\ldots,\dot{x},\dot{y},\dot{z},\ldots\ddot{x},\ddot{y},\ddot{z}\ldots,t) - F(x,y,z,\ldots,\dot{x},\dot{y},\dot{z},\ldots\ddot{x},\ddot{y},\ddot{z}\ldots,t) + \boldsymbol{K}. \tag{5.12}$$

where $\boldsymbol{K}=[1000,1000,1000]^T$ keep the error dynamics always in first guardant. Our

goal is

$$lim_{t\to\infty} e_i = lim_{t\to\infty}(G_i - F_i + K_i) = 0, (i = 1,2,3) \tag{5.13}$$

Thus we design the controller as

$$u = \begin{cases} u_1 = -2y_2 + e_1 \\ u_2 = 2 - 4y_3 + e_2 \\ u_3 = -2y_3 + 1 + e_3 \end{cases} \tag{5.14}$$

The error dynamics becomes

$$\dot{\boldsymbol{e}} = \dot{\boldsymbol{G}} - \dot{\boldsymbol{F}} - \boldsymbol{u} \tag{5.15}$$

Using partial region stability theory we can choose a Lyapunov function in the form of a positive definite function in first quadrant.

$$V(e) = e_1 + e_2 + e_3 > 0 \tag{5.16}$$

By adding u ,we obtain

$$\dot{V}(e) = -e_1 - e_2 - e_3 < 0 \tag{5.17}$$

which is a negative definite function in first quadrant. The results are shown in Fig.5.20.

Yang Sprott N and Yang Sprott K chaotic systems are used for synchronization.

Given

G(x,y,z,…,$\dot{x}$, ,$\dot{y}$, ,$\dot{z}$,…$\ddot{x}$, $\ddot{y}$, $\ddot{z}$…,t):

$$\begin{cases} G_4 = z_1 - \dot{z_3} - \frac{1}{2}\dot{y_1}\dot{y_2} + \frac{91}{30}z_3 \\ G_5 = \dot{z_2} - \dot{y_2} + y_2 + 0.3z_3 \\ G_6 = z_3 - z_2 + y_1 y_2 + 0.5y_1 \end{cases} \tag{5.18}$$

$F(x,y,z,\ldots,\dot{x},\ ,\dot{y},\ ,\dot{z},\ldots\ddot{x},\ \ddot{y},\ \ddot{z}\ldots,t)$:

$$\begin{cases} F_4 = y_1 y_2 - \frac{1}{2}\dot{y}_1 y_3^2 \\ F_5 = y_3 y_2 + \dot{y}_3 + \frac{1}{2}\dot{y}_1 y_3 + \dot{z}_3 \\ F_6 = y_1 y_3 + 0.5\dot{y}_3 y_1 \end{cases} \tag{5.19}$$

Our goal is to achieve the multiple symplectic derivative synchronization.

Define error function as Eq.(5.12).

where $\boldsymbol{K}=[300,60,400]^T$ keeps the error dynamics always in first guardant. Our goal is Eq.(5.13).

Thus we design the controller as

$$u = \begin{cases} u_4 = -z_3 - \frac{10}{3} z_1 + e_4 \\ u_5 = 2y_2 + e_5 \\ u_6 = z_2 + 0.3z_3 + e_6 \end{cases} \tag{5.20}$$

The error dynamics becomes Eq.(5.15).Using partial region stability theory we can choose a Lyapunov function in the form of a positive definite function in first quadrant.By adding u ,we obtain

$$\dot{V}(e) = -e_4 - e_5 - e_6 < 0 \tag{5.21}$$

which is a negative definite function in first quadrant. The results are shown in Fig. 5.21.

5.4 Zhen Trigram Synchronization

Zhen Trigram

$t \to -\infty \longleftarrow 0 \longrightarrow t \to \infty$ Chen-Lee

$-\infty \longleftarrow 0 \longrightarrow t \to \infty$ Sprott N

$-\infty \longrightarrow t \to \infty$ Sprott K

Given G and F of Yang Chen-Lee and Yang Sprott N system as.

$$G\begin{cases} G_1 = y_1 - x_2 - x_1\dot{x}_3 \\ G_2 = \dot{y}_2 - \dot{x}_1 + 3x_1 \\ G_3 = y_3 - x_3 - \dot{x}_3 \end{cases} \tag{5.22}$$

$$F\begin{cases} F_1 = 0.2\dot{x}_2 + 1.2x_1x_3 - \frac{1}{3}x_1^2x_2 \\ F_2 = -x_2x_3 \\ F_3 = -\frac{1}{2}y_1 - \frac{1}{3}x_1x_2 \end{cases} \tag{5.23}$$

Our goal is to achieve the multiple symplectic derivative synchronization.

Define error function as

$e = G(x,y,z,\ldots,\dot{x},\dot{y},\dot{z},\ldots\ddot{x},\ddot{y},\ddot{z}\ldots,t)\text{-}F(x,y,z,\ldots,\dot{x},\dot{y},\dot{z},\ldots\ddot{x},\ddot{y},\ddot{z}\ldots,t)+\boldsymbol{K}$.

where $\boldsymbol{K}=[1000,1000,1000]^T$ keep the error dynamics always in first guardant.

Thus we design the controller.

$$lim_{t\to\infty}\, e_i = lim_{t\to\infty}(G_i - F_i + K_i) = 0, (i = 1,2,3 \tag{5.24}$$

Thus we design the controller as

$$u = \begin{cases} u_1 = -2y_2 + e_1 \\ u_2 = 2 - 4y_3 + e_2 \\ u_3 = -2y_3 + 1 + e_3 \end{cases} \tag{5.25}$$

Given G and F of Yin Chen-Lee and Yin Sprott N system as.

$$\mathrm{G}\begin{cases} G_4 = y_4 - x_5 - 0.2\dot{x_5} - 1.8x_4\dot{x_6} \\ G_5 = \dot{y_5} - \dot{x_4} - 3x_4 \\ G_6 = y_6 - x_6 - \dot{x_6} \end{cases} \tag{5.26}$$

$$\mathrm{F}\begin{cases} F_4 = x_6x_4 - \frac{4}{15}x_4^2x_5 + \frac{1}{3}x_4^2x_5 \\ F_5 = 2y_4 - x_5x_6 \\ F_6 = -\frac{1}{2}y_4 + \frac{1}{3}x_4x_5 \end{cases} \tag{5.27}$$

Our goal is to achieve the multiple symplectic derivative synchronization.

Define error function as

$e = G(x,y,z,\ldots,\dot{x},\dot{y},\dot{z},\ldots\ddot{x},\ddot{y},\ddot{z}\ldots,t)\text{-}F(x,y,z,\ldots,\dot{x},,\dot{y},\dot{z},\ldots\ddot{x},\ddot{y},\ddot{z}\ldots,t)+\boldsymbol{K}.$

where $\boldsymbol{K}=[1000,1000,1000]^T$ keep the error dynamics always in first guardant.

Thus we design the controller.

$$lim_{t\to\infty}\, e_i = lim_{t\to\infty}(G_i - F_i + K_i) = 0, (i = 1,2,3) \tag{5.28}$$

Thus we design the controller as

$$u = \begin{cases} u_4 = -2y_5 + e_4 \\ u_5 = 2 + 4y_6 + e_5 \\ u_6 = -1 - 2y_6 + e_6 \end{cases} \tag{5.29}$$

Combining Yin and Yang synchronization. the results are shown in Fig.5.22.

Given G and F of Yang Sportt N and Yang Sprott K system as.

$$\mathrm{G}\begin{cases} \mathrm{G}_7 = \mathrm{z}_1 - \dot{\mathrm{z}_3} - \frac{1}{2}\dot{\mathrm{y}_1}\dot{\mathrm{y}_2} + \frac{91}{30}\mathrm{z}_3 \\ \mathrm{G}_8 = \dot{\mathrm{z}_2} - \dot{\mathrm{y}_2} + \mathrm{y}_2 + 0.3\mathrm{z}_3 \\ \mathrm{G}_9 = \mathrm{z}_3 - \mathrm{z}_2 + \mathrm{y}_1\mathrm{y}_2 + 0.5\mathrm{y}_1 \end{cases} \tag{5.30}$$

$$F\begin{cases} F_7 = y_1y_2 - \frac{1}{2}\dot{y}_1y_3^2 \\ F_8 = y_3y_2 + \dot{y}_3 + \frac{1}{2}\dot{y}_1y_3 + \dot{z}_3 \\ F_9 = y_1y_3 + 0.5\dot{y}_3y_1 \end{cases} \tag{5.31}$$

Our goal is to achieve the multiple symplectic derivative synchronization.

Define error function as

$e = G(x,y,z,\ldots,\dot{x},\dot{y},\dot{z},\ldots\ddot{x},\ddot{y},\ddot{z}\ldots,t)$-$F(x,y,z,\ldots,\dot{x},\dot{y},\dot{z},\ldots\ddot{x},\ddot{y},\ddot{z}\ldots,t)+\boldsymbol{K}$.

where $\boldsymbol{K}=[300,60,400]^T$ keep the error dynamics always in first guardant. Thus we design the controller.

$$lim_{t\to\infty}\, e_i = lim_{t\to\infty}(G_i - F_i + K_i) = 0, (i = 1,2,3) \tag{5.32}$$

Thus we design the controller as

$$u\begin{cases} u_7 = -z_3 - \frac{10}{3}z_1 + e_7 \\ u_8 = 2y_2 + e_8 \\ u_9 = z_2 + 0.3z_3 + e_9 \end{cases} \tag{5.33}$$

Given G and F of Yin Sportt N and Yin Sprott K system as.

$$G\begin{cases} G_{10} = z_4 - \dot{z}_6 + y_5y_6^2 \\ G_{11} = \dot{z}_5 - \dot{y}_5 - \dot{z}_6 - \frac{1}{2}y_6\dot{y}_4 \\ G_{12} = z_6 - y_4 - z_5 + \dot{y}_5 + y_6^3 \end{cases} \tag{5.34}$$

$$F\begin{cases} F_{10} = y_4y_5 - \frac{91}{30}z_6 - y_5\dot{y}_5 \\ F_{11} = y_6y_5 - 0.3z_6 + \dot{z}_5 - z_4 + 2y_6 \\ F_{12} = y_4y_6 - y_6^2 - \dot{y}_5y_6 \end{cases} \tag{5.35}$$

Our goal is to achieve the multiple symplectic derivative synchronization.

Define error function as

$e = G(x,y,z,\ldots,\dot{x},\dot{y},\dot{z},\ldots\ddot{x},\ddot{y},\ddot{z}\ldots,t)$-$F(x,y,z,\ldots,\dot{x},\dot{y},\dot{z},\ldots\ddot{x},\ddot{y},\ddot{z}\ldots,t)+\boldsymbol{K}$.

where $\boldsymbol{K}=[300,60,400]^T$ keeps the error dynamics always in first guardant. Thus

we design the controller.

$$lim_{t\to\infty} e_i = lim_{t\to\infty}(G_i - F_i + K_i) = 0, (i = 1,2,3) \tag{5.36}$$

Thus we design the controller as

$$u = \begin{cases} u_{10} = \frac{10}{3}z_4 + z_6 + e_{10} \\ u_{11} = 2y_5 + e_{11} \\ u_{12} = z_5 + 0.3z_6 + e_6 \end{cases} \tag{5.37}$$

Combining Yin and Yang synchronization, the results are shown in Fig.5.23.

5.5 Kun-Zhen Hexagram Multiple Symplectic Derivative Synchronization by Partial Region Stability Theory

Kun-Zhen Hexagram is used for synchronization.

Given

$G(x,y,z,\ldots,\dot{x},\dot{y},\dot{z},\ldots\ddot{x},\ddot{y},\ddot{z}\ldots,t)$:

$$G\begin{cases} G_1 = 2y_1 - 2x_2 - 2x_1\dot{x}_3 \\ G_2 = 2\dot{y_2} - 2\dot{x}_1 + 6x_1 \\ G_3 = 2y_3 - 2x_3 - 2\dot{x}_3 \end{cases} \tag{5.38}$$

$F(x,y,z,\ldots,\dot{x},\dot{y},\dot{z},\ldots\ddot{x},\ddot{y},\ddot{z}\ldots,t)$:

$$F\begin{cases} F_1 = 0.4\dot{x}_2 + 2.4x_1x_3 - \frac{2}{3}x_1^2x_2 \\ F_2 = -2x_2x_3 \\ F_3 = -y_1 - \frac{2}{3}x_1x_2 \end{cases} \tag{5.39}$$

Our goal is to achieve the multiple symplectic derivative synchronization.

Define error function as

$$e = G(x,y,z,\ldots,\dot{x},\dot{y},\dot{z},\ldots\ddot{x},\ddot{y},\ddot{z}\ldots,t) - F(x,y,z,\ldots,\dot{x},\dot{y},\dot{z},\ldots\ddot{x},\ddot{y},\ddot{z}\ldots,t) + \boldsymbol{K}. \tag{5.40}$$

where $\boldsymbol{K}=[2000,2000,2000]^T$ keep the error dynamics always in first guardant. Our goal is

$$lim_{t\to\infty}\, e_i = lim_{t\to\infty}(G_i - F_i + K_i) = 0, (i = 1,2,3) \tag{5.41}$$

Thus we design the controller as

$$u\begin{cases} u_1 = -4y_2 + e_1 \\ u_2 = 4 - 8y_3 + e_2 \\ u_3 = -4y_3 + 2 + e_3 \end{cases} \tag{5.42}$$

The error dynamics becomes

$$\dot{\boldsymbol{e}} = \dot{\boldsymbol{G}} - \dot{\boldsymbol{F}} - \boldsymbol{u} \tag{5.43}$$

Using partial region stability theory we can choose a Lyapunov function in the form of a positive definite function in first quadrant.

$$V(e) = e_1 + e_2 + e_3 > 0 \tag{5.44}$$

By adding u ,we obtain

$$\dot{V}(e) = -e_1 - e_2 - e_3 < 0 \tag{5.45}$$

which is a negative definite function in first quadrant, the results are shown in Fig. 5.24.

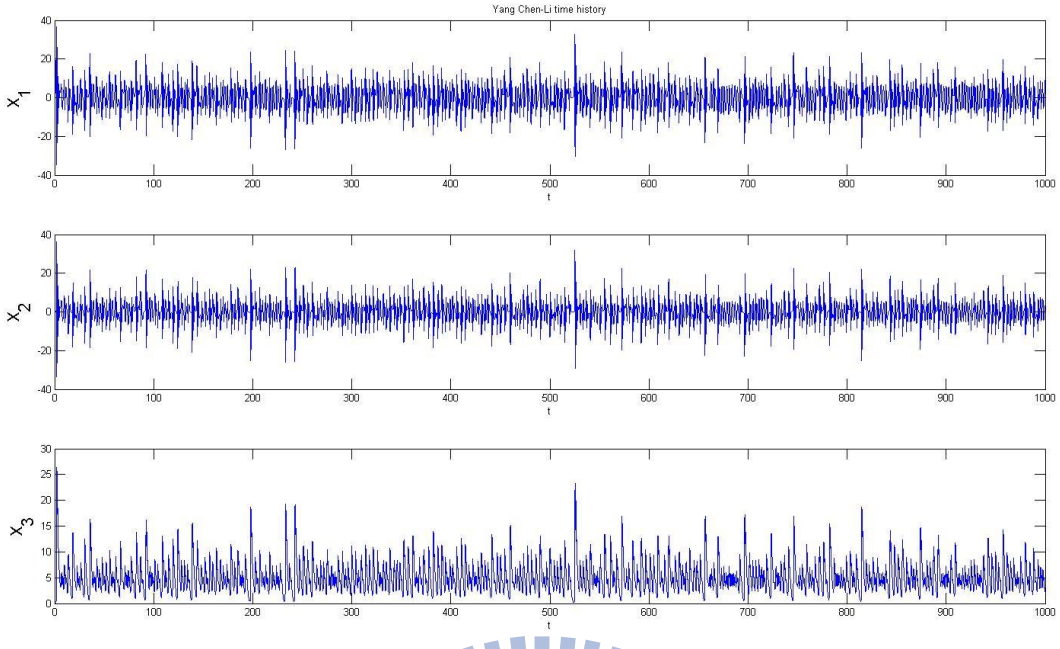

Fig.5.1 Time histories of the Yang Chen-Lee system.

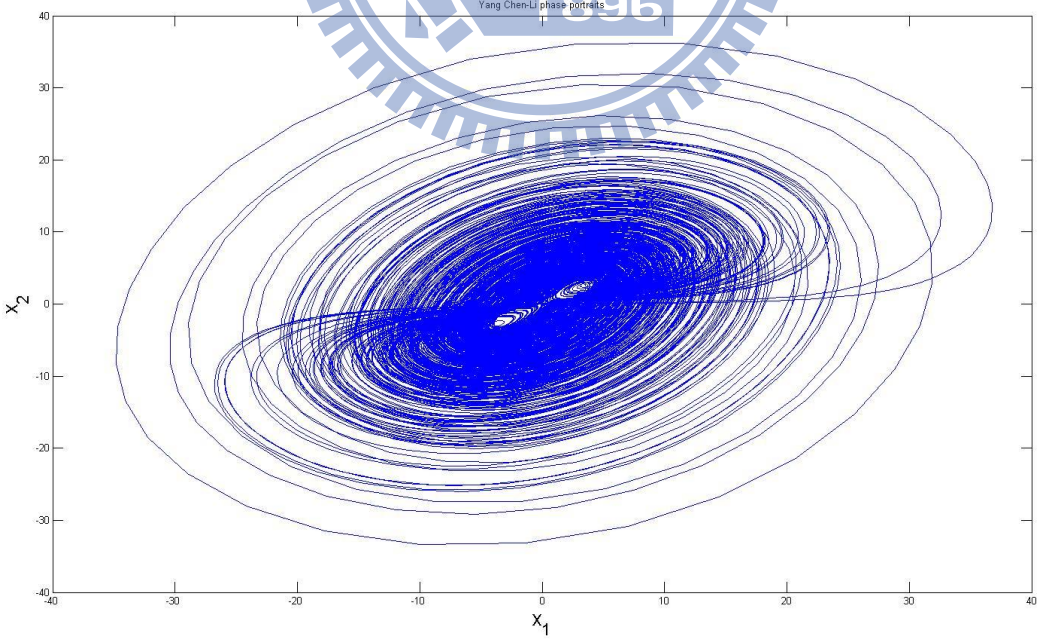

Fig.5.2 Phase portrait of the Yang Chen-Lee system.

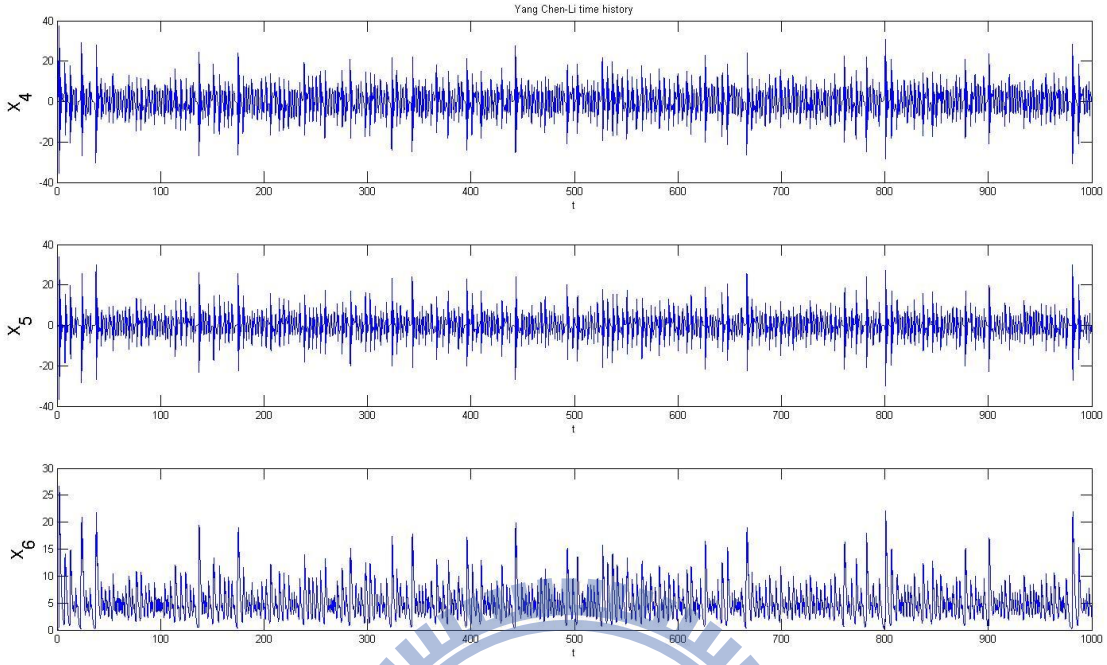

Fig.5.3 Time histories of the Yin Chen-Lee system.

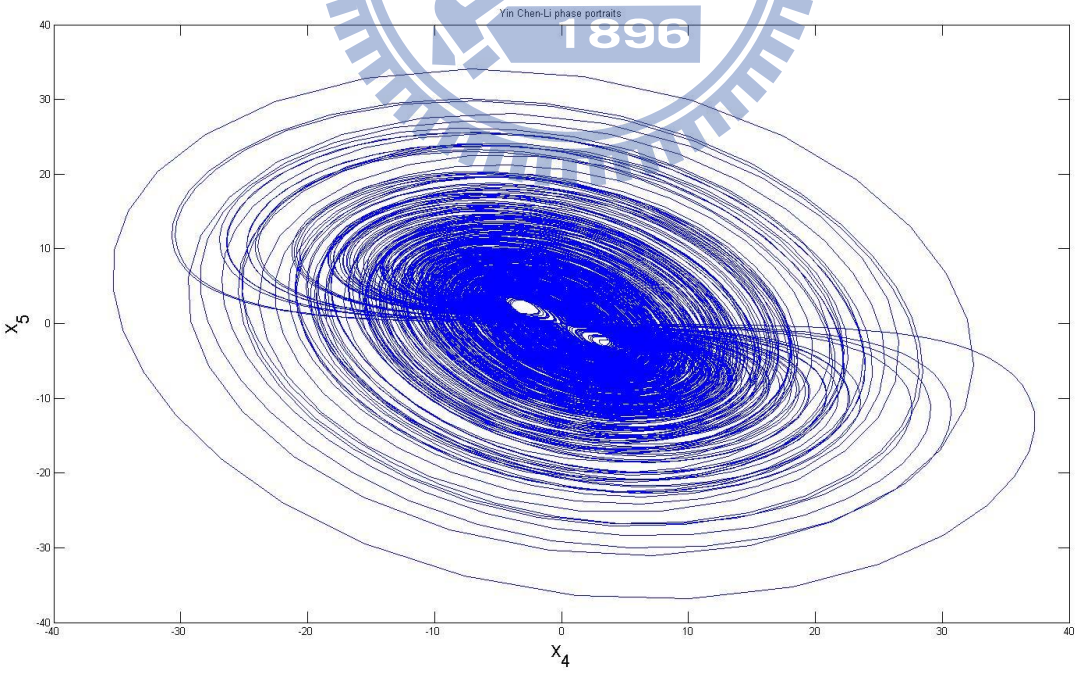

Fig.5.4 Phase portrait of the Yin Chen-Lee system.

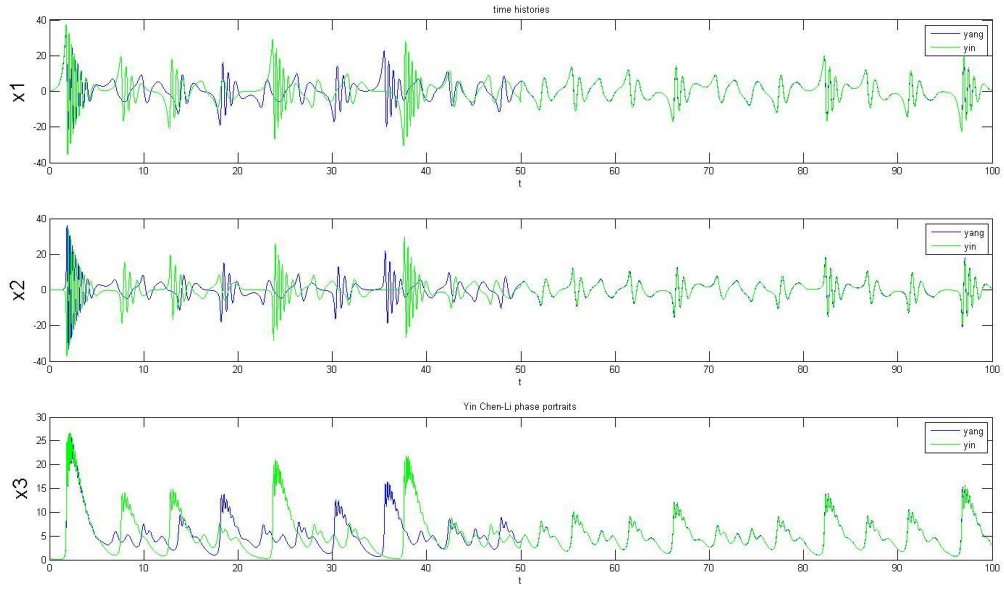

Fig. 5.5 Synchronization for Yin Chen-Lee system and Yang Chen-Lee system.

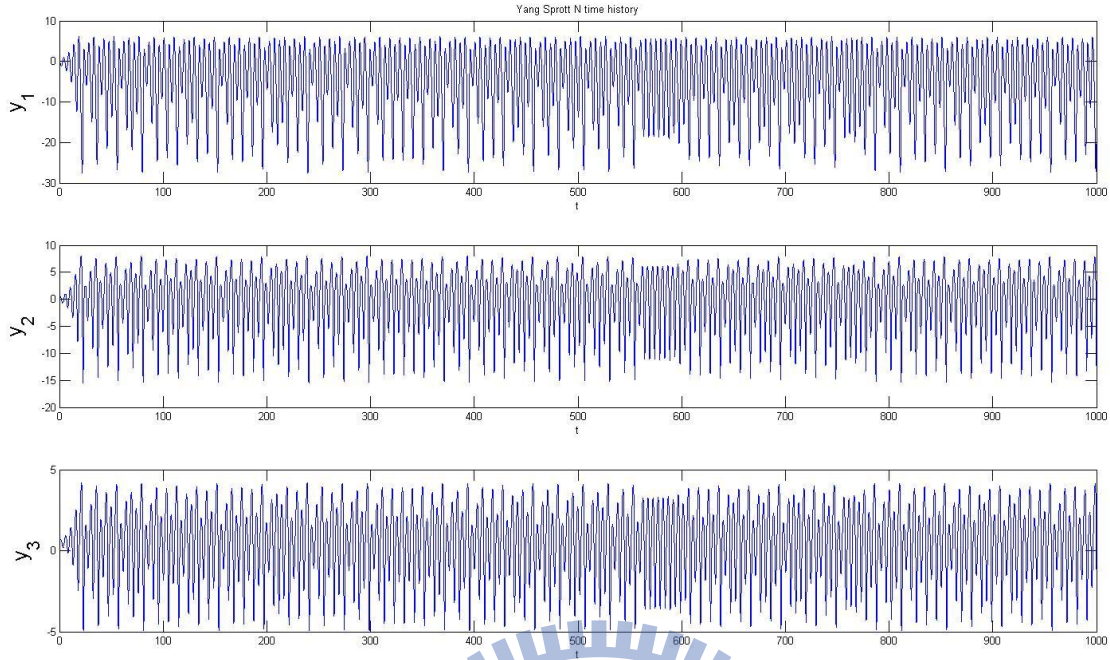

Fig.5.6 Time histories of the Yang Sprott N system.

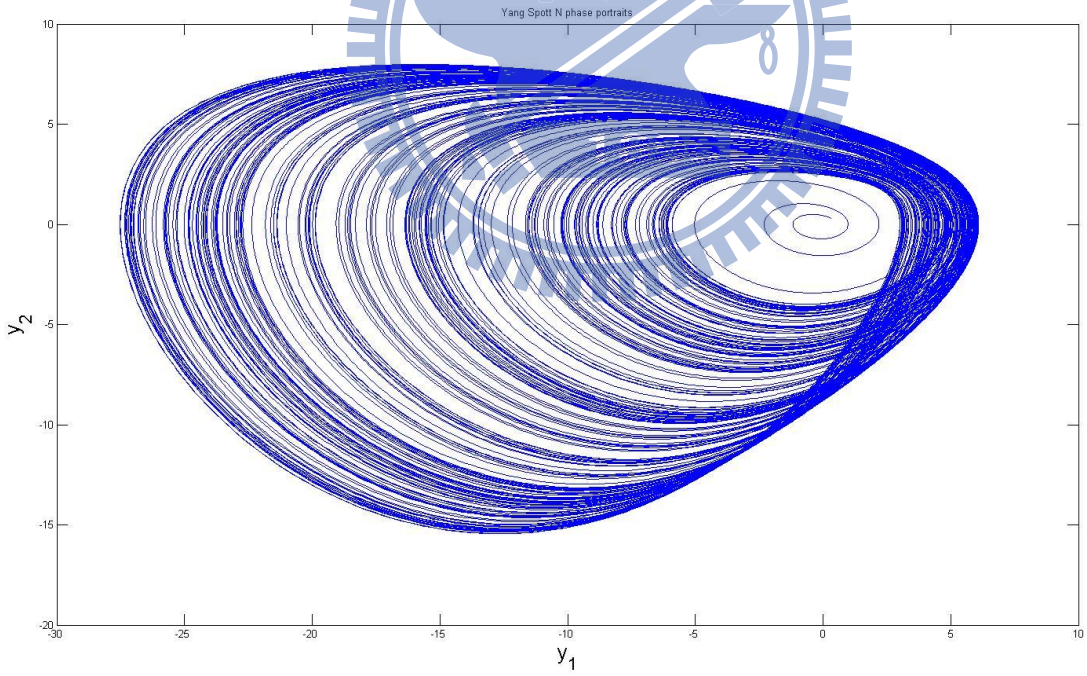

Fig.5.7 Phase portrait of the Yang sprott N system.

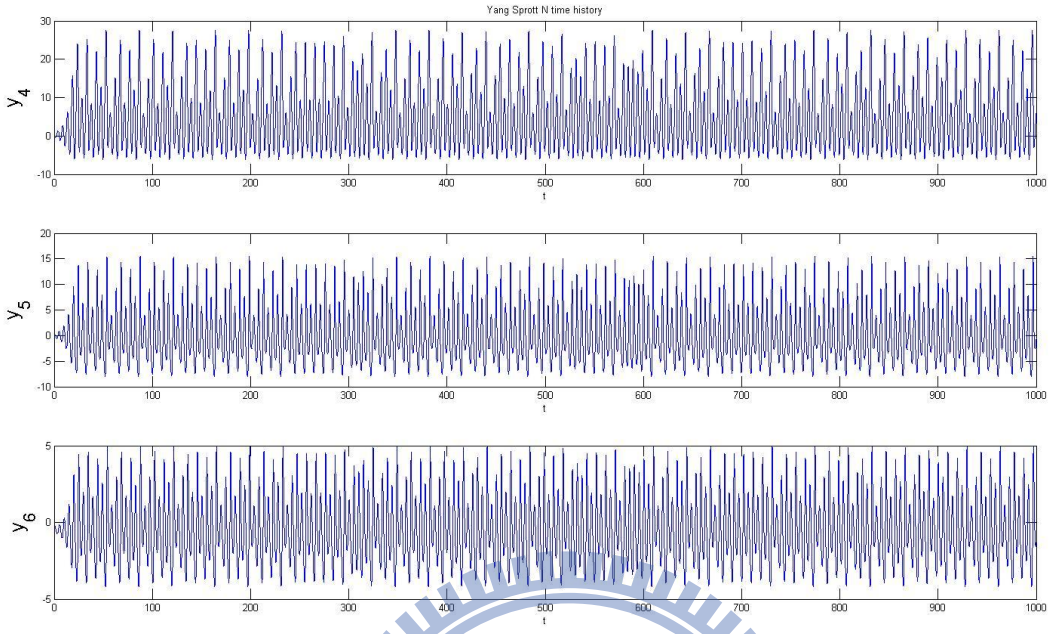

Fig.5.8 Time histories of the Yin Sprott N system.

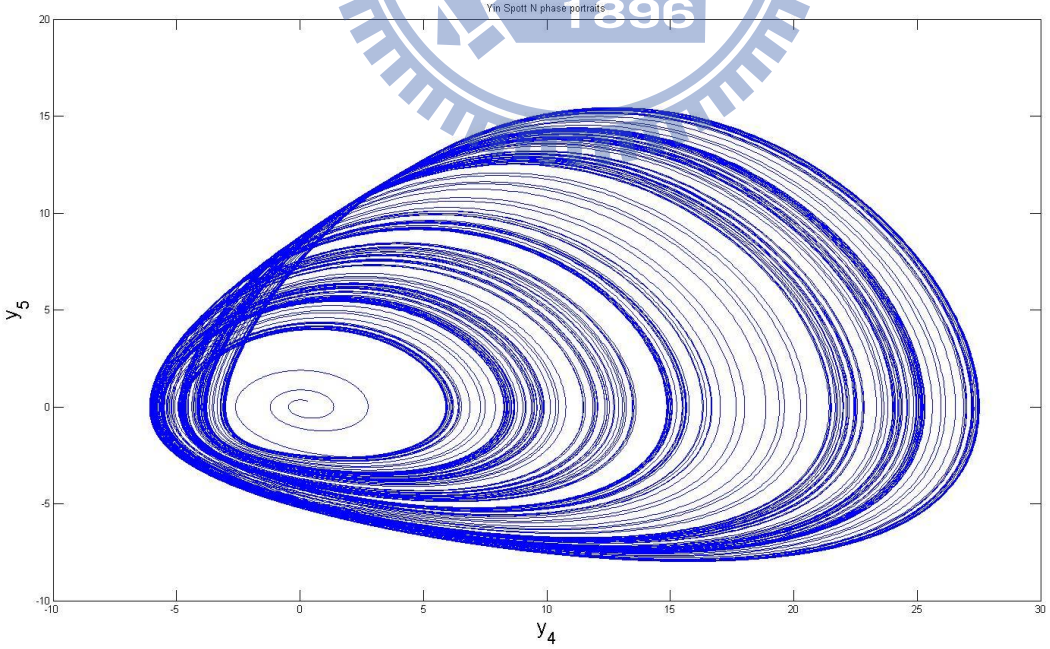

Fig.5.9 Phase portrait of the Yin Sprott N system.

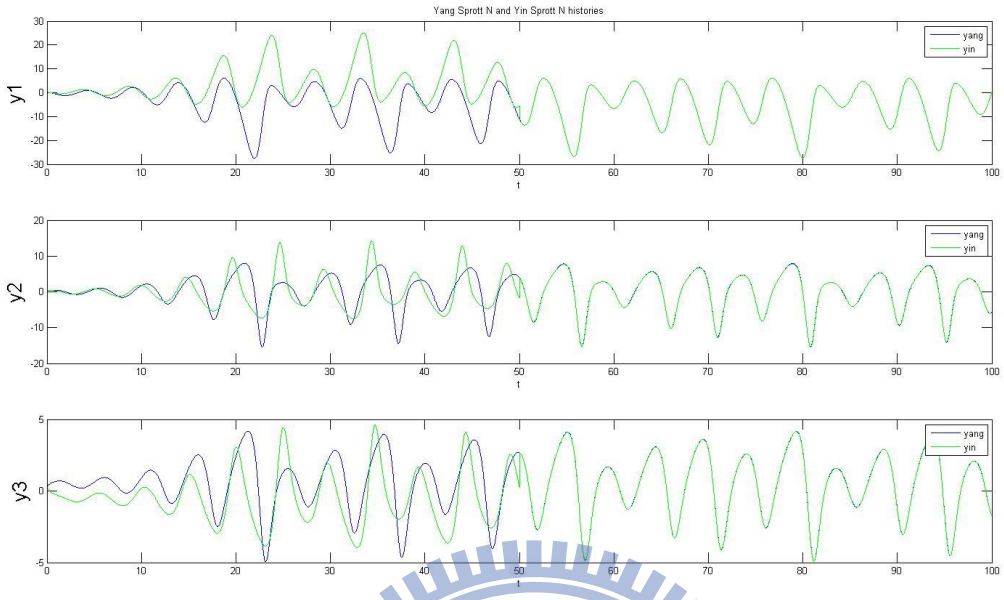

Fig. 5.10 Synchronization for Yin Sprott N system and Yang Sprott N system.

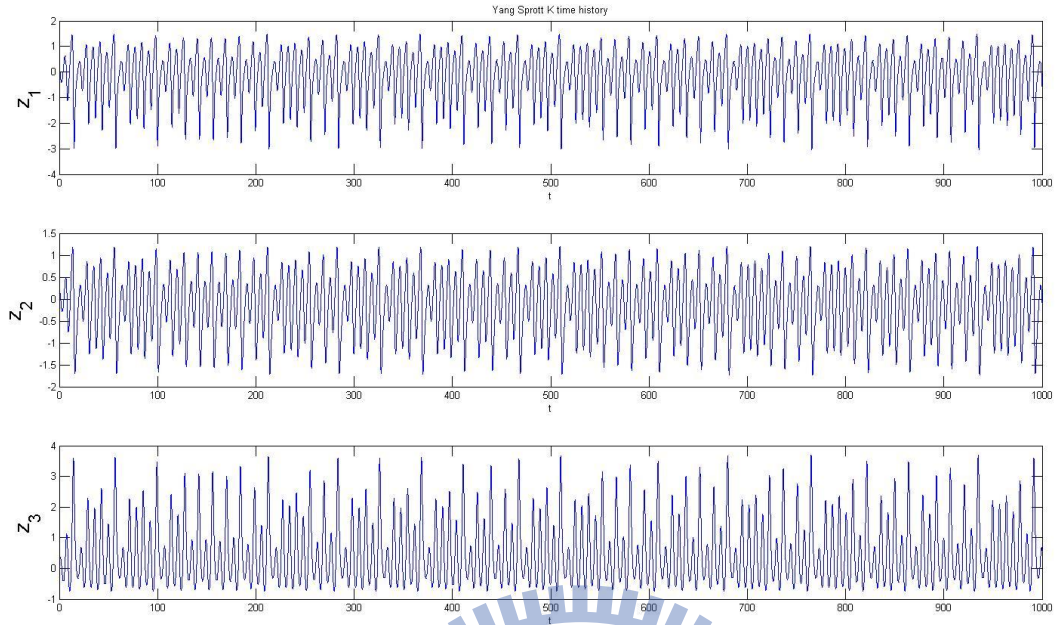

Fig.5.11 Time histories of the Yang Sprott K system.

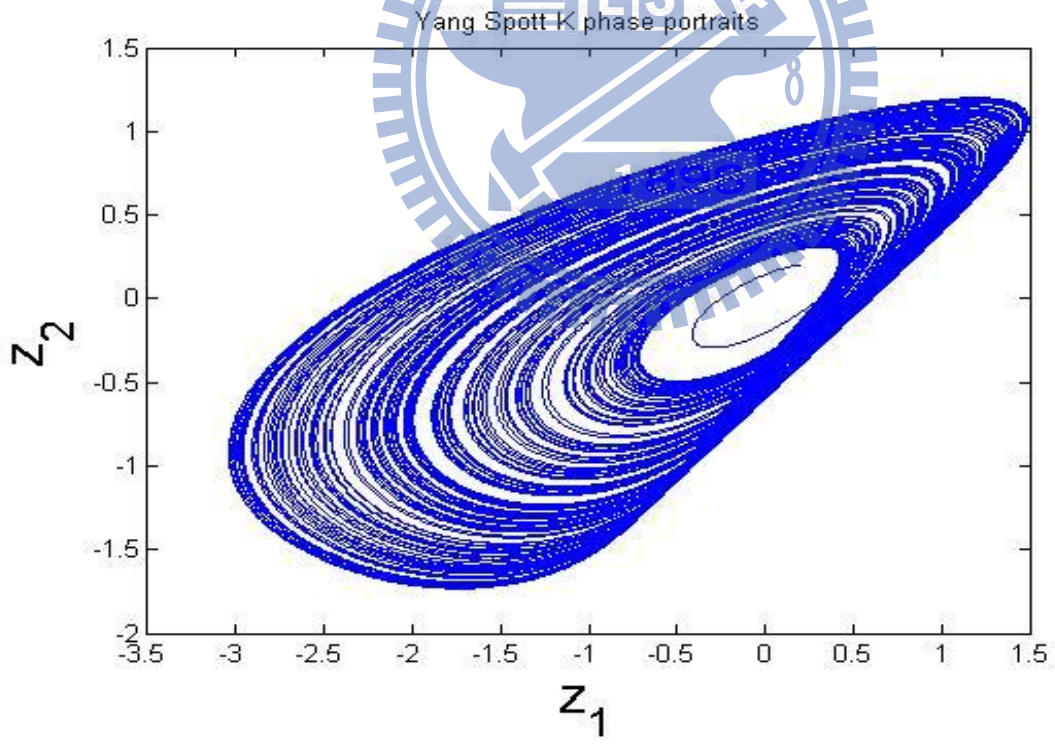

Fig.5.12 Phase portrait of the Yang Sprott K system.

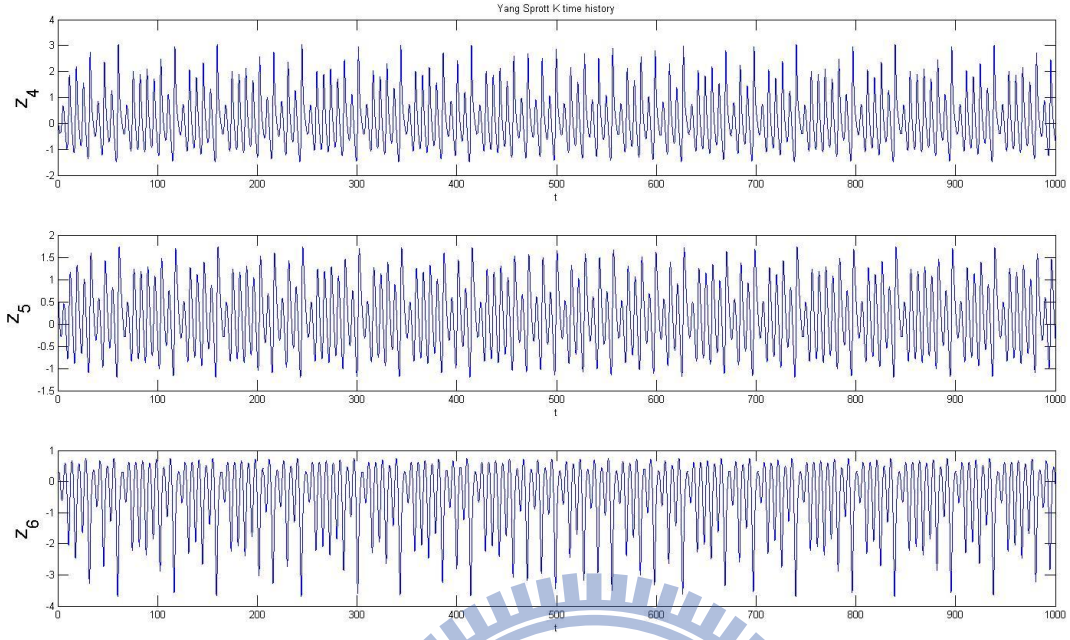

Fig.5.13 Time histories of the Yin Sprott K system.

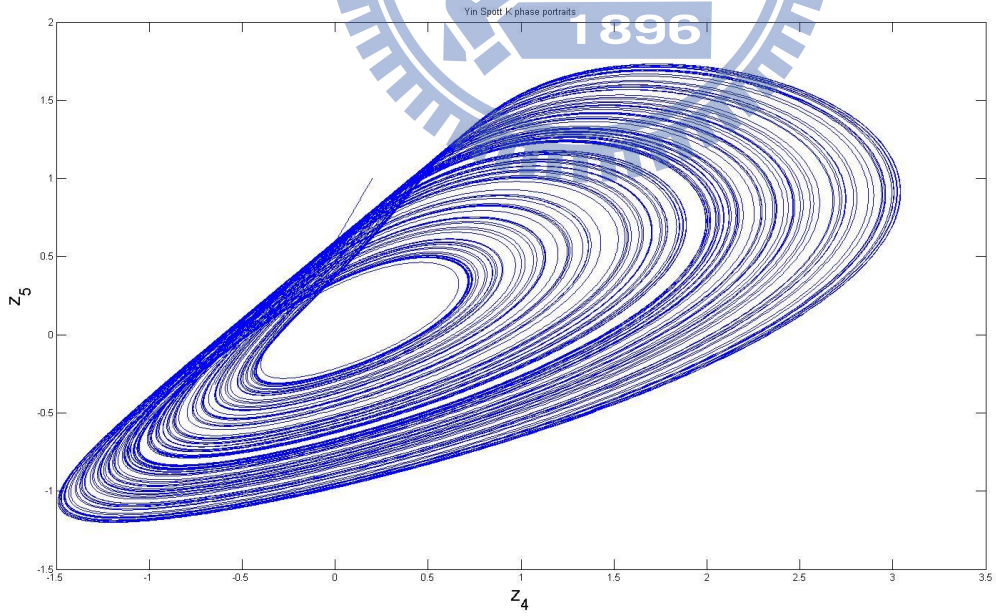

Fig.5.14 Phase portrait of the Yin Sprott K system.

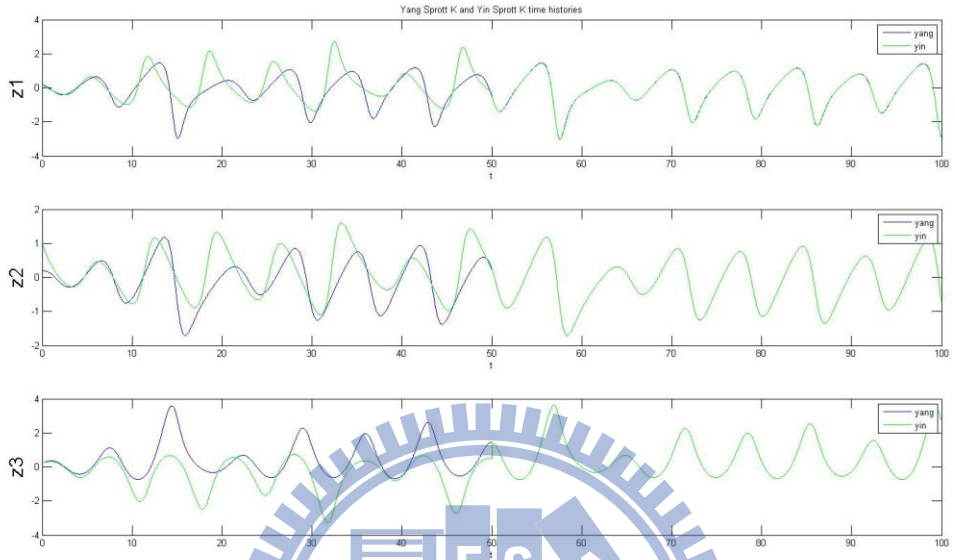

Fig. 5.15 Synchronization for Yin Sprott K system and Yang Sprott K system.

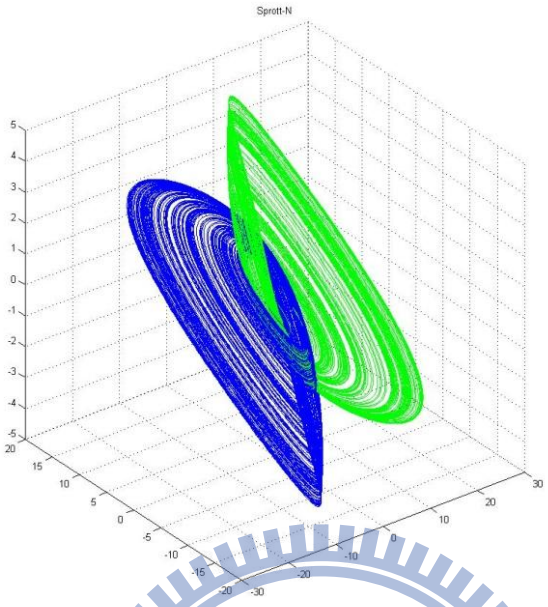

Fig. 5.16 Phase portraits of Sportt N system.

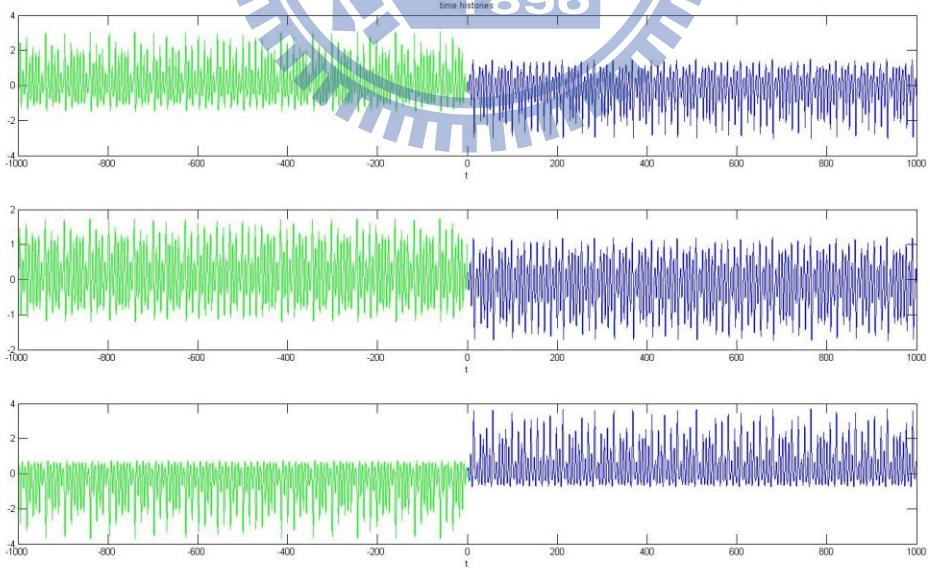

Fig. 5.17 Time histories of Tai Ji Sportt N system.

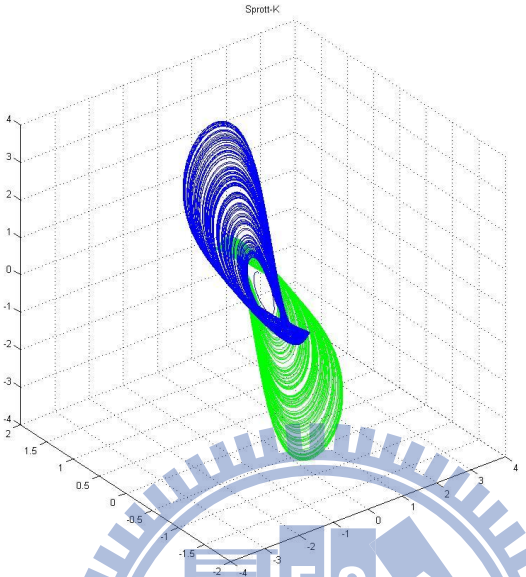

Fig.5.18 Phase portraits of Sportt K system.

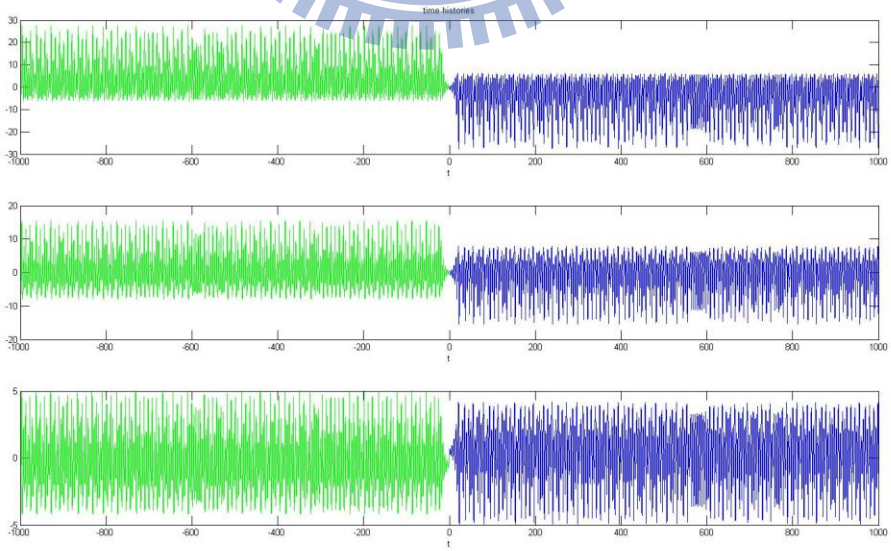

Fig.5.19 Time histories of Tai Ji Sportt K system.

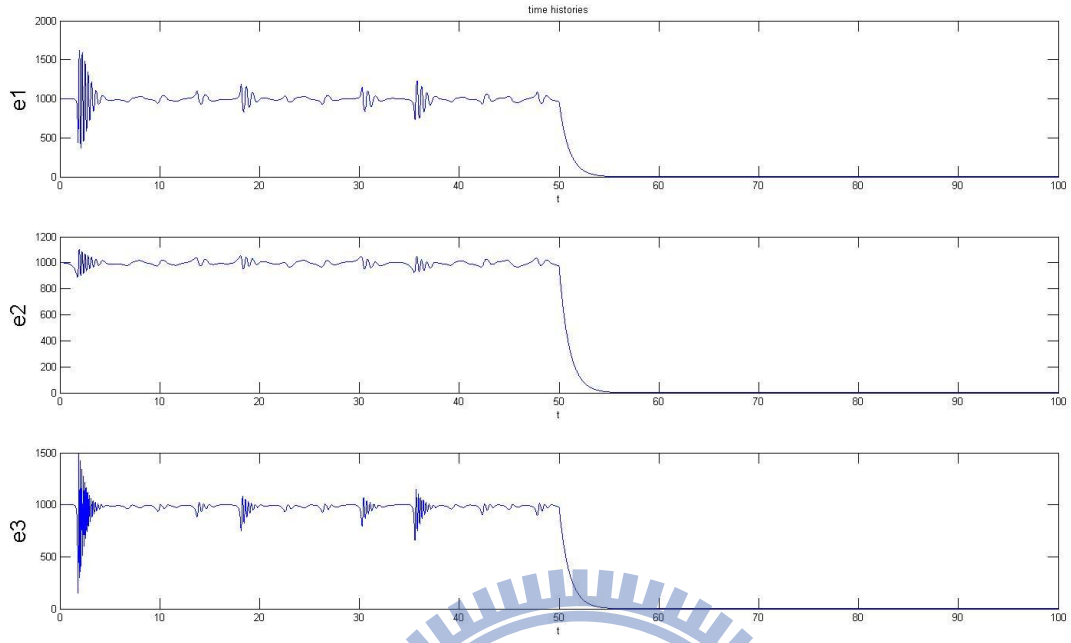

Fig.5.20 Time histories of e_1, e_2, e_3 before and after control.

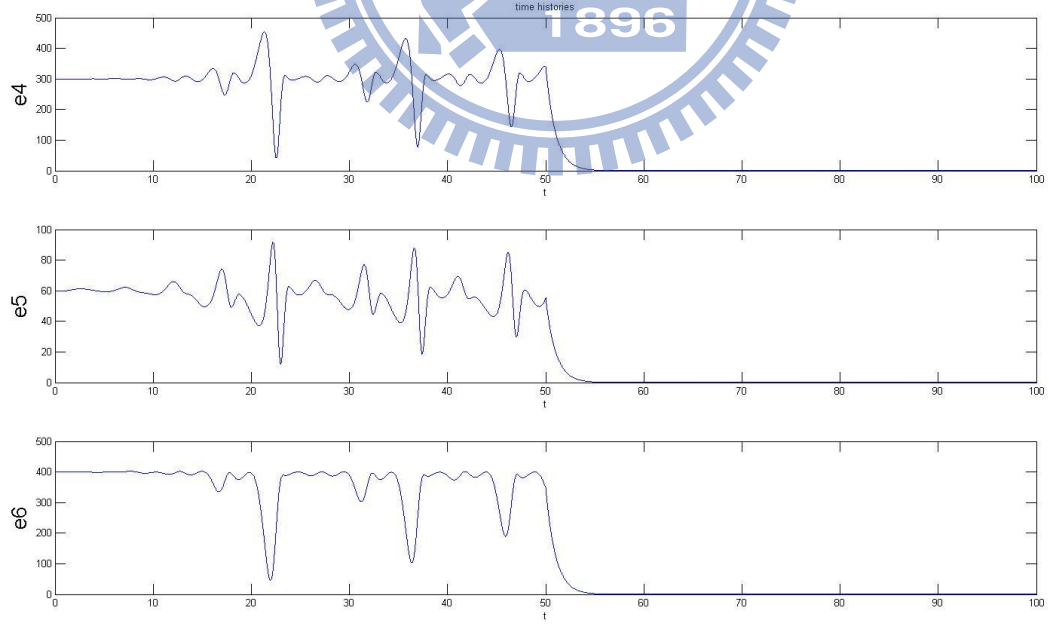

Fig.5.21 Time histories of e_4, e_5, e_6 before and after control.

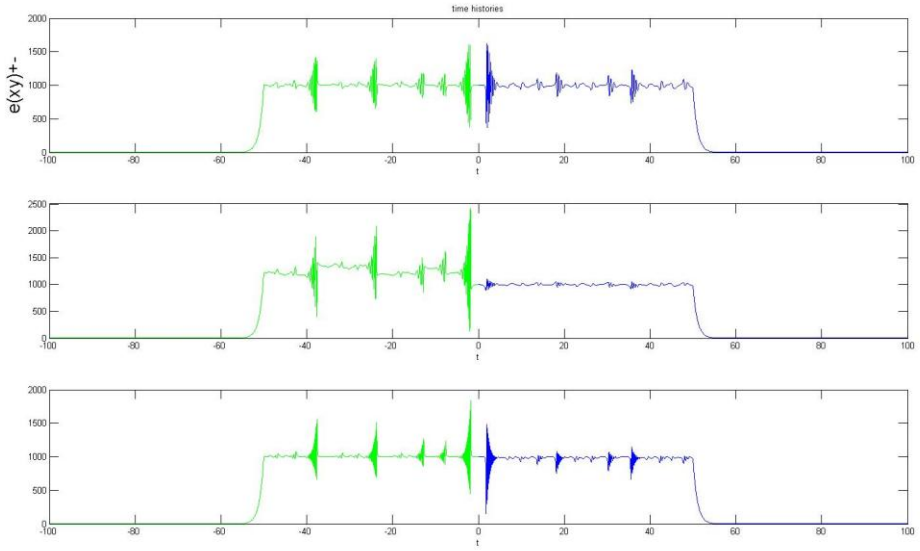

Fig..5.22 Time histories of error in Chen-lee and Sprott N systems.

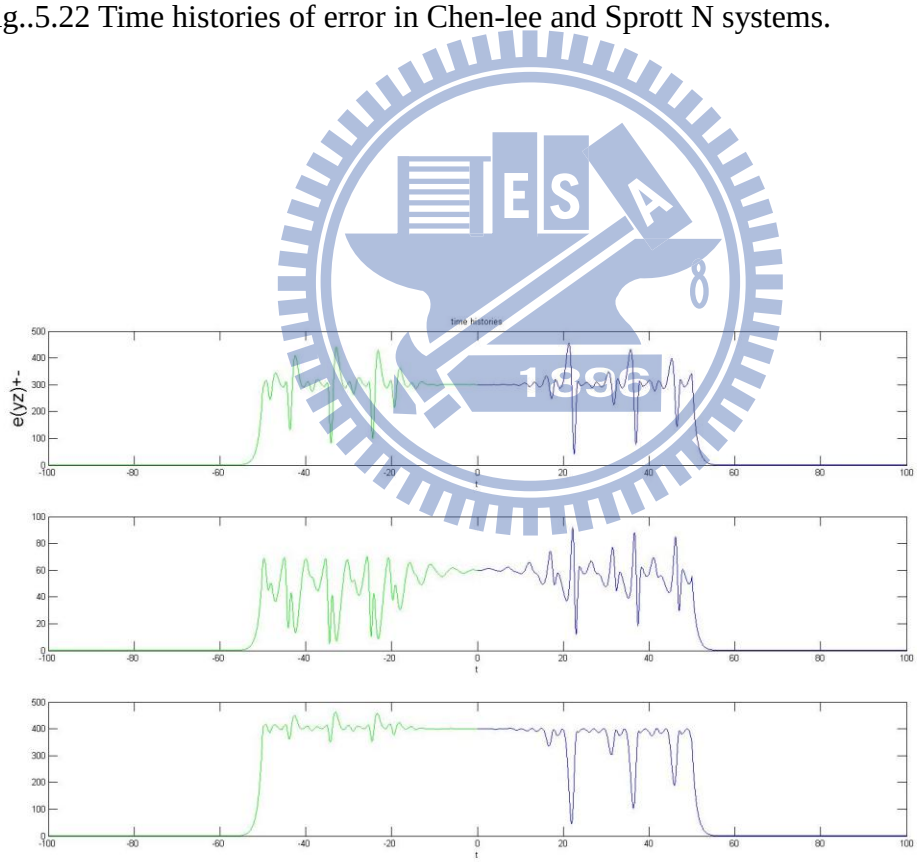

Fig.5.23 Time histories of error in SprottN and Sprott K systems.

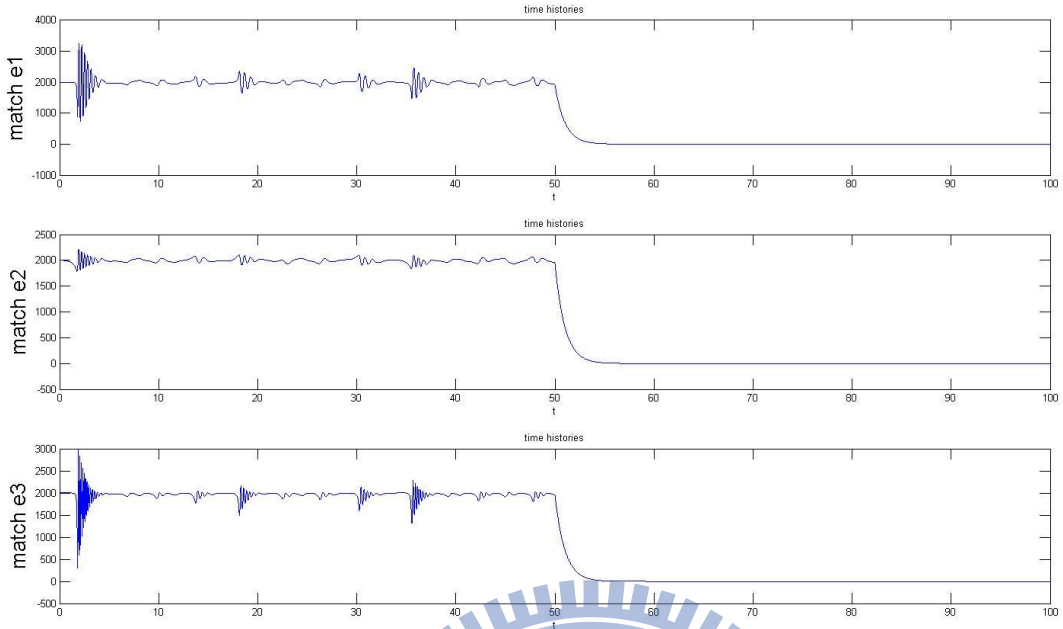

Fig.5.24 Time histories of e_1, e_2, e_3 before and after control.

Chapter 6

Conclusions

In Chapter 2, Chen-Lee system is divided into Yang, Yin and “Tai Ji” systems and the “Tai Ji” Chen-Lee system is introduced firstly. Chaos of Yang system is studied by time histories, phase portraits, bifurcation diagrams and Lyapunov exponents. Next, the past of the system, Yin system, is studied. Finally, “Tai Ji” system is studied for past and future chaos and is compared with Yang and Yin systems via numerical simulations.

It is firstly discovered that the exact scientific chaos phenomena marvelously match with the ancient Chinese philosophy, “The Yin Classic” with English translation “The book of Change” which states that the original chaotic substance, Tai Ji, begets two fundamental opposites, Yin and Yang. Correspondingly, Tai Ji chaos consists of two opposites, Yin chaos and Yang chaos.

In Chapter 3, a new synchronization is presented. We not only use the variables but also their derivatives in two given function. New strategy to achieve chaos control by GYC partial region stability is used, by which we can synchronize system quickly comparing with traditional method. Finally, Tables and figures are given to prove that the new strategy do synchronize system more quickly.

In Chapter 4, new synchronization and new strategy is presented. New synchronization have variable time scale τ and new strategy use variable quadrant to arrive synchronization. By using the partial region stability theory, the controllers become simple functions. The simulation results are given.

New strategy are superior than traditional method in high convergence rate and

low error value, it can be applied widely in the future.

In Chapter 5,Kun Trigram is one of Eight Trigrams. which consists of three broken lines. Zhen Trigram is two broken line and one unbroken lines.Kun-Zhen Hexagram has two parts, upper is Kun Trigram , and low is Zhen trigram.

The multiple derivative synchronizations of Kun and Zhen trigram are given by partial stability theory and “Kun trigrams”, “Zhen trigrams” synchronizations are obtained. Finally, Kun-Zhen hexagram are produced by synchronizations of Kun trigram and Zhen trigram.

From the previous sections, symplectic derivative chaos synchronization by partial region stability theory are shown.

To achieve chaos control , GYC partial region stability theory is used for searching controller easily and synchronizing system quickly. The new synchronization seems be rather complex, and the confidential property would be difficult to decipher.

References

[1] Lacitignola D., Petrosillo I., Zurlini G., "Time-dependent regimes of a tourism-based social–ecological system period-doubling route to chaos." Ecol.Complex.7 (2010) 44–54

[2] Huang L.-L., Feng R.-P. and Wang M., "Synchronization of chaotic systems via nonlinear control", Phys Lett A 320(4) (2004) 271.

[3] Fuh C.C. and Tung P.C., ''Controlling chaos using differential geometric method'', Phys Rev Lett 75 (1995) 2952.

[4] Hassell M. P., Comins H. N., Mayt R. M., "Spatial structure and chaos in insect population dynamics", Nature, Volume 353, Issue 6341(1991) 255-258.

[5] Chen HK, Lee CI. Anti-control of chaos in rigid body motion. Chaos, Solitons & Fractals 2004; 21: 957-65.

[6] Li Guo-Hui and Zhou Shi-Ping, "An observer-based anti-synchronization", Chaos, Solitons and Fractals 29 (2006) 495.

[7] L.M. Tam,W.M. SiTou, Parametric study of the fractional order Chen–Lee System,Chaos Solitons Fractals (2006) doi:10.1016/j.chaos.2006.09.067.

[8] Yin Li and Biao Li, "Chaos Control and Projective Synchronization of a Chaotic Chen-Lee System", Chinese Academy of Sciences(2008)

[9] Lorenz E.N., "Deterministic non-periodic flows", J. Atoms.20 (1963) 130.

[10] Ge Zheng-Ming and Li Shich-Yu, "Yang and Yin parameters in the Lorenz system", Nonlinear Dynamics 62 (2010) 105

[11] Ge, Z.-M. and Yang, C.-H. "Symplectic synchronization of different chaotic systems", Chaos, Solitons and Fractals 40 (2009) 2532–2543

[12] Sprott J.C., "Some simple chaotic flows", Physical Review E, 2 (1994) 5

[13] Petrov V., Gaspar V., Masere J. and Showalter K., "Controlling chaos in the

Belousov–Zhabotinsky reaction", Nature 361 (1993) 240–243.

[14] Yu, X., Song, Y. "Chaos synchronization via controlling partial state of chaotic systems", Int J Bifurcat Chaos 11 (2001) 1737-1741.

[15] Wang, C, Ge, SS. "Adaptive synchronization fo uncertain chaotic via backstepping design", Chaos Solitons & Fractals 12 (2001) 1199-1206.

[16] Elabbasy, E. M., Agiza, H. N., and El-Desoky, M. M., ''Adaptive synchronization of a hyperchaotic system with uncertain parameter'', Chaos, Solitons and Fractals, 30 (2006) 1133-1142.

[17] Garfinkel A, Spano ML, Ditto WL and Weiss JN, "Controlling cardiac chaos", Science 257 (1992) 1230–1235.

[18] Park Ju H., ''Adaptive synchronization of Rossler system with uncertain parameters'', Chaos, Solitons and Fractals, 25 (2005) 333-338.

[19] Yamada T. and Fujisaka H., "Stability theory of synchronized motion in coupled-oscillator systems", Progr. Theor. Phys. **70** (1983) (5) 1240–1248.

[20] Pecora LM and Carroll TL, "Synchronization in chaotic systems", Phys Rev Lett, 64 (1990) 821-824.

[21] Ge Z.-M. and Yang C.-H., "Synchronization in chaotic system of chaotic systems with uncertain parameters by adaptive control", Physica D: Nonlinear Phenomena **231** (2007) 87–94.

[22] Krawiecki A. and Sukiennicki A., "Generalizations of the concept of marginal synchronization of chaos", Chaos, Solitons & Fractals **11** (9) (2000) 1445–1458.

[23] Mainieri R. and Rahacek J., "Projection synchronization in three-dimensional chaotic systems", Phys. Rev. Lett. 82 (1999) 3042-3045.

[24] Ge Z.-M., Yang C.-H., Chen H.-H. and Lee S.-C., "Non-linear dynamics and chaos control of a physical pendulum with vibrating and rotation support", J

Sound Vib **242** (2) (2001) 247–264.

[25] Ge, Z.-M., Ho, C.-Y., Li, S.-Y. and Chang, C.-M., “Chaos control of new Ikeda–Lorenz systems by GYC partial region stability theory”, Math. Meth. Appl. Sci., 32 (2009) 1564–1584

[26] Ge, Z.-M. and Chen, Y.-S., “Synchronization of unidirectional coupled chaotic systems via partial stability”, Chaos, Solitons & Fractals, 21 (2004) 101.

[27] Ge, Z.-M., Yao, C.-W. and Chen, H.-K., “Stability on partial region in dynamics”, Journal of Chinese Society of Mechanical Engineer, 15 (2) (1994) 140-151.

[28] Ge, Z.-M. and Chen, H.-K., “Three asymptotical stability theorems on partial region with applications”, Japanse Journal of Applied Physics, 37 (1998) 2762-2773.

[29] Ge, Z.-M., “Necessary and sufficient conditions for the stability of a sleeping top described by three forms of dynamic equations”, Physical Review E, 77 (2008) 046606.